IEEE/CIC ICCC
IEEE/CIC International Conference on Communications in China
10–12 August 2023 // Dalian, China
Integrating Space-Air-Ground-Sea Communications

# Beamforming Technologies for Ultra-Massive MIMO in Terahertz Communications

**Chong Han**
Shanghai Jiao Tong University
chong.han@sjtu.edu.cn

**Linglong Dai**
Tsinghua University
daill@tsinghua.edu.cn

**Zhi Chen**
University of Electronic Science and Technology of China
chenzhi@uestc.edu.cn

# Outline

# 6G Key Capability Vision

- **6G Application scenarios："Broadband, ubiquitous, smart"**

Metaverse

AR automatic drive

Intelligent manufacturing 2025

Holographic intelligent medical service

Networked UAV

Smart city

# 6G Key Capability Vision

| | Peak rate | User data rate | Delay | Reliability | Spectral efficiency | Connection density |
|---|---|---|---|---|---|---|
| 5G | 0.01Tbit/s | 0.1-0.5 Gbit/s | 1 ms | 99.999% | 30 bps/Hz | $10^2$ devices/100 $m^2$ |
| **6G** | **1 Tbit/s** | **10 Gbit/s** | **0.1 ms** | **99.99999%** | **100 bps/Hz** | **$10^3$ devices/100 $m^2$** |

**Rich spectrum resources**

**Ultra-high frequency (mmWave, THz)**

**Ultra-massive MIMO (256 and above)**

**Multiple times of spectral efficiency**

**Ultra-high frequency and ultra-large scale MIMO are recognized as key technologies**

Chong Han, Linglong Dai, and Zhi Chen ©

B. Ning, Z. Tian, Z. Chen, C. Han, S. Li, J. Yuan, and R. Zhang, **"Prospective Beamforming Technologies for Ultra-Massive MIMO in Terahertz Communications: A Tutorial,"** IEEE Open Journal of the Communications Society, 2023

# Trend One: Higher Carrier Band

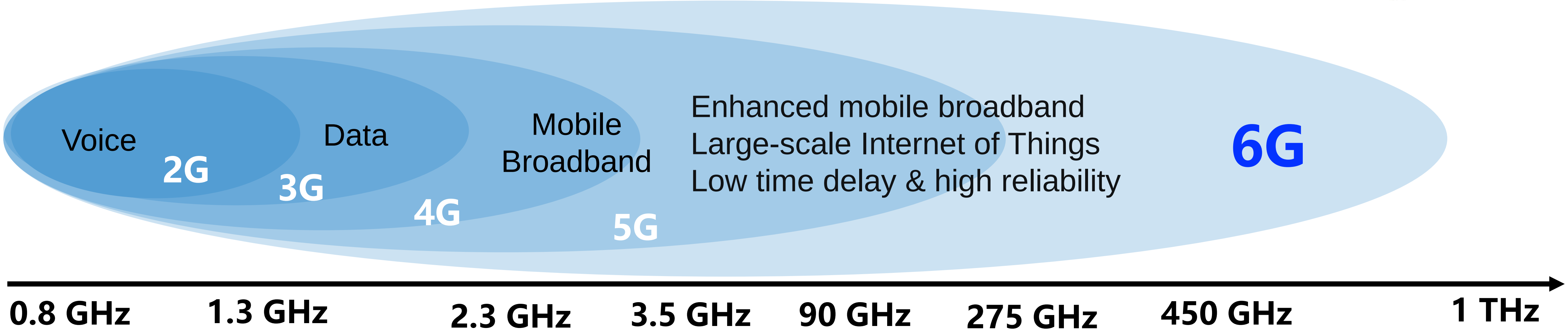


The 2019 World Radiocommunication Conference (WRC) identified 0.275-0.45THz as the 6G mobile communication band with an available bandwidth of up to tens of GHz.

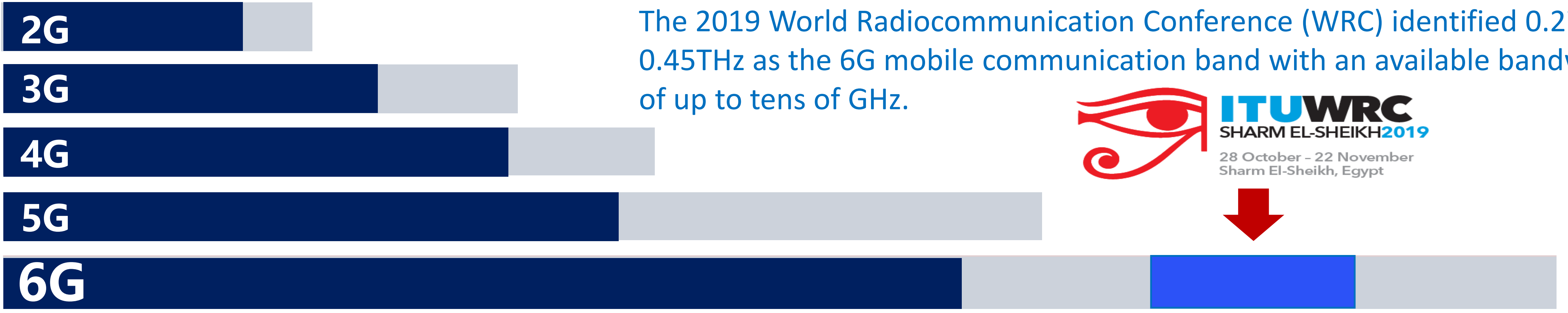


**Ultra-high frequency band (millimeter wave, terahertz) will become important supports for 6G communication ultra-wideband real-time service.**

# Trend Two: Larger Antenna Array Scale

| 1G | 2G | 3G | 4G | 5G | 6G |
|---|---|---|---|---|---|
| Omni-directional antenna | Single-polarized directional antenna | Bipolar antenna | MIMO antennas (2 – 8) | Massive MIMO antennas (64 – 128) | Ultra-massive MIMO antennas (256 – 1024) |

**Very large scale MIMO (256 and above) will become an important support for 6G multi-mode intensive deployment**

 White Paper on **"6G Vision and Candidate Technologies,"** IMT-2030 (6G), 2021 

# Motivations for Terahertz

- THz has ultra-wideband, high-speed communication capability and high precision sensing imaging capability, which is an important candidate technology for 6G
- Key technologies to meet the requirements of 6G communication scenarios become research hotspots

**THZ Band**

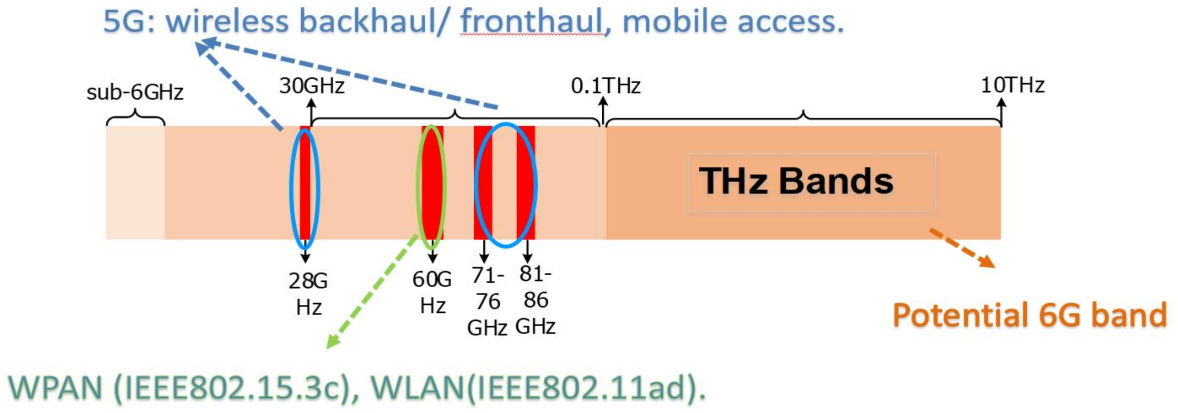


**Researches on key and difficult points**

- Coverage
  - THz spectrum sharing
- Energy efficiency
  - THz nano array
- Reliability
  - THz UM-MIMO
- Movability
  - THz beam tracking
- AI fusion service
  - THz wideband

# Research Progress of THz

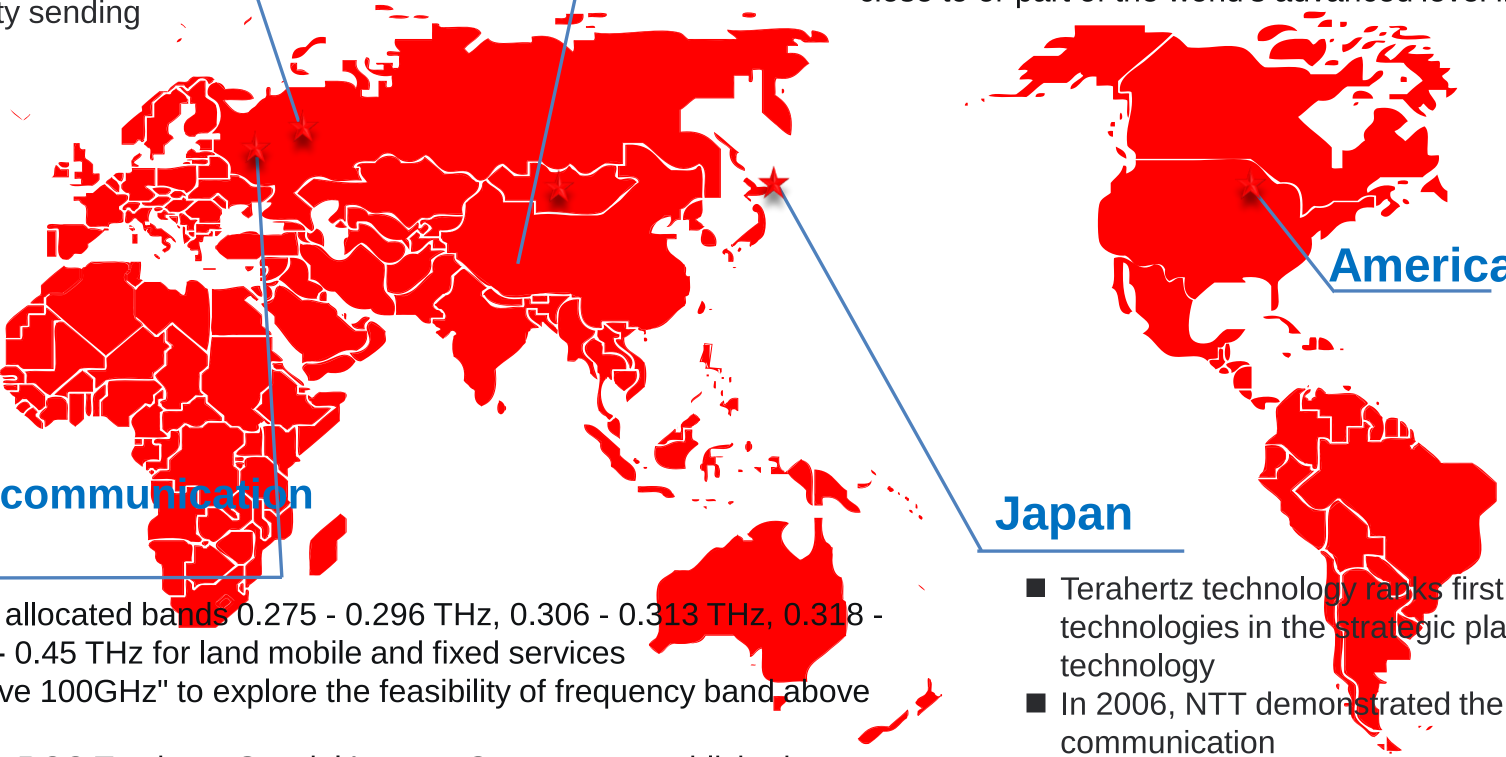

## Europe

- **Eu framework programme:**
  Horizon 2020、Horizon Europe
- **Transnational terahertz project：**
  Heterogeneous networking
  Ultrahigh capacity sending

## China

- Terahertz research launched at the "Terahertz Science and Technology" conference in 2005
- "Terahertz Wireless Communication Technology and System" major project of Ministry of Science and Technology in 2018
- Terahertz Core Devices and Transceiver Chips in 2019
- Domestic universities, research institutes and other joint research institutions, close to or part of the world's advanced level in 2020

## America

- DARPA and NASA launched the terahertz system Bell LABS 0.625 THz communication system is the highest frequency fully electronic architecture terahertz communication system realized to date in 2009.
- The FCC approved the opening of future wireless mobile communications research in August 2020.

## International Telecommunication Union ITU

- In 2019, ITU WRC-19 allocated bands 0.275 - 0.296 THz, 0.306 - 0.313 THz, 0.318 - 0.333 THz, and 0.356 - 0.45 THz for land mobile and fixed services
- August 2021 "IMT Above 100GHz" to explore the feasibility of frequency band above 100GHz
- In 2021, IEEE ComSoc RCC Terahertz Special Interest Group was established

## Japan

- Terahertz technology ranks first among the top ten technologies in the strategic planning of future science and technology
- In 2006, NTT demonstrated the first terahertz communication
  The government and the people will work together to formulate the 2030 "post-5G" strategy

# ITU-R timeline for IMT-2030

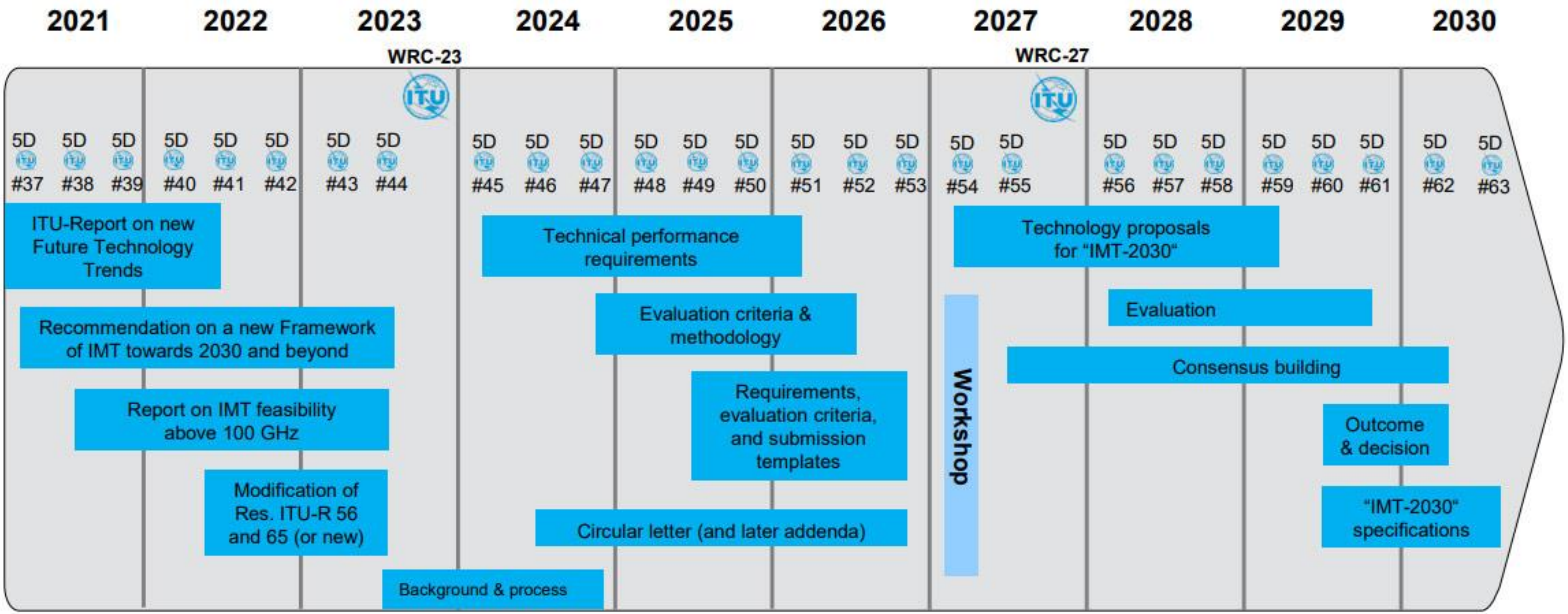


*Note 1: WP 5D #59 will additionally organize a workshop involving the Proponents and registered Independent Evaluation Groups (IEGs) to support the evaluation process*

*Note 2: While not expected to change, details may be adjusted if warranted. Content of deliverables to be defined by responsible WP 5D groups*

***Note by the ITU-R Radiocommunication Bureaux:*** *This document is taken from Attachment 2.12 to Chapter 2 of Document 5D/1361 (Meeting report WP 5D #41, June 2022) and adjustments could be made in the future. ITU holds copyright in the information – when used, reference to the source shall be done.*

# THz Application Scenarios

- Tbps wireless communications rate




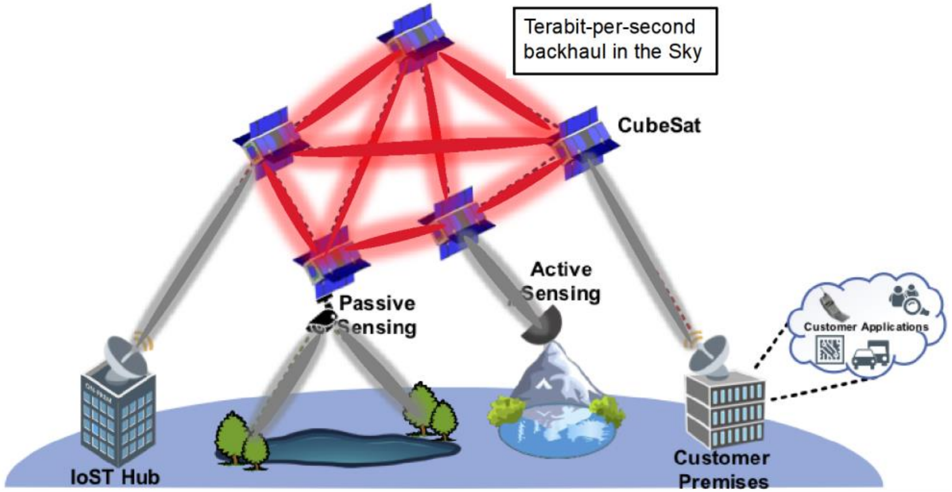


Z. Chen, C. Han, et. al., Wen Tong **"Terahertz Wireless Communications for 2030 and Beyond: A Cutting-Edge Frontier,"** Communications Magazine, 2021

# THz Application: Practical Example

- Tbps wireless communications rate
  - Sports event broadcasting: Ultra-low latency, uncompressed 8K ultra HD video



- Real-time transmission rate exceeding 80Gbps
- Distance coverage of over 1 kilometer
- New milestone in real-time transmission distance

# THz Application Scenarios

- Tbps wireless communications rate and millimeter-level sensing accuracy

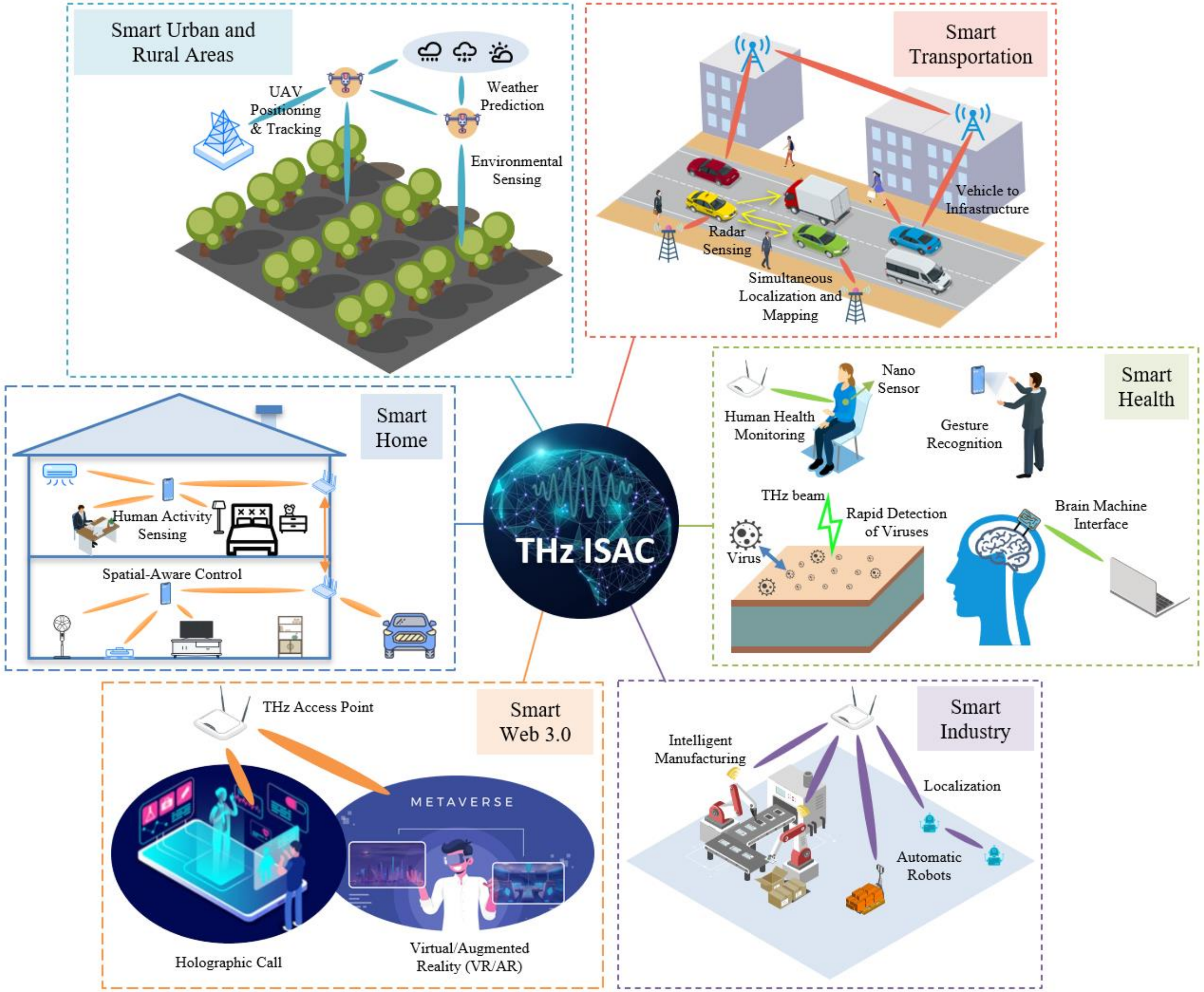


C. Han, Y. Wu, Z. Chen, Y. Chen, and G. Wang, **"THz ISAC: A Physical Layer Perspective of Terahertz Integrated Sensing and Communication,"** IEEE Communications Magazine, 2023

# THz Application Scenarios

- Terahertz nano-micro-scale communication scenarios

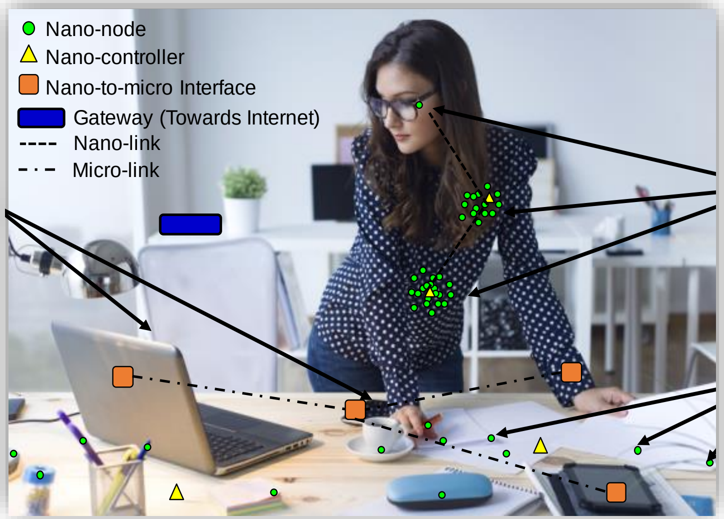


Smart Wearable Device

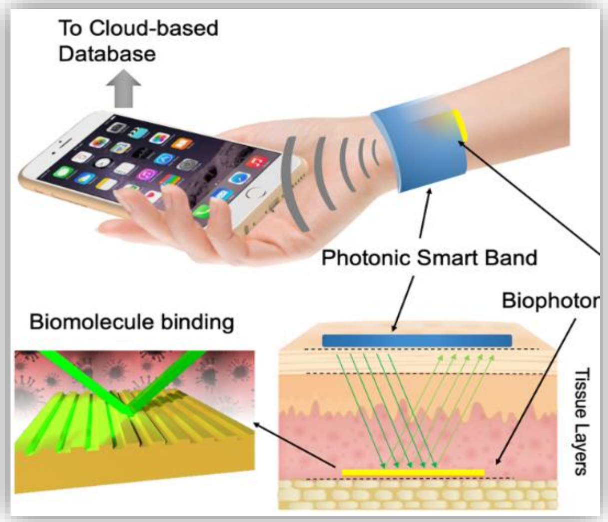


In Vivo Nanocommunication

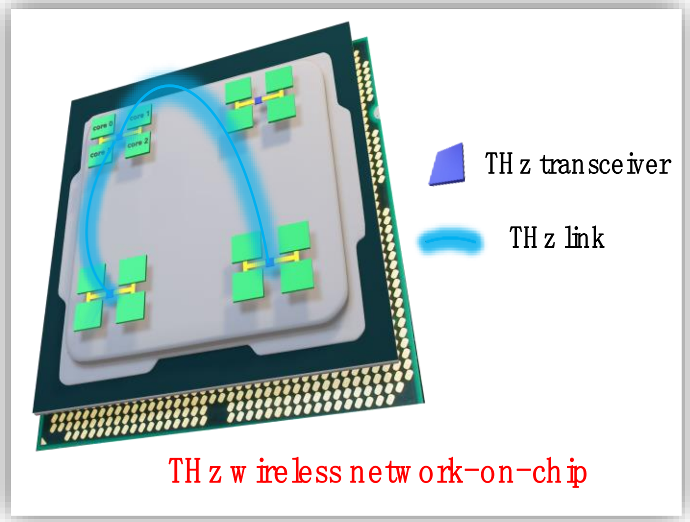


On-chip Communication

# Motivations for THz Ultra-Massive MIMO

- **Coverage challenge for THz communications**

High frequency

Short wavelength

- Large free space loss
- Large reflection and diffraction loss
- Huge molecular absorption loss

Short transmission distance

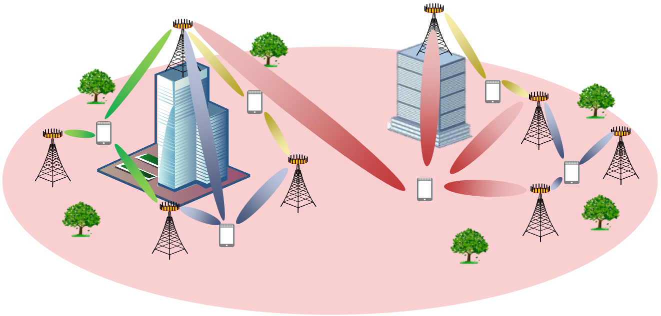

- **Solution: THz ultra-massive MIMO (UM-MIMO) systems**

Decreasing size of THz antennas → use large number of antennas to compose a large-scale antenna array, e.g., 1024 antennas

- Provide **high-speed mobile access services**
- Improve **system capacity** and **signal quality** through centralized deployment of UM-MIMO and beamforming technology
- Improves **signal coverage** and **transmission rate** through distributed deployment of UM-MIMO
- Improve the accuracy of **3D location service** and realize **spatial positioning and perception**

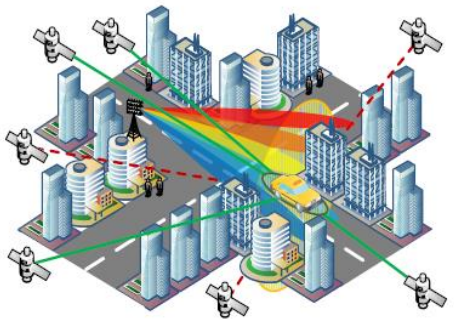

# Outline

# THz UM-MIMO Systems

Fabrication can be roughly divided into three categories:

- **Electronic-based**
  - horns, reflectors
  - cavity-backed slot antenna arrays
- **Photonics-based**
  - photo-conductive antennas
  - silicon-based lenses
- **New materials-based**
  - vanadium dioxide (VO2)
  - graphene and liquid crystal (LC)

B. Ning, Z. Tian, Z. Chen, C. Han, S. Li, J. Yuan, and R. Zhang, **"Prospective Beamforming Technologies for Ultra-Massive MIMO in Terahertz Communications: A Tutorial,"** IEEE Open Journal of the Communications Society, 2023

# Electronic approaches

- As the efficacy of electronic components is constrained in the THz band, a feasible solution is to modulate the phase in the lower frequency and then convert to the THz region

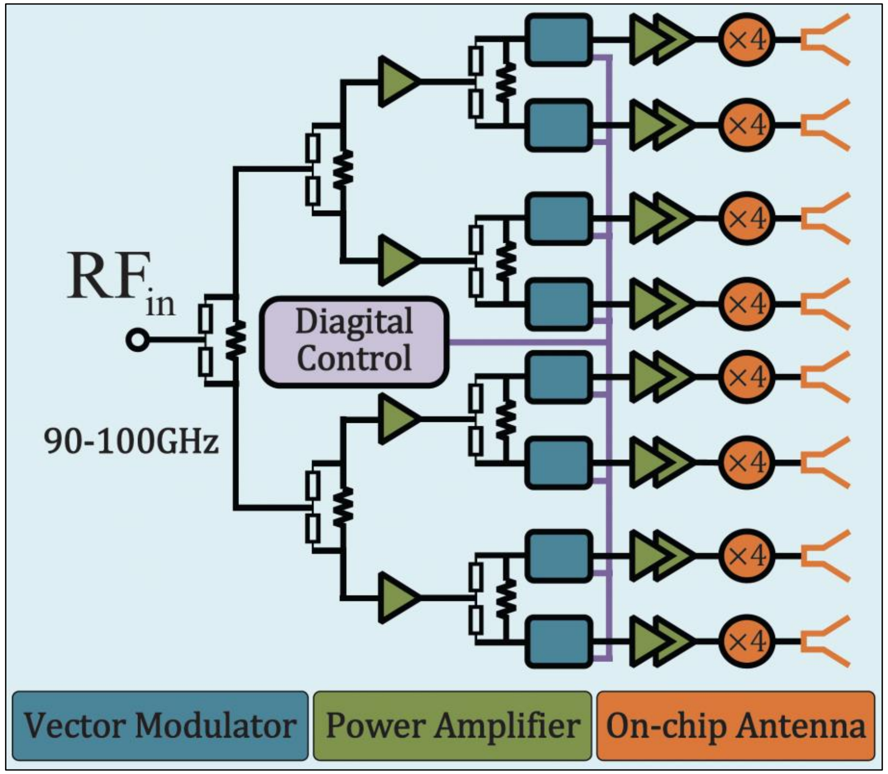


370 – 410 GHz 8 × 1 ULA



Y. Yang et al., **"An Eight-Element 370-410-GHz Phased-Array Transmitter in 45-nm CMOS SOI with Peak EIRP of 8–8.5 dBm,"** IEEE Trans. Microwave Theory Tech., vol. 64, no. 12, Dec. 2016, pp. 4241–49.

# Electronic approaches

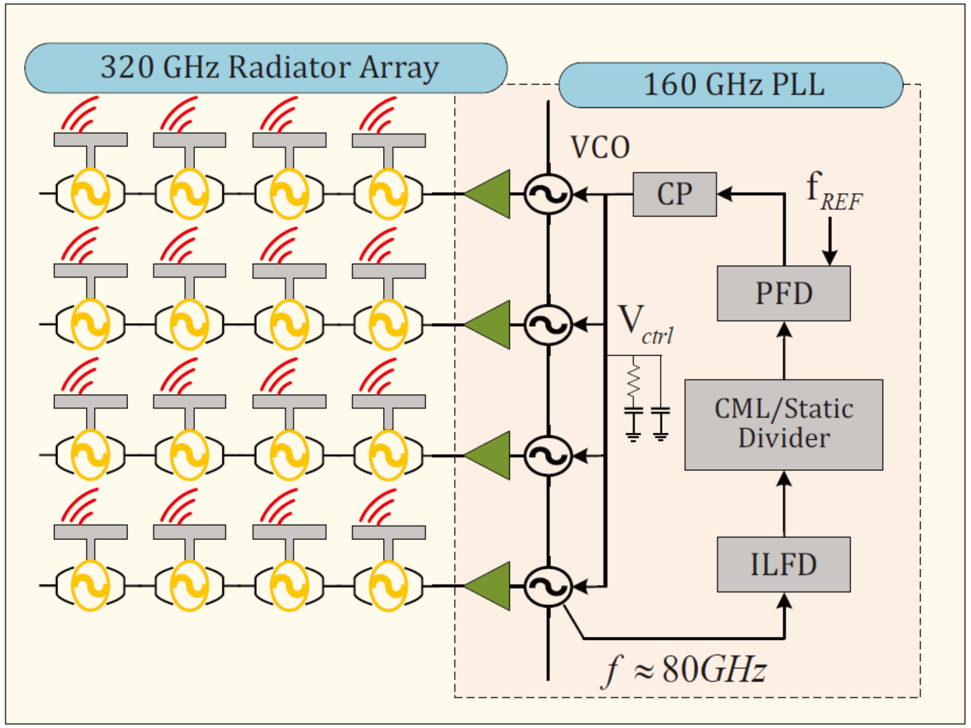


4 × 4 URPA using 130 nm SiGe bipolar-CMOS (BiCMOS) technology at 320 GHz [a]

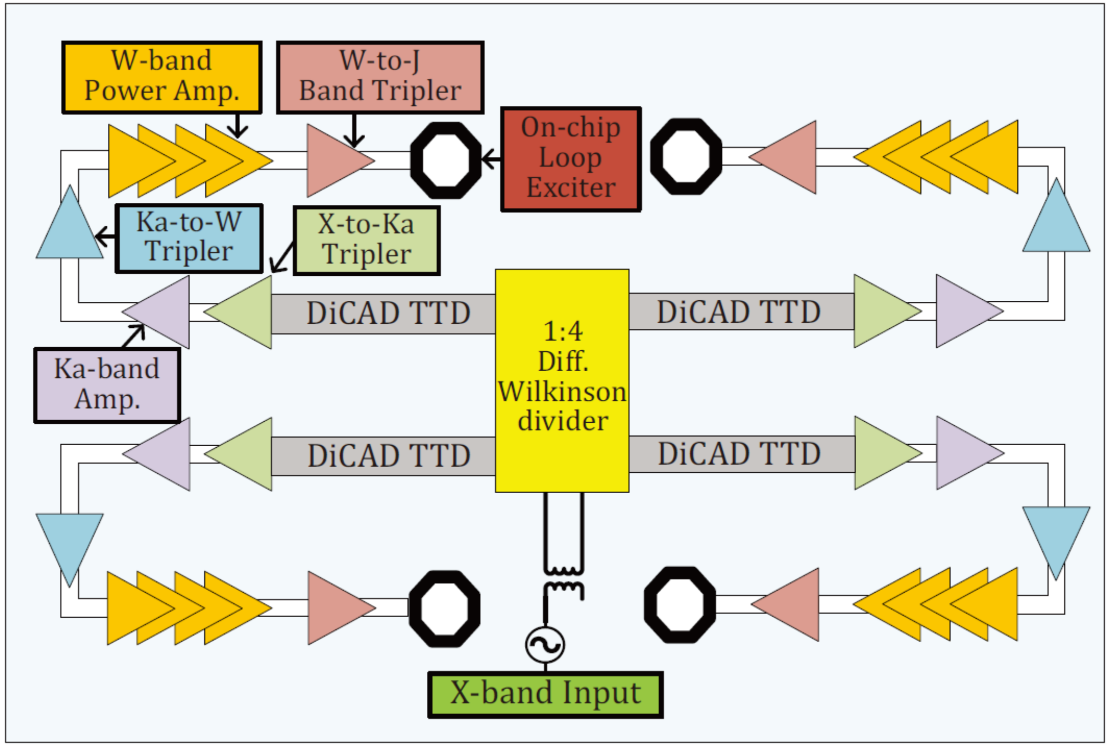


280 GHz 2 × 2 chip-scale dielectric resonator antenna array [b]


[a] R. Han et al., **"A SiGe Terahertz Heterodyne Imaging Transmitter with 3.3 mW Radiated Power and Fully-Integrated Phase-Locked Loop,"** IEEE J. Solid-State Circuits, vol. 50, no. 12, Dec. 2015, pp. 2935–47.

[b] N. Buadana et al., **"A 280-GHz Digitally Controlled Four Port Chip-Scale Dielectric Resonator Antenna Transmitter with DiCAD True Time Delay,"** IEEE Solid-State Circuits Lett., vol. 3, 2020, pp. 454–57

# Photonic approaches

In the photonic approach, schemes for THz dynamic beam scanning are designed.

- Frequency-scanning antennas can be used to control THz beam steering
- A proposed photoelectric phase shifter can control 300 GHz beam scanning within 50 degree
- The optical TTD phase shifters are also employed to offer stable time delay for wideband communications

# Photonic approaches

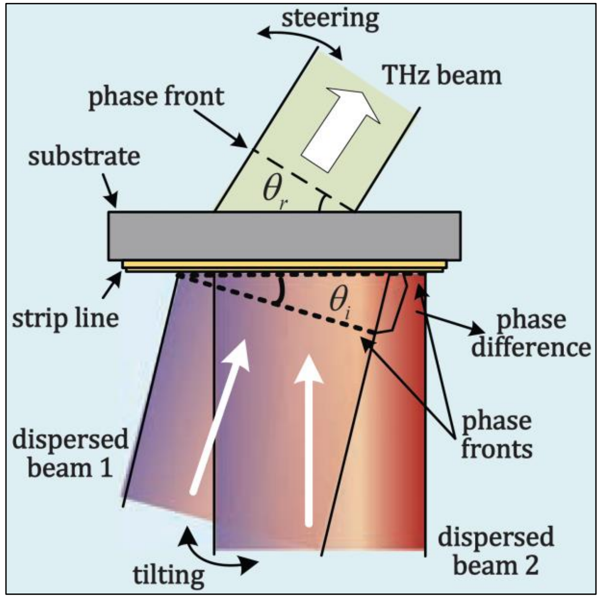


Changing the phase difference of two laser beams [a]

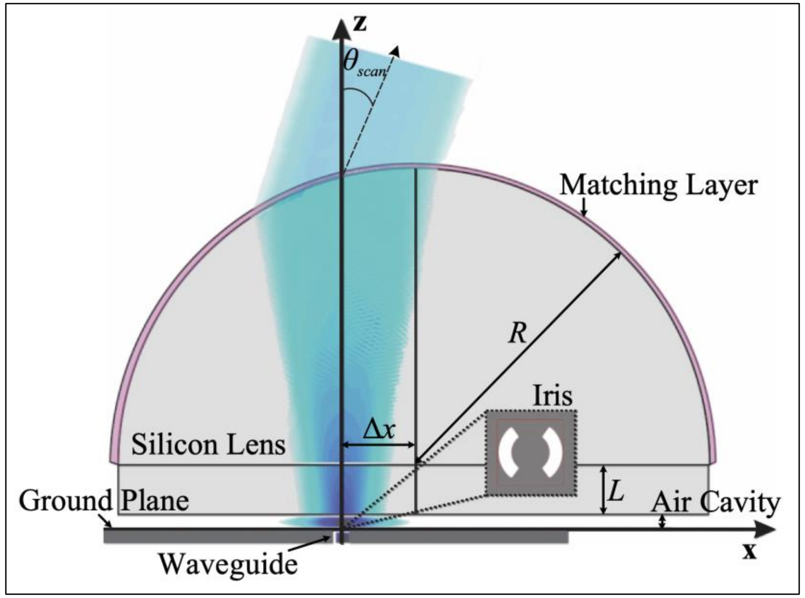


Refraction based on the optical lens antennas [b]

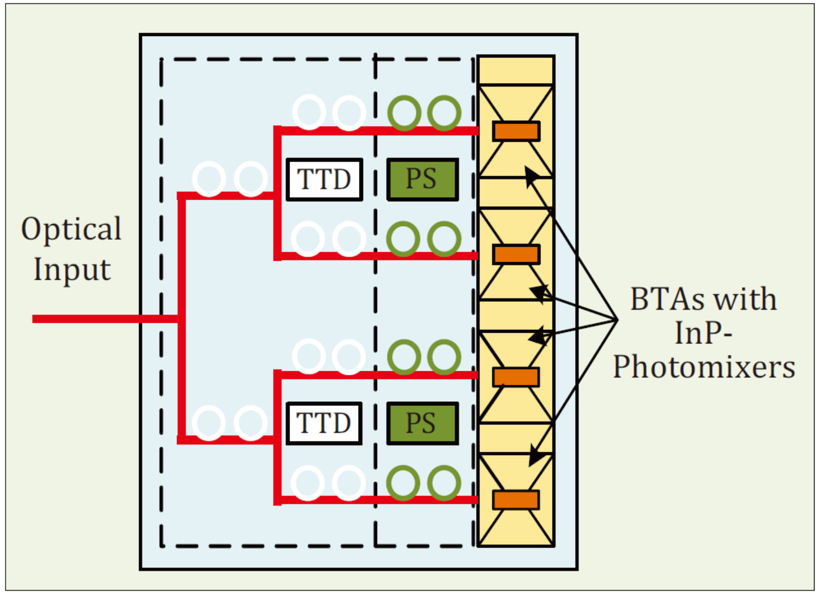


The schematic view of an optical TTD-based chip [c]

[a] K.-i. Maki and C. Otani, **"Terahertz Beam Steering and Frequency Tuning by Using the Spatial Dispersion of Ultrafast Laser Pulses,"** Opt. Express, vol. 169, July 2008, pp. 10,158–69.

[b] M. Alonso-delPino et al., **"Beam Scanning of Silicon Lens Antennas Using Integrated Piezomotors at Submillimeter Wavelengths,"** IEEE Trans. THz Sci. Tech., vol. 9, no. 1, Nov. 2019, pp. 47–54.

[c] P. Lu et al., **"Photonic Assisted Beam Steering for Millimeter- Wave and THz Antennas,"** IEEE Conf. Antenna Meas. & Appl., Sweden, 2018, pp. 1–4.

# New material approaches

- Graphene, i.e., a two-dimensional form of graphite, has attracted the attention of the scientific community due to its unique electronic and optical properties.

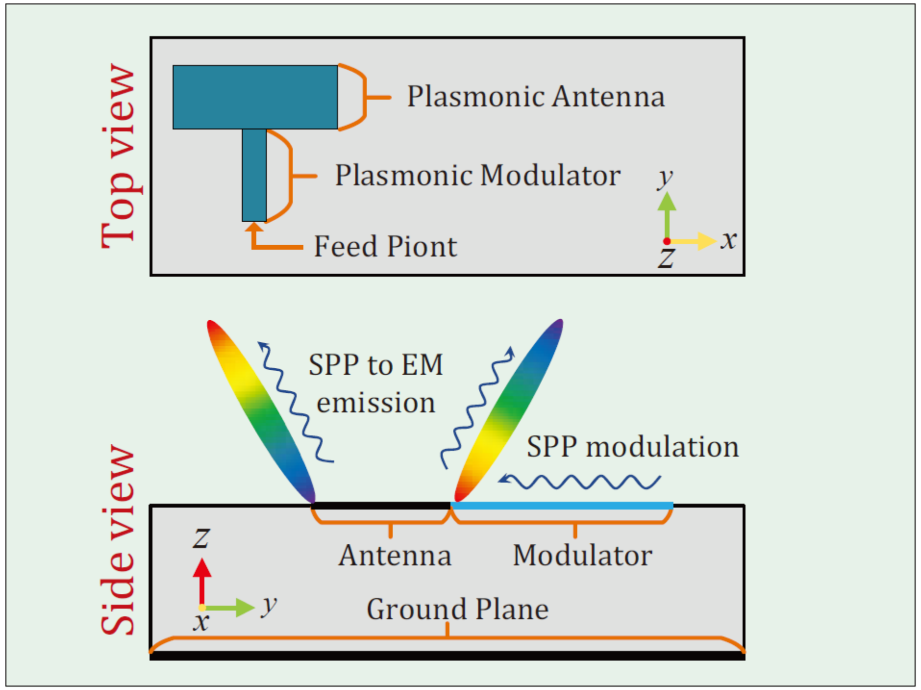


The working principle and design of the THz front end


A. Singh et al., **"Design and operation of a graphene-based plasmonic nano-antenna array for communication in the terahertz band,"** IEEE J. Sel. Areas Commun., vol. 38, no. 9, pp. 2104-2117, Sept. 2020.

# New material approaches

- Individual graphene antennas at the THz band
  - with reconfigurable radiation patterns
- Small-scale graphene antenna
  - the beam scanning range has not been piratically tested
- Reconfigurable MIMO antenna system for THz communications
- The use of graphene to implement UM-MIMO plasmonic nano-antenna arrays
  - implement a 1024×1024 UM-MIMO system at 1THz with arrays that occupy just 1 $mm^2$
- Liquid crystal and graphene also show application potential in reconfigurable reflect arrays

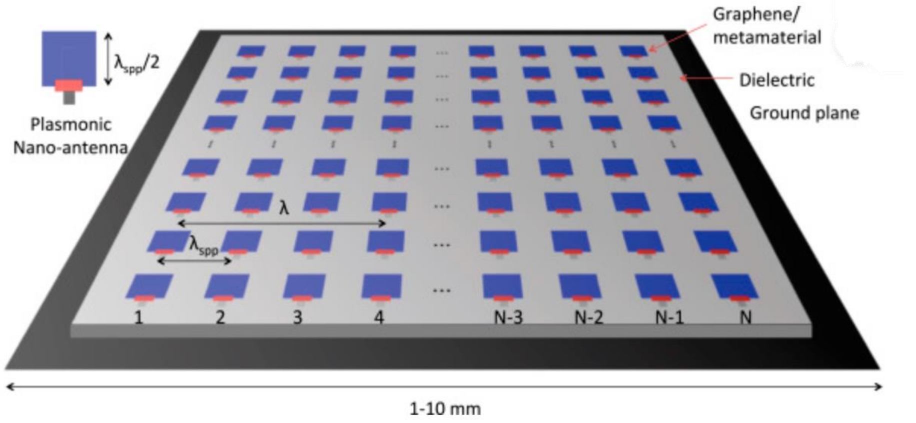


I. F. Akyildiz and J. M. Jornet, "Realizing ultra-massive MIMO (1024×1024) communication in the (0.06-10) terahertz band," Nano Commun. Networks, vol. 8, pp. 46-54, Nov. 2016.

# New material approaches

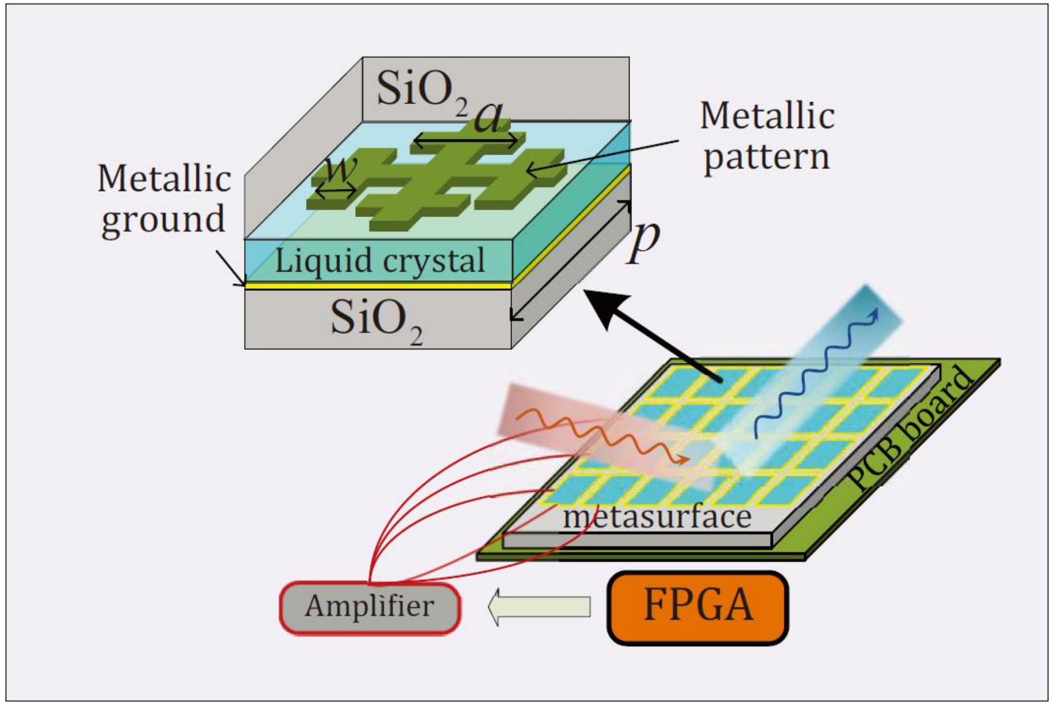


The LC reflect array at 0.67 THz

This array is made up of :

- a 24 element linear array
- each element is composed of 50 rows and 2 columns of unit cells with meta-insulator metal-resonator structure



Wu, Jingbo et al. **"Liquid crystal programmable metasurface for terahertz beam steering,"** Appl. Phys. Lett., vol. 116, no. 13, pp. 131104, 2020.

# New material approaches

- The reported THz antenna arrays with dynamic beam scanning capability

| Freq (Hz) | Size | Process | Beam scan | Gain | Antenna type |
|---|---|---|---|---|---|
| 280 G | $4 \times 4$ arrays | 45 nm SOI CMOS | 80°/80° [1] | 16 dBi | on-chip |
| 140 G | $2 \times 4$ arrays | 65 nm CMOS | 40° | - | multi-chip |
| 0.53 T | $1 \times 4$ arrays | 40 nm CMOS | 60° | 11.7 dBi | patch |
| 400 G | $1 \times 8$ arrays | 45 nm SOI CMOS | 75° | 12 dBi | patch |
| 0.34 T | $2 \times 2$ arrays | 130 nm SiGe BiCMOS | 128°/53° [1] | - | patch |
| 320 G | $1 \times 4$ arrays | 130 nm SiGe BiCMOS | 24° | 13 dBi | patch |
| 338 G | $4 \times 4$ arrays | 65 nm CMOS | 45°/50° [1] | 18 dBi | microstrip |
| 317 G | $4 \times 4$ arrays | 130 nm SiGe BiCMOS | - | 17.3 dBi | return-path gap coupler |
| 280 G | $2 \times 2$ arrays | 65 nm CMOS | 30° | 12.5 dBi | dielectric resonator |
| 300 G | $1 \times 4$ arrays | photonic | 90° | 10.6 dBi | bow-tie antenna |
| 1.05 T | $4 \times 4$ arrays | graphene | - | 13.9 dBi | dipole |
| 1.1 T | $2 \times 2$ arrays | graphene | 60° | 8.3 dBi | patch |
| 220 – 320 G | 600 elements | metallic | 48° | 28.5 dBi | frequency scanning |
| 0.8 T | $2 \times 2$ arrays | graphene | - | - | photoconductive |
| 1.3 T | 25448 elements | graphene | - | 29.3 dBi | reflectarray |
| 220 – 320 G | $8 \times 8$ arrays | brass sheets | 50°/45° [1] | 17 dBi | frequency scanning |
| 100 G | $54 \times 52$ cells | liquid crystals | 55° | 15 dBi | reflectarray |
| 345 G | - | liquid crystals | 20° | 35 dBi | reflectarray |
| 100 G | - | VO2 | 44°/44° | - | metasurfaces |
| 115 G | $39 \times 39$ cells | liquid crystals | 20° | 16.55 dBi | reflectarray |

# Device technologies

- Lesson 1: some promising fabrication techniques for implementing UM-MIMO antenna arrays have been developed in the THz range → we are almost ready
- Lesson 2: future research may focus on seeking potential solutions for better beam flexibility as well as a larger array size → we still can do better
  - Improve the dynamic beamforming capabilities of the THz arrays, including adjustment accuracy and scanning range
  - Increase the size of the antenna array and pushing it to the level of thousands of elements
  - Reduce mutual coupling effects caused by large-scale integration

# Molecular Absorption Effect

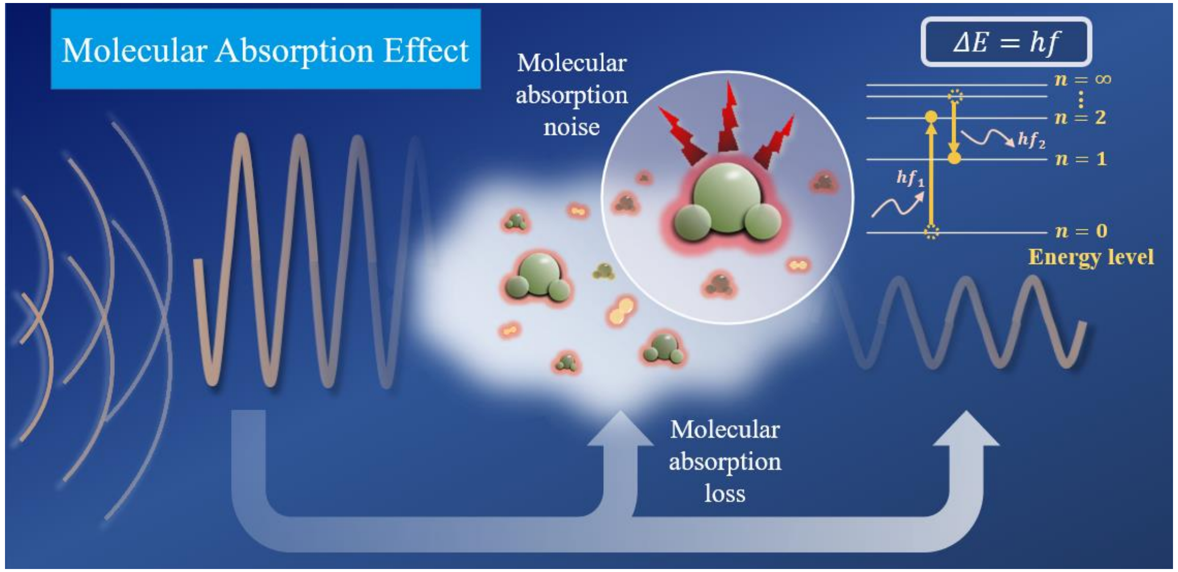


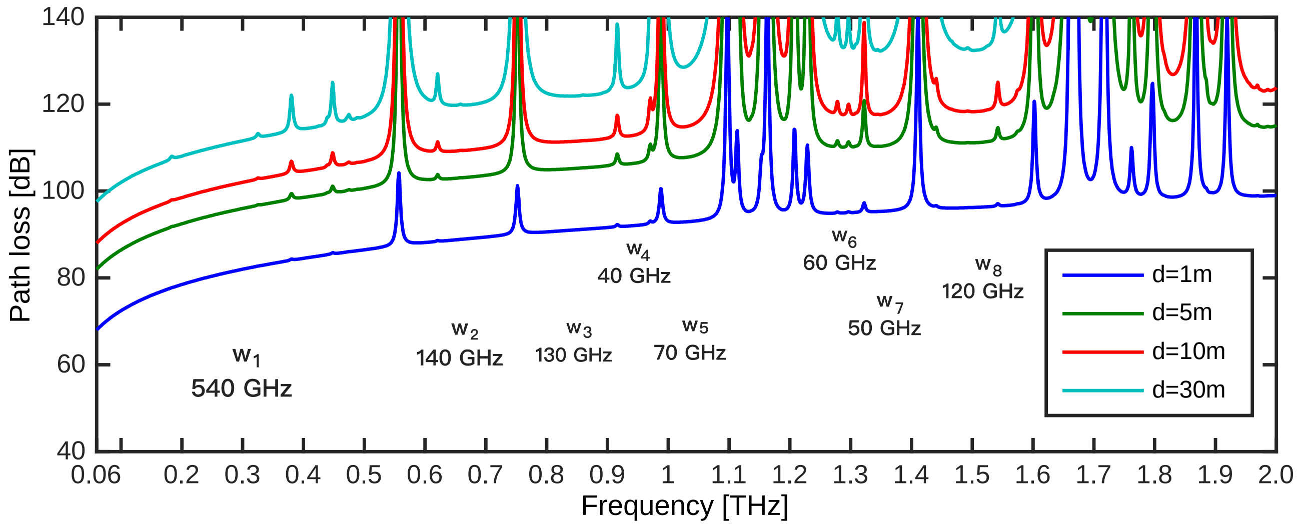


**Spectral windows created by molecular absorption effects**

**Each window has multi-GHz BW, sensitive to f, d, env.**



C. Han, W. Gao, N. Yang, and J. M. Jornet, **"Molecular Absorption Effect: A Double-edged Sword of Terahertz Communications,"** IEEE Wireless Communications, 2023

# Channel Characteristics

- Path loss exponent (PLE)
  - ➢ Larger PLEs in NLoS
  - ➢ Mostly close to 2, indicating the dominance of LoS path in the THz band (sparsity)

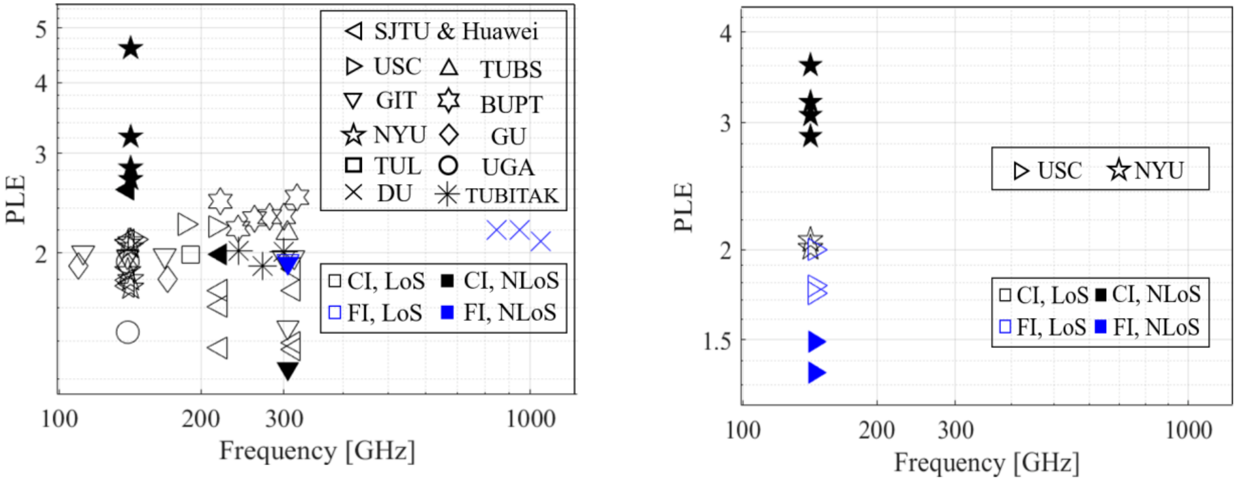


(a) Indoor scenarios (b) Outdoor scenarios

- Shadow fading (SF): additional loss caused by blockage; mostly calculated as the deviation of path loss to path loss models
  - ➢ Severer shadow fading in NLoS
  - ➢ Mostly lower than 1 in indoor scenarios

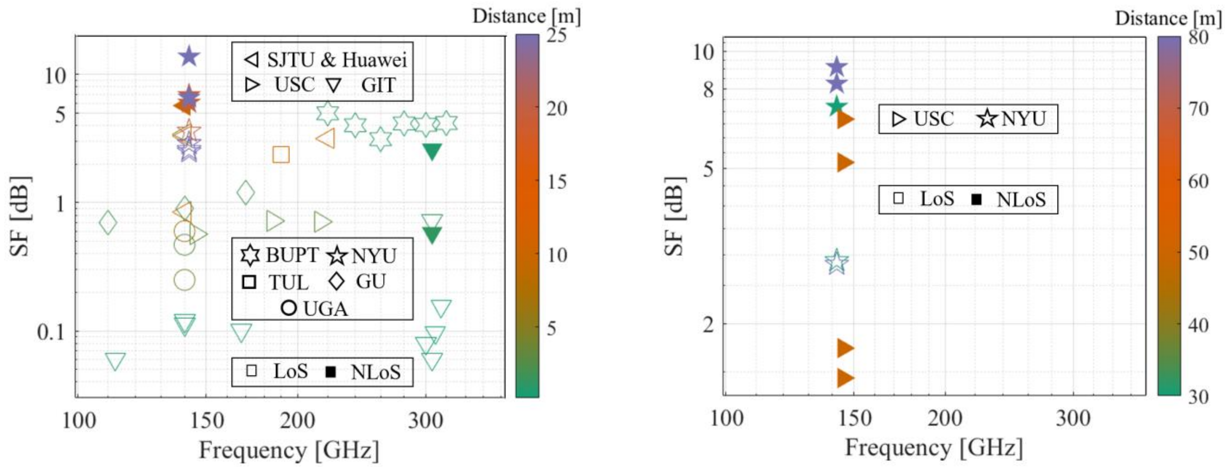


(a) Indoor scenarios (b) Outdoor scenarios

**C. Han**, Y. Wang, Y. Li, Y. Chen, N. Abbasi, T. Kurner, and A. Molisch, **"Terahertz Wireless Channels: A Holistic Survey on Measurement, Modeling, and Analysis,"** IEEE Communications Surveys and Tutorials, 2022

# Channel Characteristics

- K-factor (KF): power ratio between the strongest path and other paths
  - Generally larger KF in outdoor scenarios
  - Mostly very large in the THz band (>10 dB), indicating high sparsity

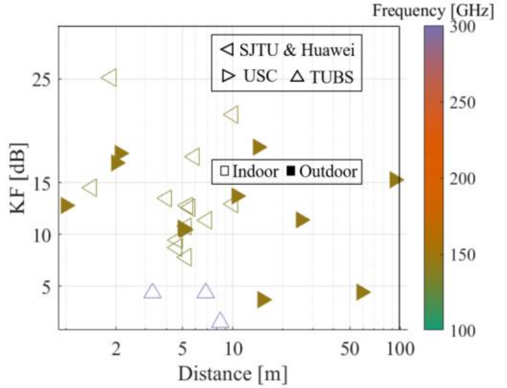


- Delay spread (DS): power dispersion in temporal domain
  - Generally larger DS in outdoor scenarios
  - Smaller DS for higher frequencies
  - Typically around 5~30 ns in indoor scenarios
  - 5-60 ns in outdoor scenarios

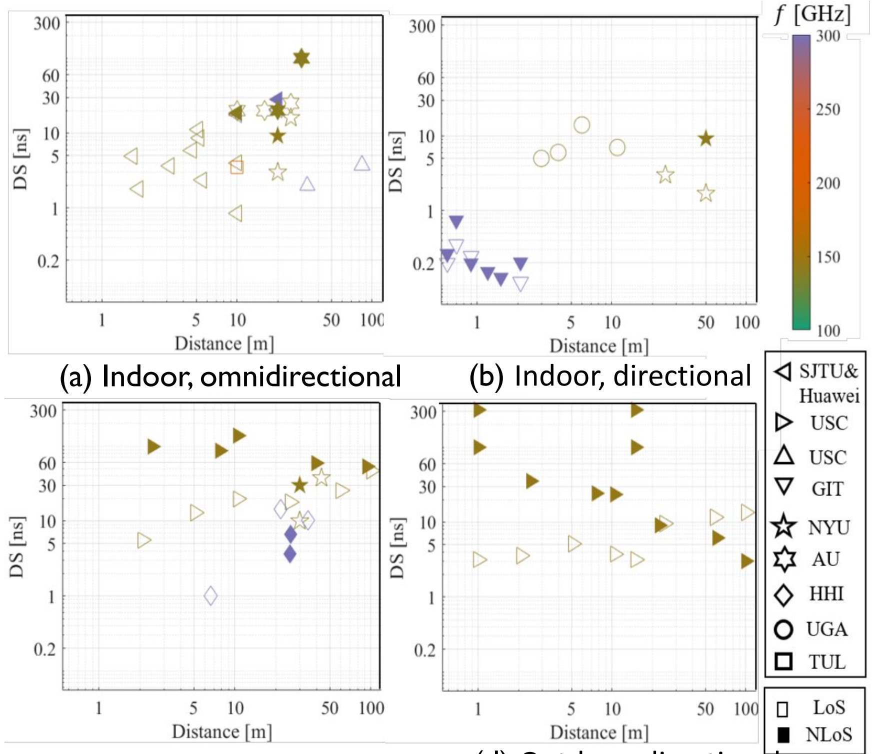

(a) Indoor, omnidirectional (b) Indoor, directional
(c) Outdoor omnidirectional (d) Outdoor, directional

# Channel Characteristic – Angular Spread

- Angular spread (AS): the power dispersion in the spatial domain
  - ➢ Close AS in indoor and outdoor scenarios
  - ➢ Typically around 10-60° for ASA and ASD

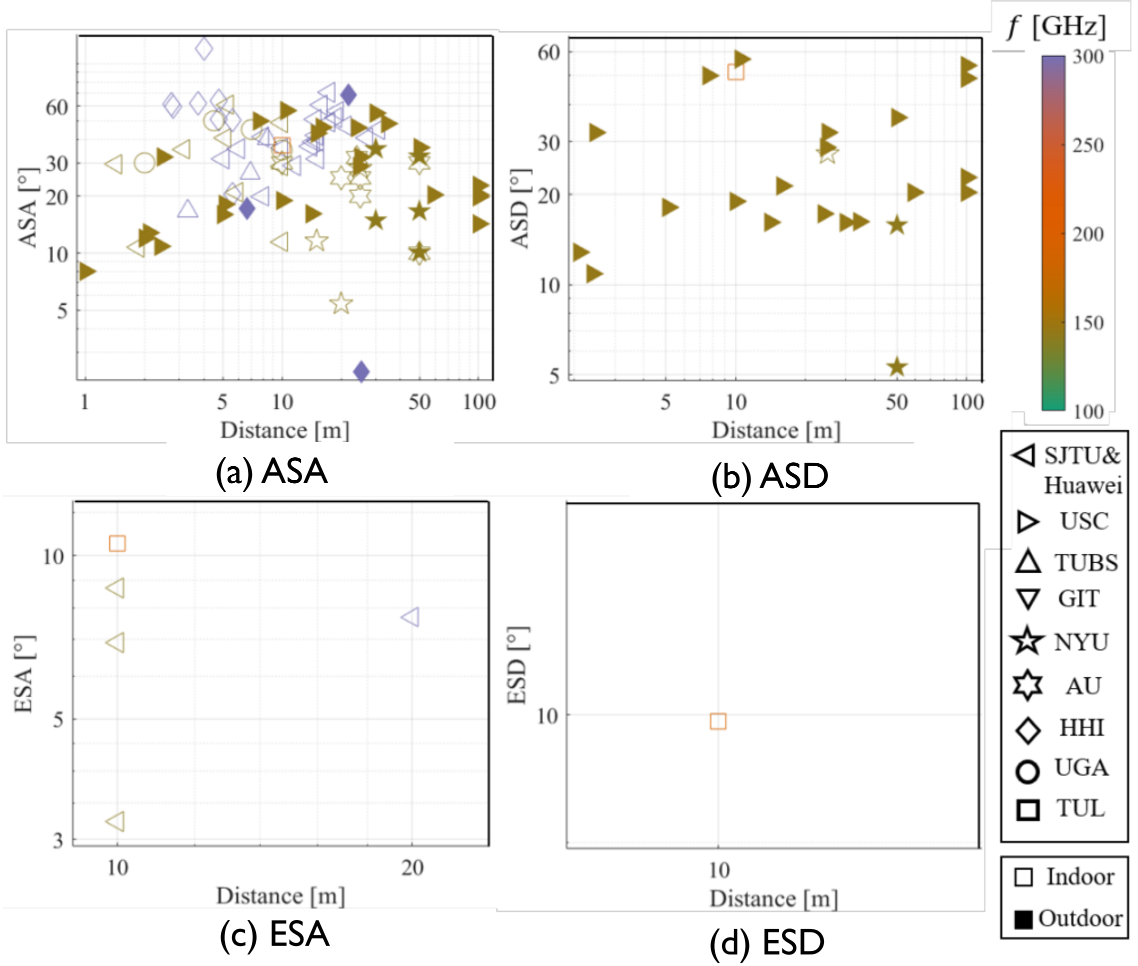

# UM-MIMO Channel Model

- **Spherical-wave propagation** is the ground truth of electromagnetic wave propagation
  - Individually calculating the channel response of all antennas pairs between Tx and Rx
  - High complexity
- **Planar-wave assumption** is a simplification of spherical-wave propagation
  - Valid in far-field communications
  - Signal transmission is approximated as parallel and the wavefront is analyzed as a plane
  - Low complexity

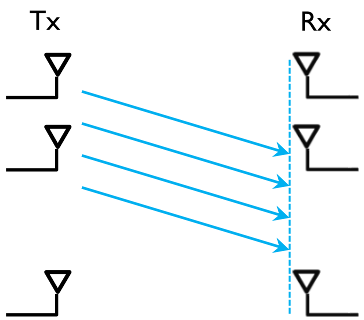


Illustration of PWM

$$\mathbf{H}_{\mathrm{P}} = \Sigma_{p=1}^{N_p} \alpha_p \mathbf{a}_{rp} \mathbf{a}_{tp}^{\mathrm{H}}$$

Neglect the non-linear phase from the spherical model

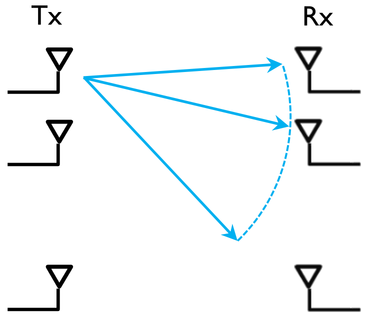


Illustration of SWM

$$\mathbf{H}_{\mathrm{S}}[n_r, n_t] = \Sigma_{p=1}^{N_p} |\alpha_p^{n_r n_t}| e^{-j\frac{2\pi}{\lambda} D_p^{n_r n_t}}$$

Chong Han, Linglong Dai, and Zhi Chen ©

# Inaccuracy of Planar-wave Channel Models

- Rayleigh distance is the classis boundary between the near-field and far-field, below which near-field propagation dominates and the planar-wave model (PWM) becomes inaccurate

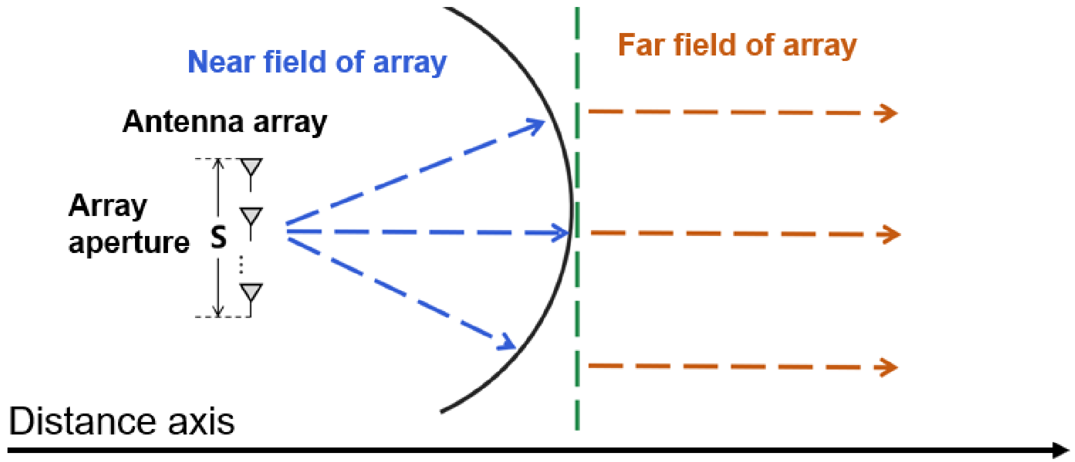


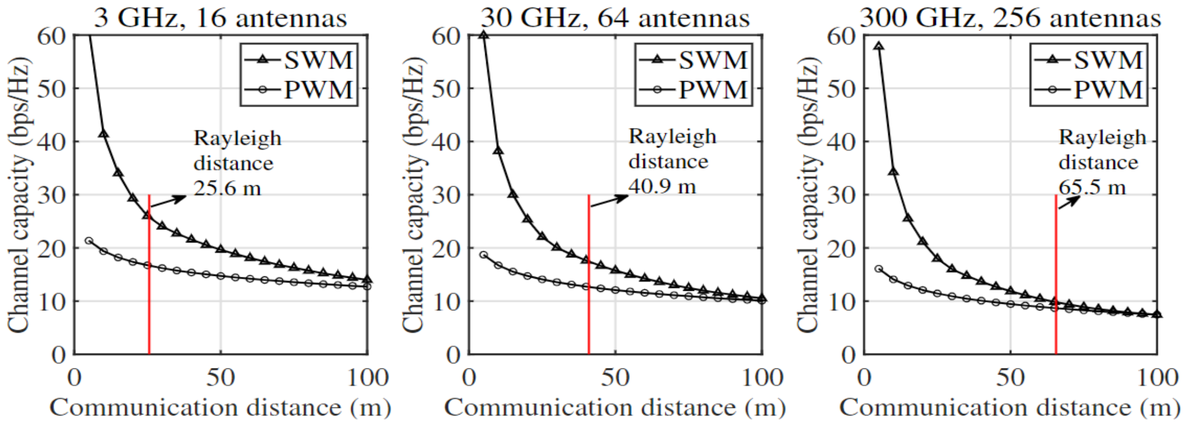


Channel capacity based on PWM and SWM in different communication distances and frequencies

**The communication distance $D \gg D_{ray}$ → Planar-wave assumption is valid**
**Otherwise, e.g., $D < D_{ray}$ → Spherical-wave propagation needs to be considered**

# Hybrid Spherical- and Planar- Wave Model

- Consider a generalized THz UM-MIMO system
  - ➢ Transmitter and receiver antennas are divided into several subarrays
- Employ PWM within one subarray
  - ➢ Remain precise due to the relatedly small array size
  - ➢ Achieve reduced complexity
- Employ SWM among subarrays
  - ➢ Improved modeling accuracy

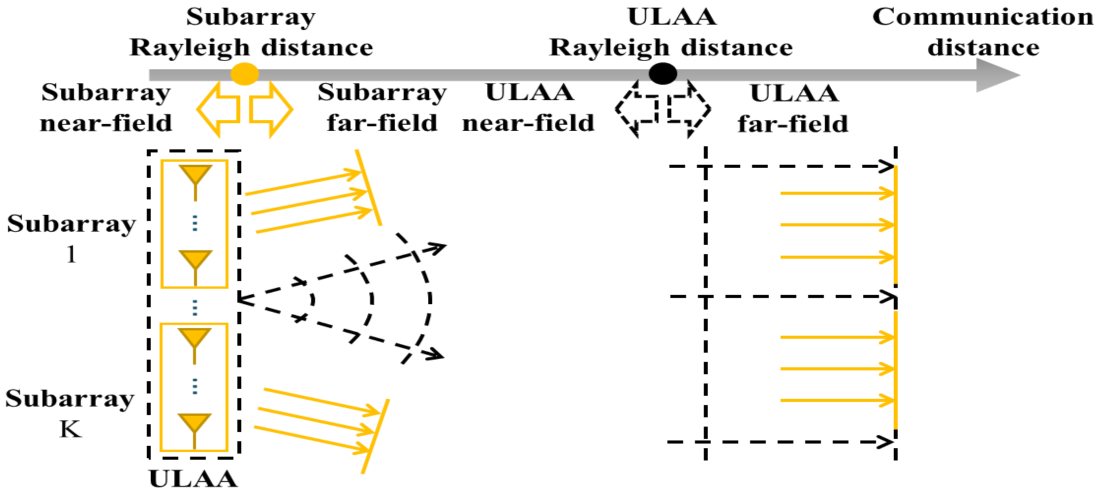


$$\mathbf{H}_{\mathrm{HSPM}} = \sum_{p=1}^{N_p} \begin{bmatrix} \alpha_p^{11}\mathbf{a}_{rp}^{11}(\mathbf{a}_{tp}^{11})^{\mathrm{H}} & \cdots & \alpha_p^{11}\mathbf{a}_{rp}^{1K_t}(\mathbf{a}_{tp}^{1K_t})^{\mathrm{H}} \\ \vdots & \ddots & \vdots \\ \alpha_p^{11}\mathbf{a}_{rp}^{K_r1}(\mathbf{a}_{tp}^{K_r1})^{\mathrm{H}} & \cdots & \alpha_p^{11}\mathbf{a}_{rp}^{K_rK_t}(\mathbf{a}_{tp}^{K_rK_t})^{\mathrm{H}} \end{bmatrix}$$

HSPM channel matrix

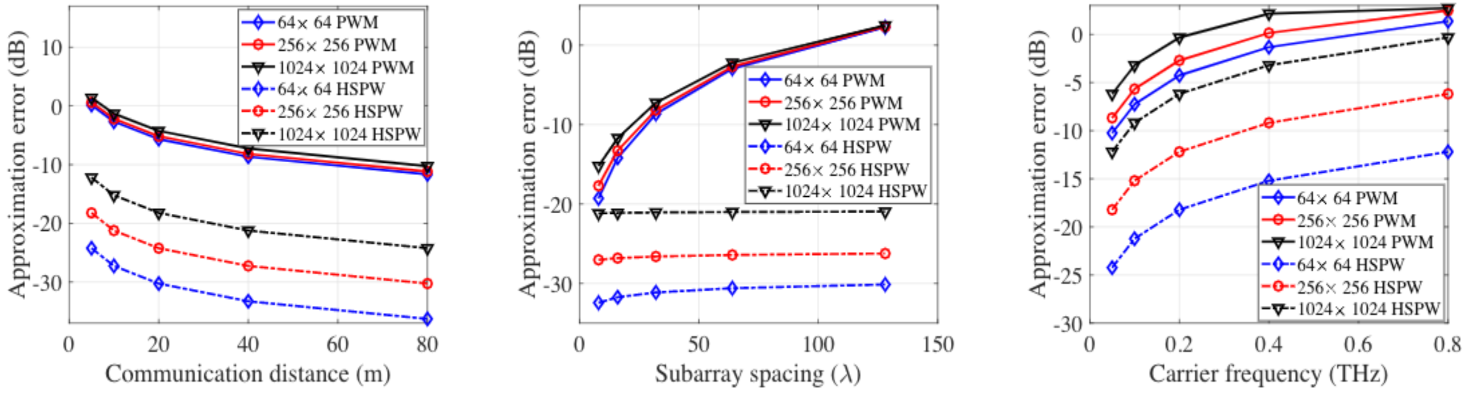


Y.-H. Chen, Longfei Yan and C. Han*, **"Hybrid Spherical- and Planar-Wave Modeling and DCNN-powered Estimation of Terahertz Ultra-massive MIMO Channels,"** IEEE Transactions on Communications, 2021.

# UM-MIMO Channel Estimation

## DCNN parameter estimation of reference subarray

- Fifteen-layer DCNN structure
- Training labels:
  - Spherical-wave channel parameters:
    Angles, communication distance,
    amplitude of channel gain
- Loss function: $L_{loss} = \iota_1 L_{angle} + \iota_2 L_{dist} + \iota_3 L_{gain}$

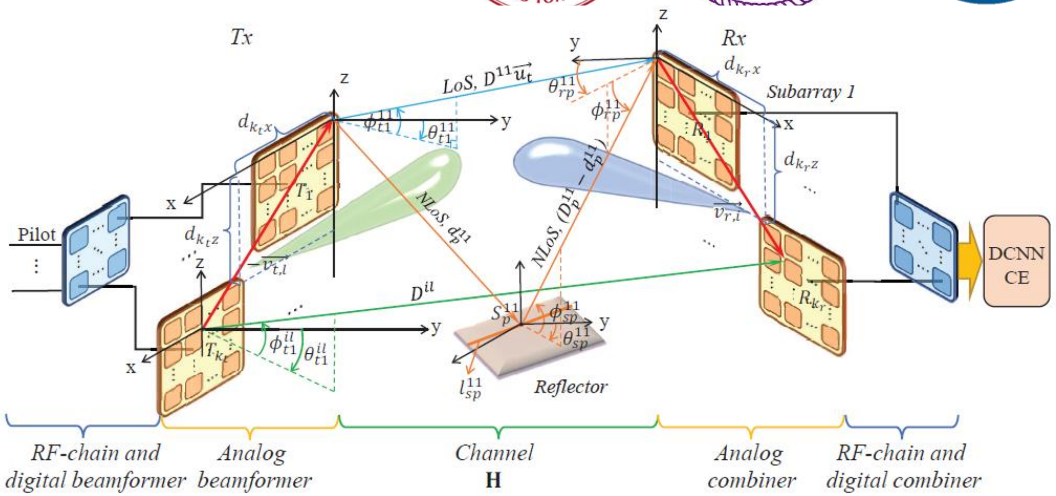


System model and channel estimation block diagram

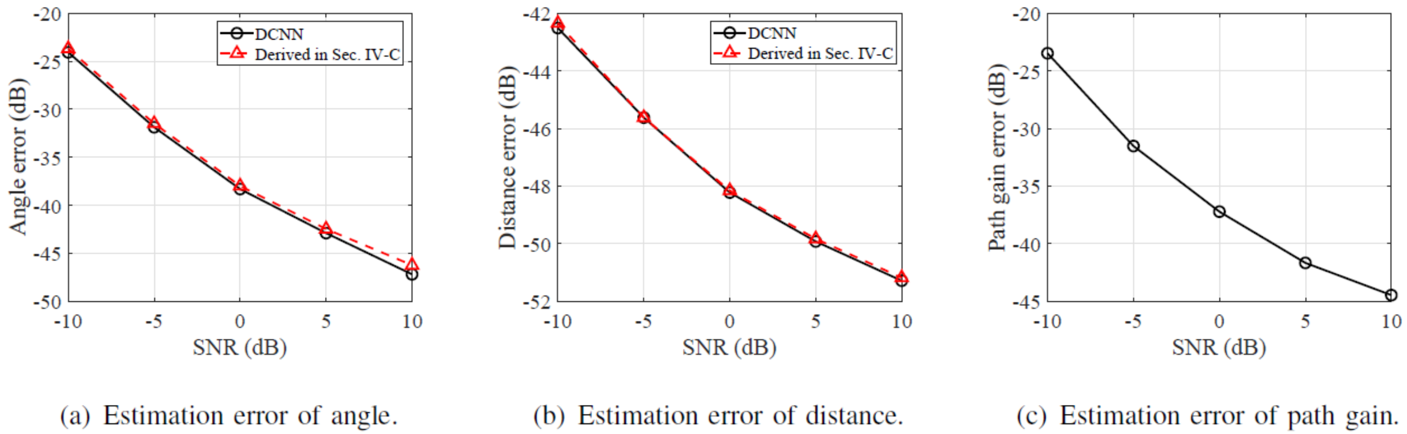


(a) Estimation error of angle. (b) Estimation error of distance. (c) Estimation error of path gain.

Channel parameter estimation accuracy of DCNN method

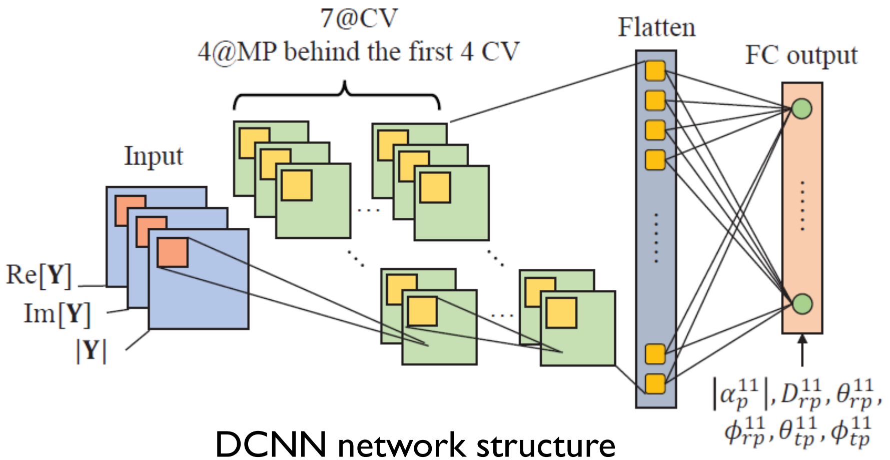


DCNN network structure



Y.-H. Chen, Longfei Yan and C. Han*, **"Hybrid Spherical- and Planar-Wave Modeling and DCNN-powered Estimation of Terahertz Ultra-massive MIMO Channels,"** IEEE Transactions on Communications, 2021.

# Geometric-based Hierarchical Channel Recovery

- **Instead of estimating for each antenna or each subarray, we propose geometric-based hierarchical channel recovery**
  - ➢ Employ the geometric relationships between channel parameters among subarrays

$$\theta_t^{k_t k_r} = \arccos\left(\frac{D_{xy}^{11}\cos\theta_t^{11}}{D_{xy}^{k_t k_r}}\right),$$

$$\theta_r^{k_t k_r} = \theta_r^{11} + \arcsin\left(\frac{\Delta d_x \cos\theta_t^{11}}{D_{xy}^{k_t k_r}}\right),$$

$$\phi_t^{k_t k_r} = \arccos\left(\frac{D_{yz}^{11}\cos\phi_{t1}^{11}}{D_{yz}^{k_t k_r}}\right),$$

$$\phi_r^{k_t k_r} = -\phi_r^{11} + \arcsin\left(\frac{\Delta d_z \cos\phi_{t1}^{11}}{D_{yz}^{k_t k_r}}\right),$$

$$D^{k_t k_r} = \frac{D_{yz}^{k_t k_r}}{\cos\theta_{t1}^{k_t k_r}} = \frac{D_{xy}^{k_t k_r}}{\cos\phi_{t1}^{k_t k_r}}.$$

Geometric relationship derivation

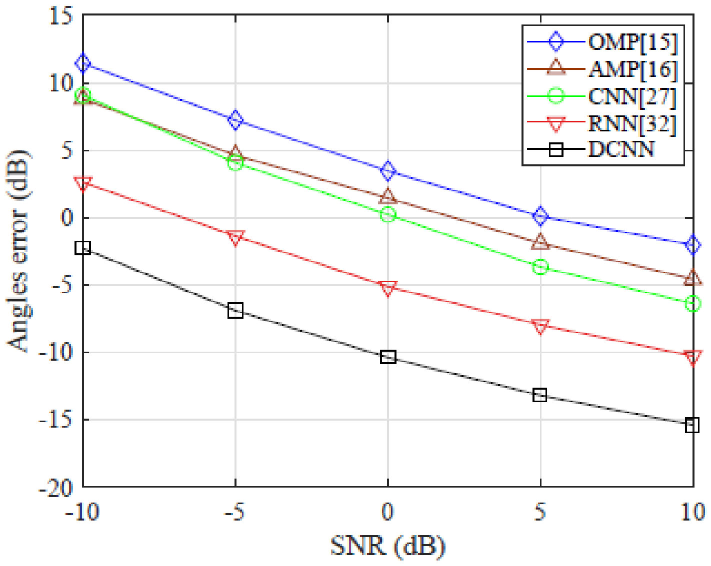


Estimation NMSE performance comparison

**Algorithm 1: DCNN for Channel Estimation**

**Input:** $\mathbf{Y}$

1. Obtain $\{|\alpha_p^{11}|, D_p^{11}, \theta_{rp}^{11}, \phi_{rp}^{11}, \theta_{tp}^{11}, \phi_{tp}^{11}\}$ by DCNN.
2. **for** $k_t = 1, ..., K_t - 1$
3.     **for** $k_r = 1, ..., K_r - 1$
4.         Calculate LoS channel parameters by (28).
5.         Calculate NLoS channel parameters by (31).
6.     **end for**
7. **end for**
8. Reconstruct $\mathbf{H}$ in (10)

**Output:** $\mathbf{H}$

DCNN channel estimation algorithm

# Outline

# Beamforming Technologies by Architectures

- **Fully-analog beamforming [1960s]:** One RF chain connects to all antennas

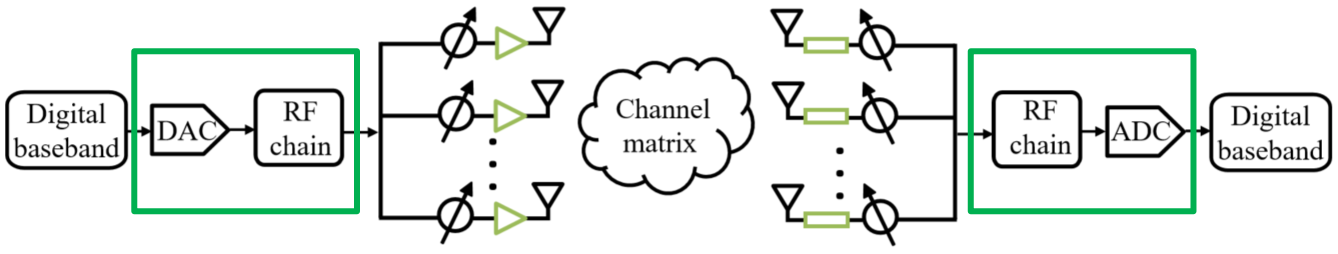


(b) Fully-analog beamforming architecture

- **Pros:** Only one RF chain and DAC/ADC → Low complexity
- **Cons:** Can not support multiple data streams→ Poor spectral efficiency

- **Fully-digital beamforming [1980s]:** Each RF chain connects to each antenna

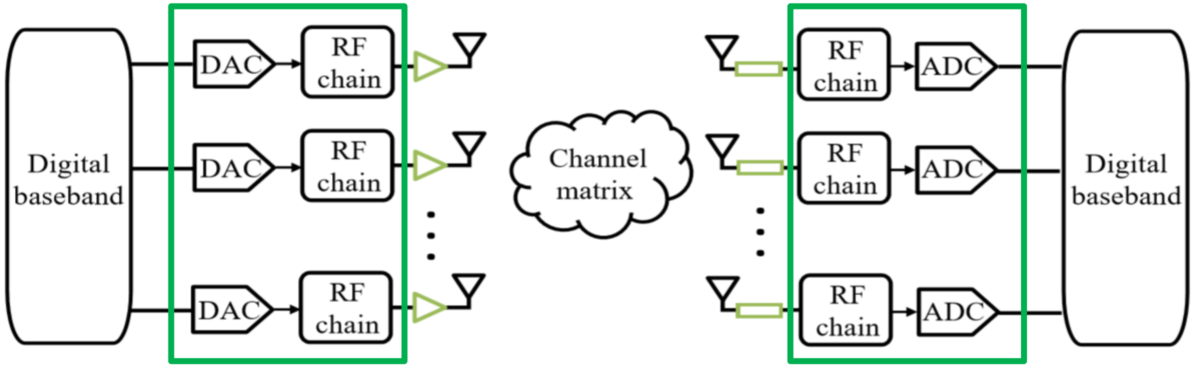


(a) Fully-digital beamforming architecture

- **Pros:** Optimal spectral efficiency
- **Cons:** Too many RF chains and DAC/ADCs → High hardware complexity and power consumption

R. W. Bickmore, **"Adaptive antenna arrays,"** IEEE Spectrum, vol. 1, no. 8, pp. 78-88, Aug. 1964.

J. Winters, **"On the capacity of radio communication systems with diversity in a Rayleigh fading environment,"** IEEE Journal on Selected Areas in Communications, pp. 871–878, Jun. 1987.

# Hybrid Beamforming

- **A more tractable solution: Hybrid beamforming**

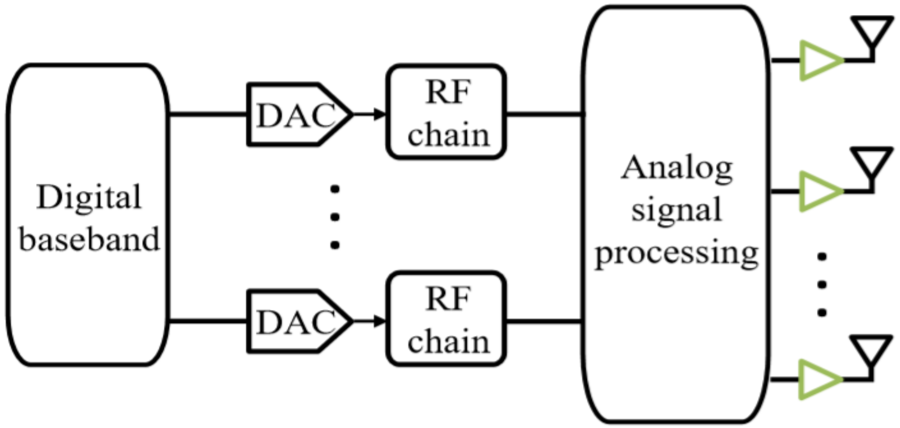


- Number of RF chains is much less than the number of antennas
  - **Few high-cost devices**, e.g., RF chains and DAC/ADCs
  - **Large number of low-cost devices**, e.g., phase shifters
- Combine the advantages of both the fully-digital and fully-analog beamforming
  - **Near-optimal** spectral efficiency and **relatively low** hardware complexity and power consumption

Two connection relationships between RF chains and antennas

fixed connection → Fixed hybrid beamforming

dynamic connection → Dynamic hybrid beamforming

C. Han, L. Yan, and J. Yuan, **"Hybrid Beamforming for Terahertz Wireless Communications: Challenges, Architectures, and Open Problems,"** IEEE Wireless Communications, 2021.

# Fixed Hybrid Beamforming

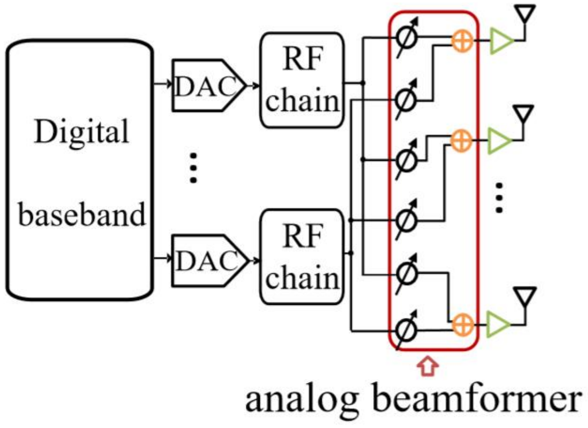


(a) Fully-connected (FC) [2014]

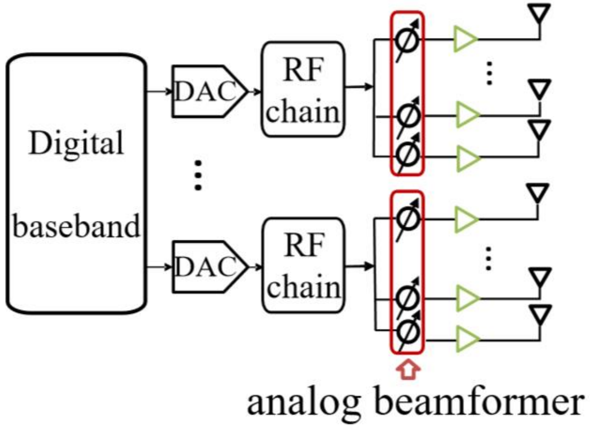


(b) Array-of-subarray (AoSA) [2015]

FC: Each RF chain connects to each antenna through a phase shifter

AoSA: Each RF chain only connects to a subset of antennas through phase shifters

| | FC | AoSA |
|---|---|---|
| Connection between RF chains and antennas | Full | Partial |
| Spectral efficiency | High | Low |
| Power consumption | High | Low |

***Both the FC and AoSA hybrid beamforming can not balance the spectral efficiency and power consumption***

***Dynamic architectures are needed!***


O. E. Ayach, S. Rajagopal, S. Abu-Surra, Z. Pi and R. W. Heath, **"Spatially Sparse Precoding in Millimeter Wave MIMO Systems,"** IEEE Transactions on Wireless Communications, vol. 13, no. 3, pp. 1499-1513, Mar. 2014.

S. Han, C. -I. I, Z. Xu and C. Rowell, **"Large-scale antenna systems with hybrid analog and digital beamforming for millimeter wave 5G,"** IEEE Communications Magazine, vol. 53, no. 1, pp. 186-194, Jan. 2015.


Chong Han, Linglong Dai, and Zhi Chen ©

# Dynamic Hybrid Beamforming

**Key idea:** Inserting switches between RF chains and phase shifters to control the connections

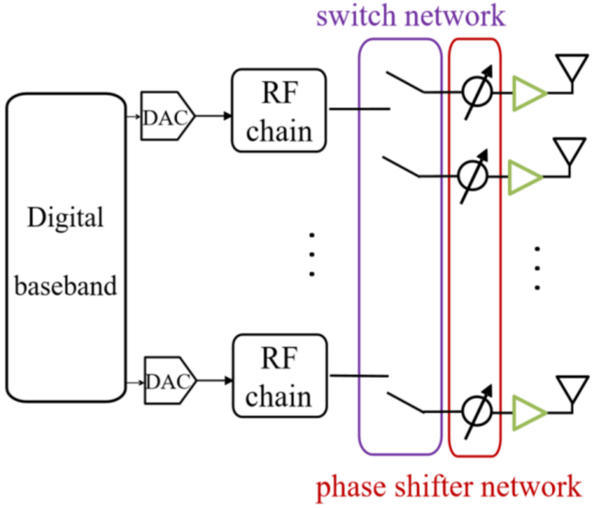


(a) Dynamic-subarray (DS) [2017]

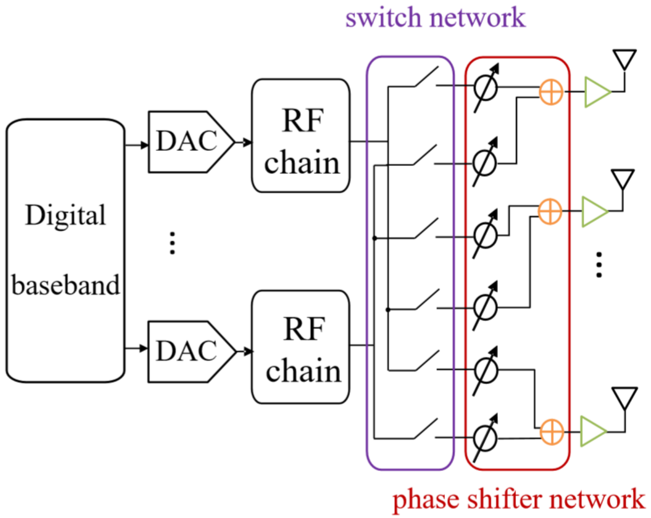


(b) Fully-adaptive-connected (FAC) [2020]

- Switch is a **low-cost** device which only has 2 states, i.e., on and off
  - **Switch on** → Closed circuit → Phase shifter is **active** and **contributes to the spectral efficiency**
  - **Switch off** → Open circuit → Phase shifter is **inactive** and **does not consume power**
- **Control the state of switch** to adjust the spectral efficiency and power consumption

S. Park, A. Alkhateeb and R. W. Heath, **"Dynamic Subarrays for Hybrid Precoding in Wideband mmWave MIMO Systems,"** IEEE Transactions on Wireless Communications, vol. 16, no. 5, pp. 2907-2920, May 2017.

X. Xue, Y. Wang, L. Yang, J. Shi and Z. Li, **"Energy-Efficient Hybrid Precoding for Massive MIMO mmWave Systems With a Fully-Adaptive-Connected Structure,"** IEEE Transactions on Communications, vol. 68, no. 6, pp. 3521-3535, Jun. 2020.

# Challenges of THz Beamforming

- **Very high path loss**
  - Distance limitation → **Beamforming is critical**
- **Very strong channel sparsity**
  - Limited number of multi-paths → Limited spatial multiplexing gains
- **Large multipath K factor**
  - Line-of-sight (LoS) dominance → Inter-intra-spatial multiplexing and blockage
- **Very large antenna array**
  - Many antennas, phase shifters, RF chains → Hardware and energy efficiency
  - Phase front fluctuation → Spherical-wave or planar-wave propagation
  - Wideband over large bandwidth → Beam squint/split mitigation

C. Han, L. Yan, and J. Yuan, **"Hybrid Beamforming for Terahertz Wireless Communications: Challenges, Architectures, and Open Problems,"** IEEE Wireless Communications, 2021.

# Outline

# Near-field and Far-field

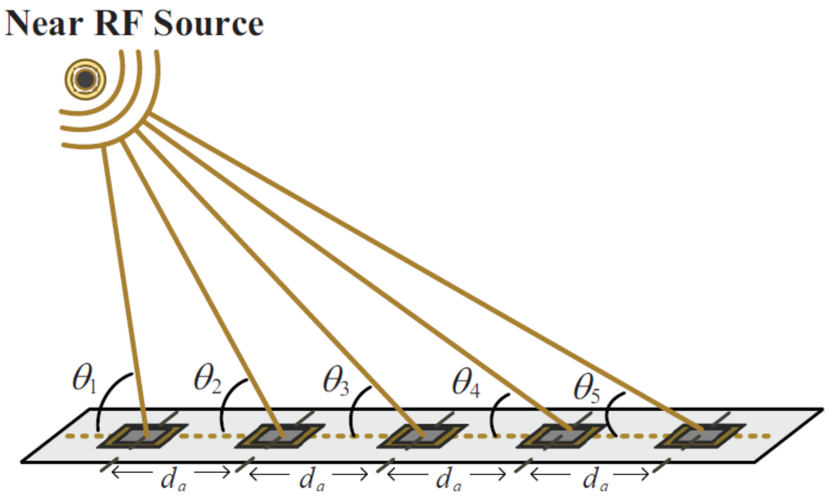


$$\theta_1 \neq \theta_2 \neq \theta_3 \neq \theta_4 \neq \theta_5$$

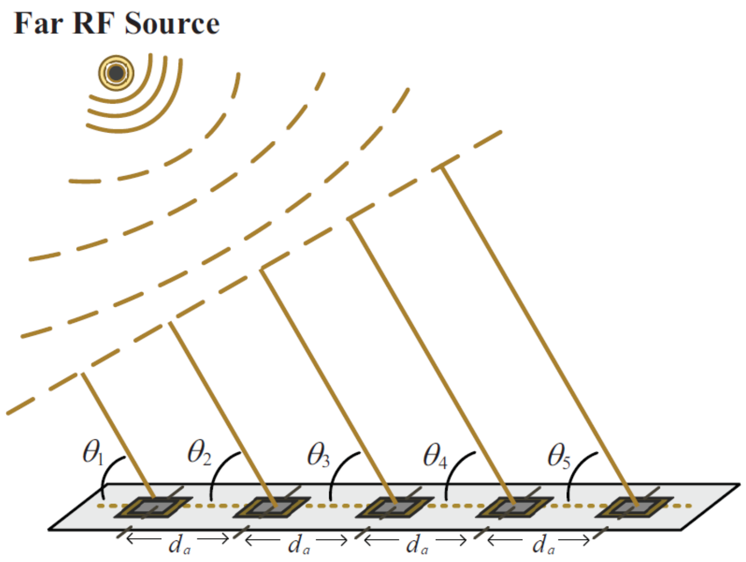


$$\theta_1 = \theta_2 = \theta_3 = \theta_4 = \theta_5 = \theta$$

**Array Response Vector：**

$$\mathbf{a}(\theta_1,\theta_2,\theta_3,\theta_4,\theta_5) = [e^{j\frac{2\pi R}{\sin\theta_1\lambda}}, e^{j\frac{2\pi R}{\sin\theta_2\lambda}}, \dots, e^{j\frac{2\pi R}{\sin\theta_5\lambda}}]^T$$

$$\mathbf{a}(\theta) = [1, e^{j\pi\cos\theta}, \dots, e^{j4\pi\cos\theta}]^T$$

The operation complexity of far-field beamforming is low

# Far-field Array Response

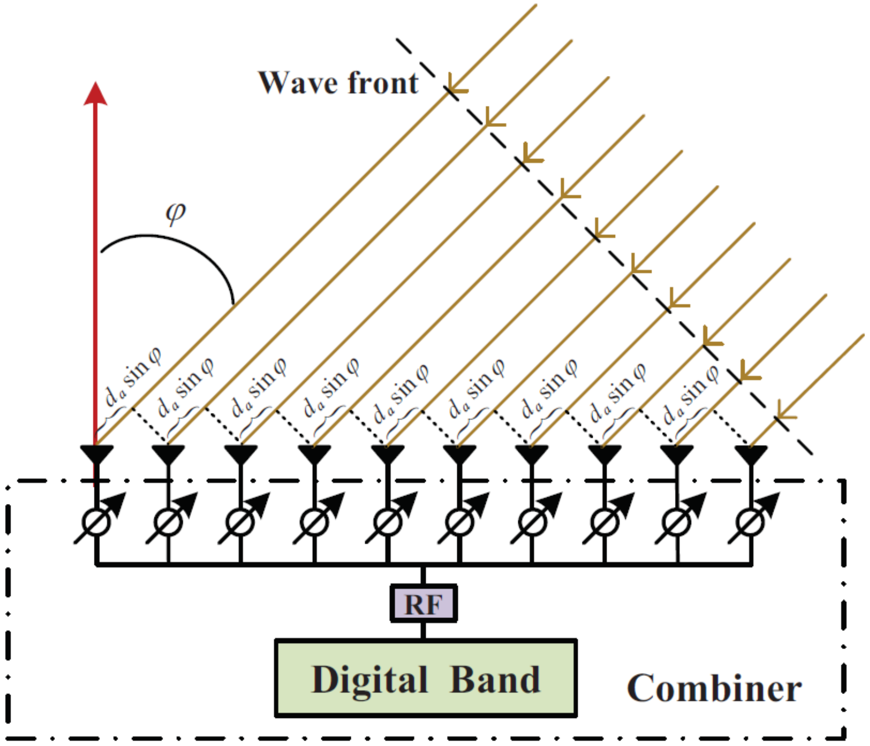


**Using array response vector to receive**

**For far-field beamforming, the phase difference between adjacent antennas is the same, and the array response vector can be written as**

$$\mathbf{a}_r(\varphi) = \frac{1}{\sqrt{N_r}}\left[1, e^{-jkd_a \sin\varphi}, \ldots, e^{-jkd_a(N_r-1)\sin\varphi}\right]^T$$

The combiner is optimized to maximize the resulting power, i.e.,

$$\max_{\mathbf{w}} \left|\mathbf{w}^H \mathbf{a}_r(\varphi)\right|^2$$
$$\text{s.t.} \quad |\mathbf{w}(i)| = \frac{1}{\sqrt{N_r}}, \quad i = 1, 2, \ldots, N_r.$$

It is easy to verify that an optimal solution is given by

$$\mathbf{w} = \mathbf{a}_r(\varphi),$$

# Far-field Beam Pattern

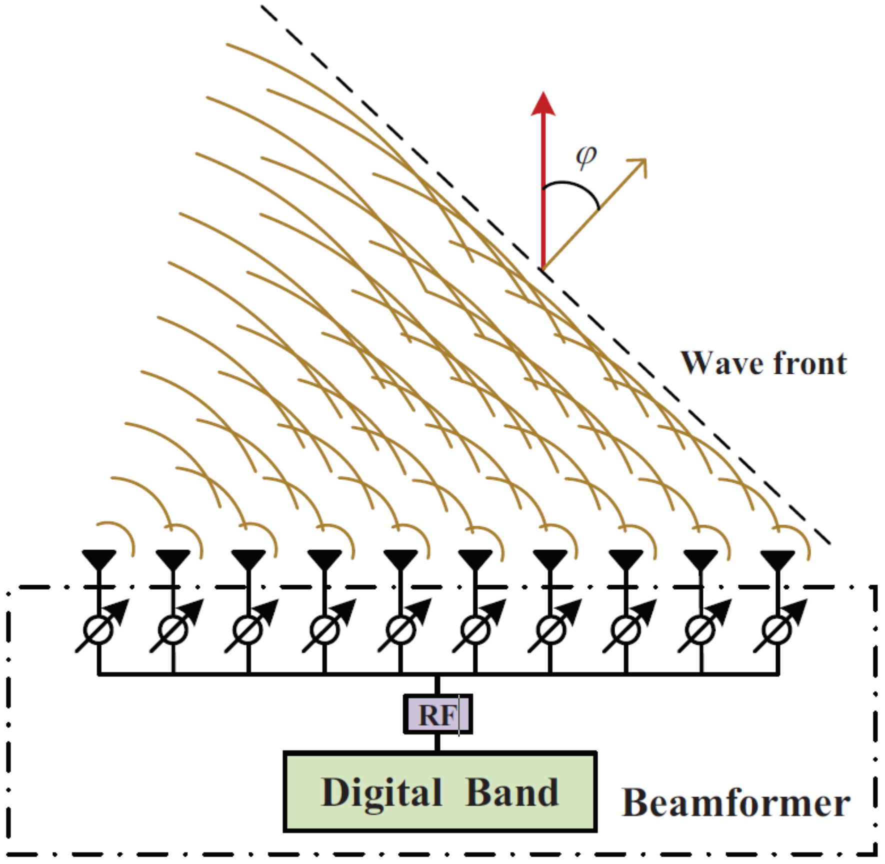


**Using array response vector to transmit**

We have known that using array response vector as a combiner can maximize the received power with AoA φ.

On the contrary, if we use array response vector as a beamformer/precoder, the wavefront moves in the direction of AoD φ.

The radiation beam pattern of array response vector:

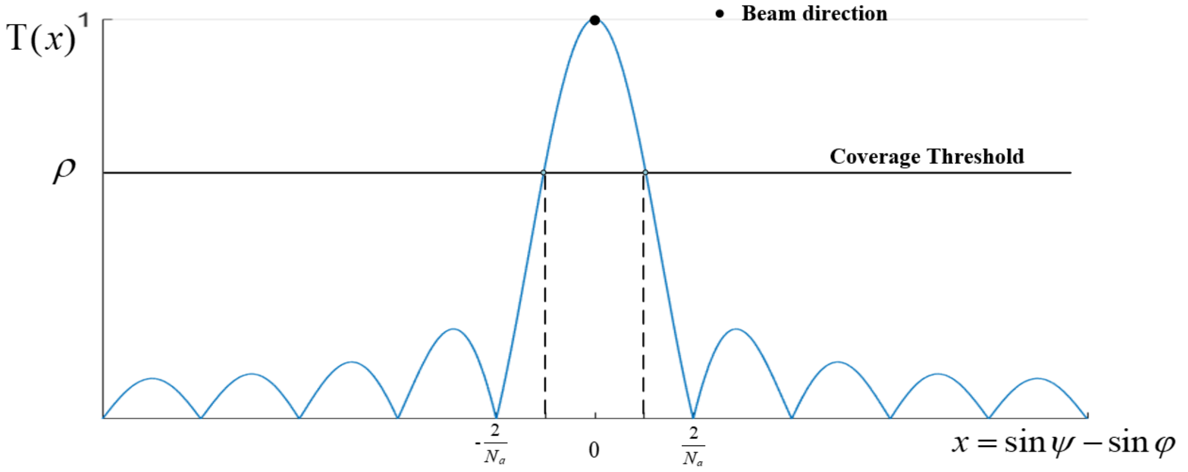


**Thus, the array response vector can be regarded as a narrow beam covering a certain zone.**

# Far-field Codebook

We can **predefine a codebook** that includes many antenna response vectors representing the narrow beams corresponding to different AoAs/AoDs.

$$\mathcal{F} = \{\mathbf{a}(\varphi_1), \mathbf{a}(\varphi_2), ..., \mathbf{a}(\varphi_N)\},$$

**Some Properties of the narrow beams:**

**Lemma 1.** *Beams within* $[-\frac{\pi}{2}, \frac{\pi}{2}]$ *and beams within* $[\frac{\pi}{2}, \frac{3\pi}{2}]$ *are isomorphic for ULA. In particular, the narrow beam in direction of* $\varphi$ *is equivalent to that in direction of* $\pi - \varphi$*, i.e.,*

$$\mathbf{a}(\varphi) = \mathbf{a}(\pi - \varphi).$$

Moreover, the beam is **narrower** with the AoA/AoD around 0 and is **wider** with the AoA/AoD around ±π/2.

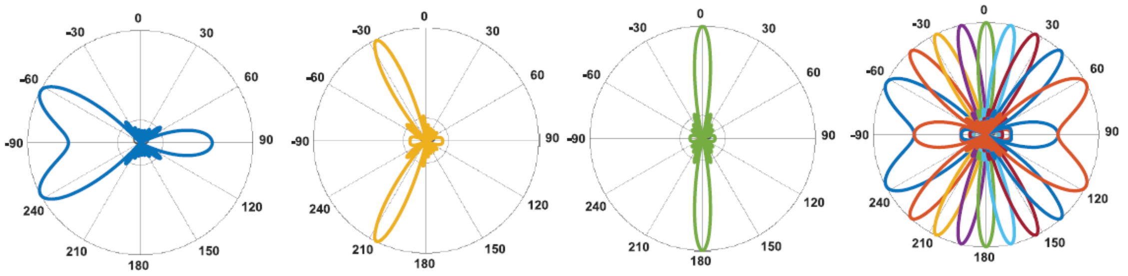

(a)

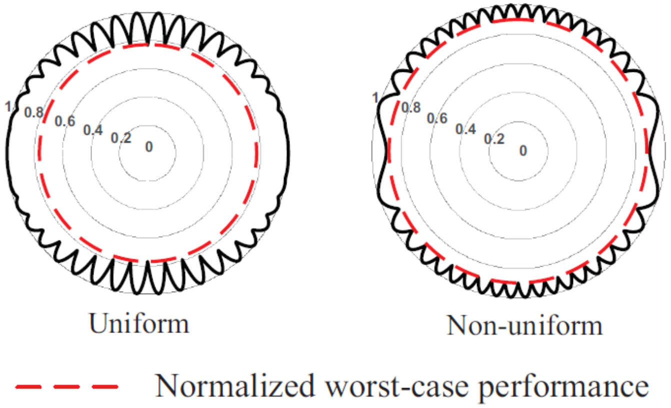


(b)

The codebook with **non-uniformly distributed beams** may achieve **a higher worst-case performance** than that with uniformly distributed beams

# Far-field Codebook

## How many narrow beams we need in a codebook?

Generally, the number of beams N required in the codebook is proportional to the number of array antennas Na.

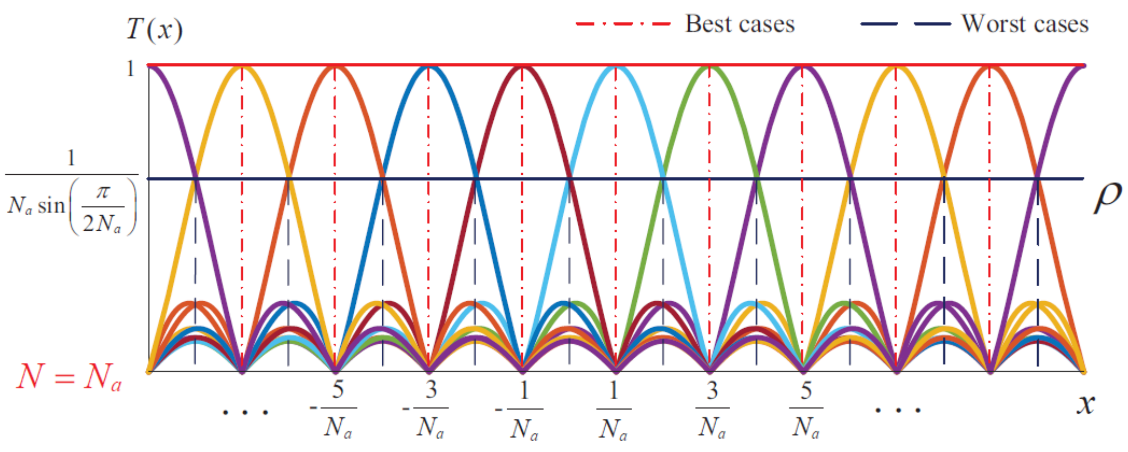


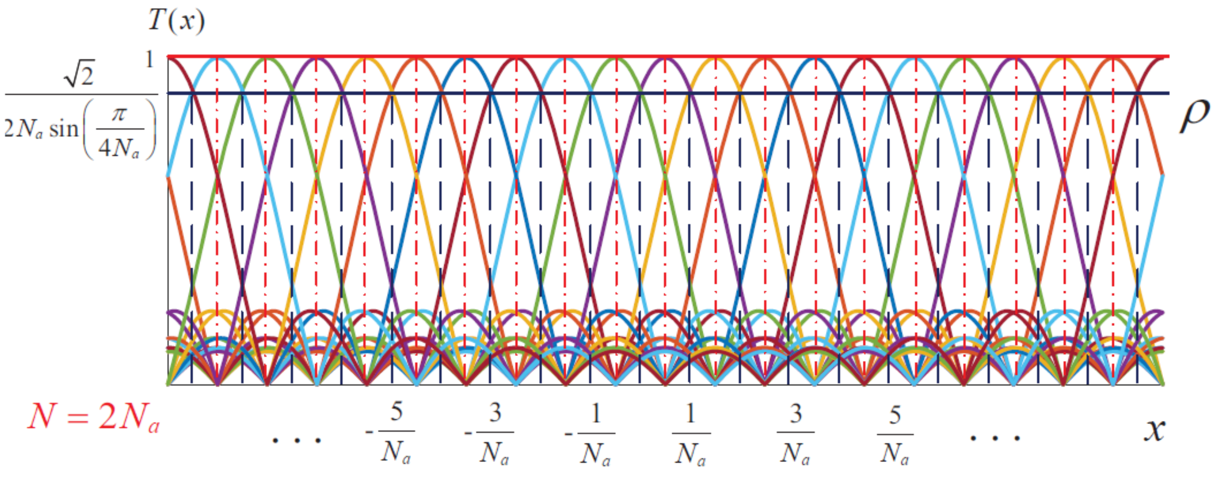


The normalized worst-case performance of the above two cases is given by

$$\frac{1}{N_a \sin\left(\frac{\pi}{2N_a}\right)}, \qquad N = N_a \qquad\qquad \frac{\sqrt{2}}{2N_a \sin\left(\frac{\pi}{4N_a}\right)}, \qquad N = 2N_a$$

# Far-field Codebook

## How many narrow beams we need in a codebook?

Thus, the numbers of narrow beams in the UM-MIMO THz systems **is much larger** than that in conventional MIMO systems, which incurs difficulty in beam alignment and management.

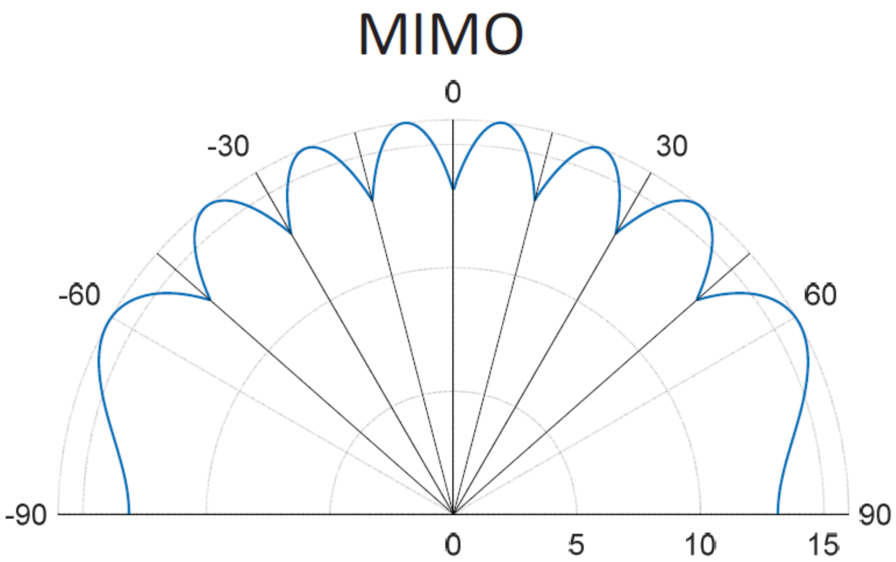


$N_a = 16$

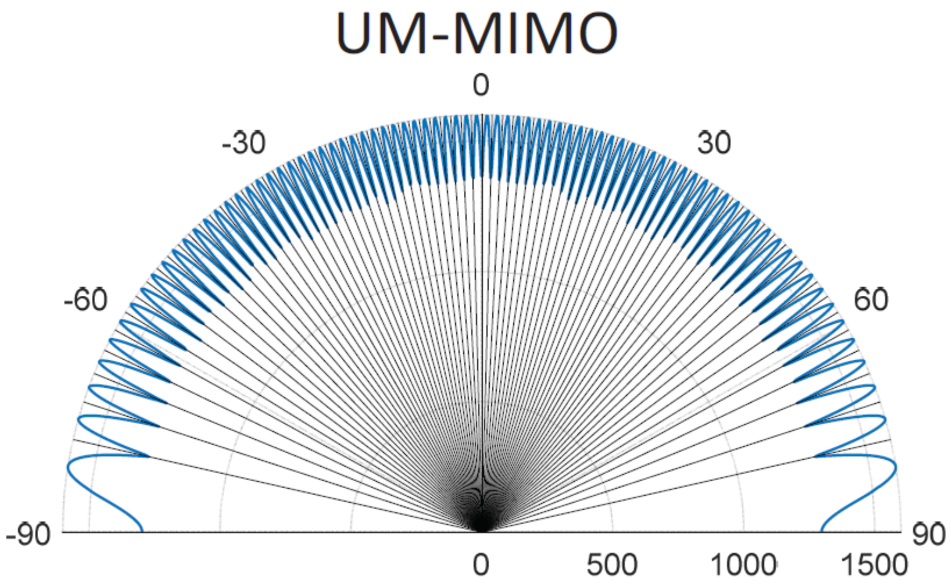


$N_a = 1600$

## 3D beamforming

3D beamforming allows higher transmission gain and stronger directivity for THz communication to provide large-capacity and less-interference multiple access.

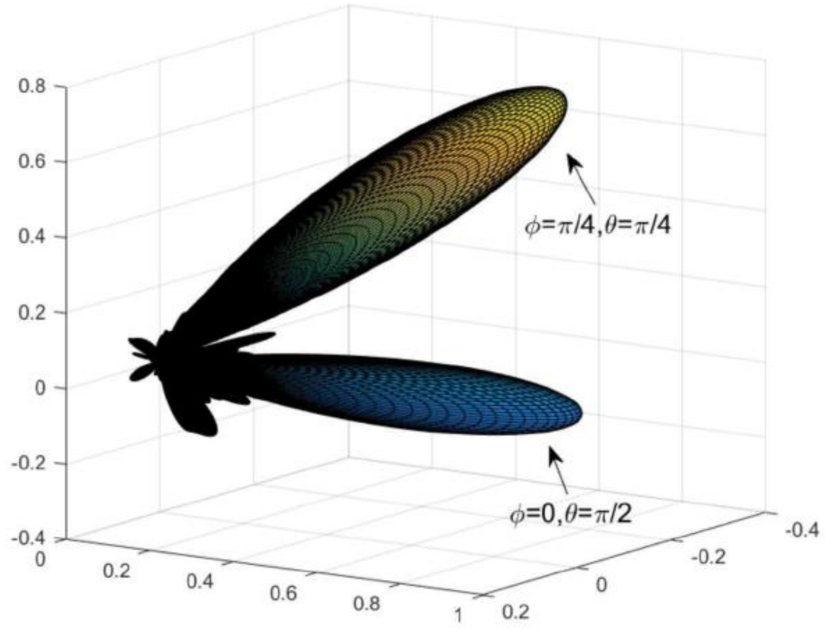


This feature will help the connection management of a large number of air targets (e.g. cellular-connected drones) in the future air-ground integrated wide-area coverage network.

# Far-field Beamforming

## Quadruple-UPA (QUPA) architecture

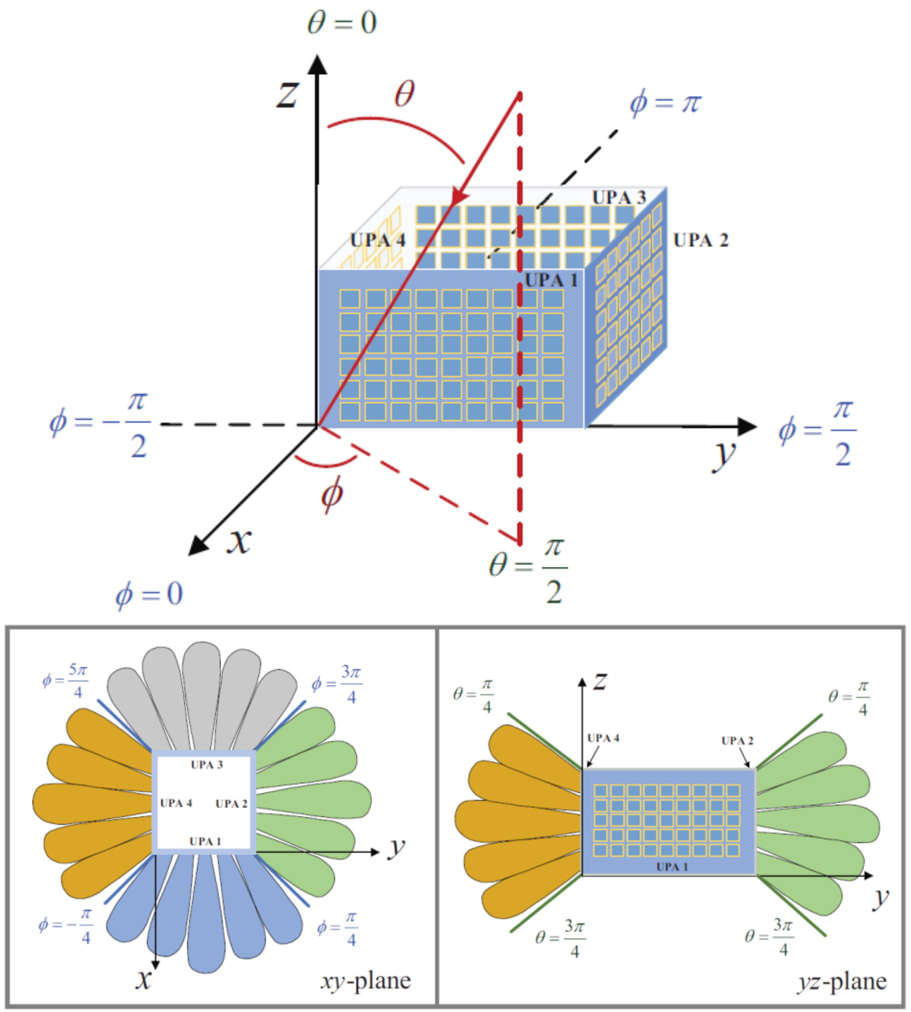


As THz channel is LoS dominant, the signal coverage by one array is limited, which significantly reduces the flexibility of the beam control.

### Merits:

- QUPA architecture can cover omni-direction in the azimuth, which has an improved signal coverage range.
- As each UPA only serves a confined range, higher antenna gain can be achieved by using the directional antenna element.
- As each UPA in the QUPA has substantially less angular deflection and the beam squint loss can be reduced.

B. Ning, Z. Chen et al., **"A unified 3D beam training and tracking procedure for terahertz communication,"** IEEE Trans. Wireless Commun., 2022.

# Far-field Beamforming

## Quadruple-UPA (QUPA) architecture

The Codebook for QUPA should be customized.

If straightforwardly using the Kronecker product of existing 2D codewords, the azimuth coverage expands when beams are above/below 90 degrees of elevation angle, which makes the total coverage of the QUPA cannot constitute an exact sphere.

The worst-case performance is maximized

$$\eta_{\text{worst}} = \frac{\sin\left[\left(\sqrt{2}N_z\pi\right)/4N\right]\sin\left[\left(\sqrt{2}\beta N_y\pi\right)/4N\right]}{N_y N_z \sin\left[\left(\sqrt{2}\pi\right)/4N\right]\sin\left[\sqrt{2}\beta\pi/4N\right]}$$

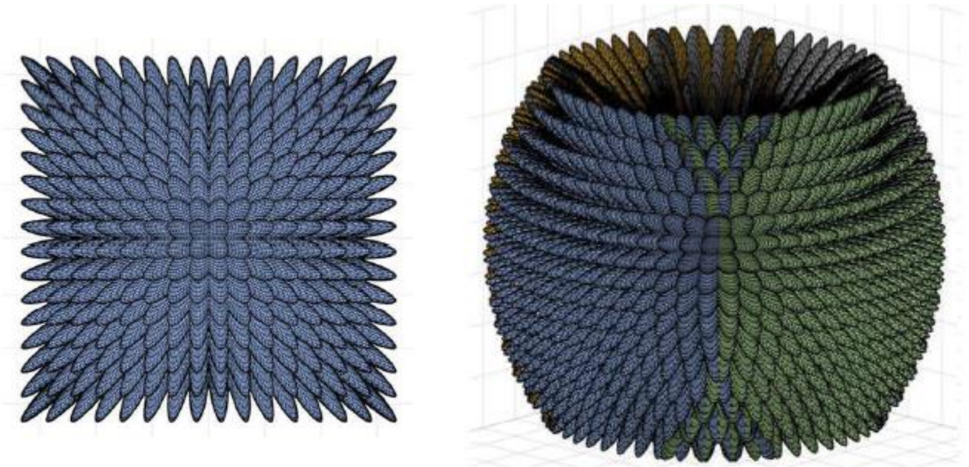

Kronecker product of 2D codebook

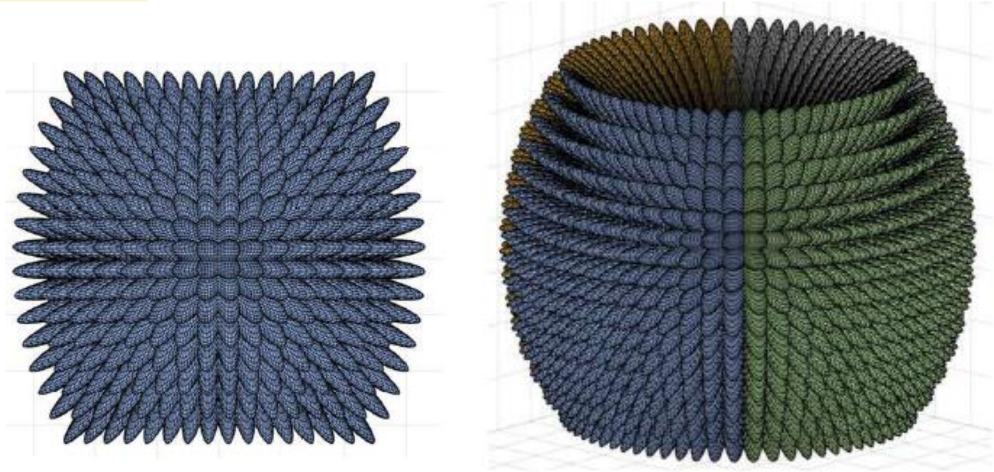

Customized 3D codebook

Chong Han, Linglong Dai, and Zhi Chen ©

B. Ning, Z. Chen et al., **"A unified 3D beam training and tracking procedure for terahertz communication,"** IEEE Trans. Wireless Commun., vol. 21, no. 4, pp. 2445-2461, Apr. 2022.

# Hybrid Far-field Beamforming

Recall two typical hybrid beamforming architectures

- Fully-connected (FC) and array-of-subarrays (AoSA) architectures:

| | Hardware Complexity | Quantity of Devices | Spectral Efficiency |
|---|---|---|---|
| Fully-connected | Higher | Larger | Higher |
| Array-of-subarrays | Lower | Smaller | Poorer |

  - Total power = Quantity of devices × Individual power
    - High operation frequency of THz → Large individual device power → Power consumption of FC architecture is too high
  - Data rate = Spectral efficiency × Bandwidth
    - Huge bandwidth of THz → Large data rate loss of AoSA architecture
- Both FC and AoSA can not achieve low power consumption and high data rate concurrently

**A balanced trade-off between FC and AoSA → Dynamic array-of-subarrays (DAoSA)**

# Dynamic Array-of-Subarrays Hybrid Beamforming

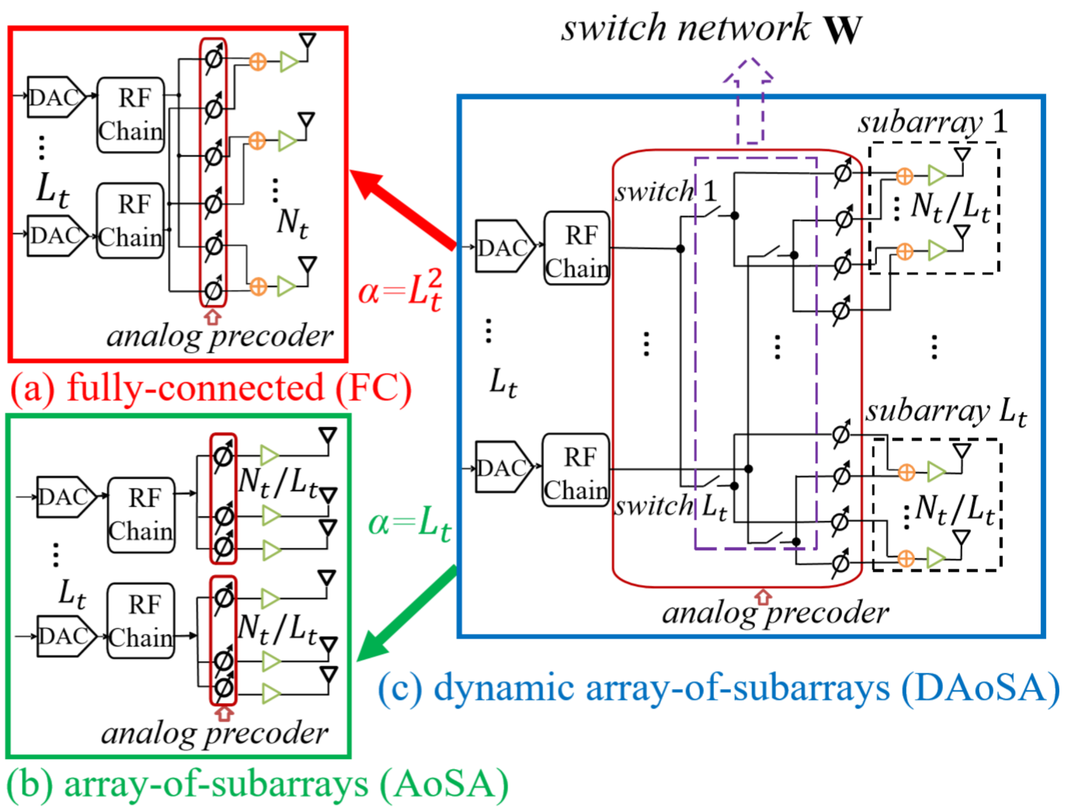


Hybrid beamforming architectures. (a) FC architecture; (b) AoSA architecture; (c) Proposed DAoSA architecture

## DAoSA

- Antennas are divided into $L_t$ subarrays
- Insert one switch between each RF chain and each subarray
  - **Switch on** → phase shifters in one subarray are **active** and **contribute to the spectral efficiency**
  - **Switch off** → phase shifters in one subarray are **inactive** and **do not consume power**
- Carefully disconnect some switches to **reduce the power consumption while still achieving high spectral efficiency**
- Denote $\alpha$ as the number of connected switches
  - The FC architecture is a special case with $\alpha = L_t^2$
  - The AoSA architecture is another special case with $\alpha = L_t$

L. Yan, C. Han and J. Yuan, **"A dynamic array-of-subarrays architecture and hybrid precoding algorithms for terahertz wireless communications,"** IEEE JSAC, 2020.

# Dynamic Array-of-Subarrays Hybrid Beamforming

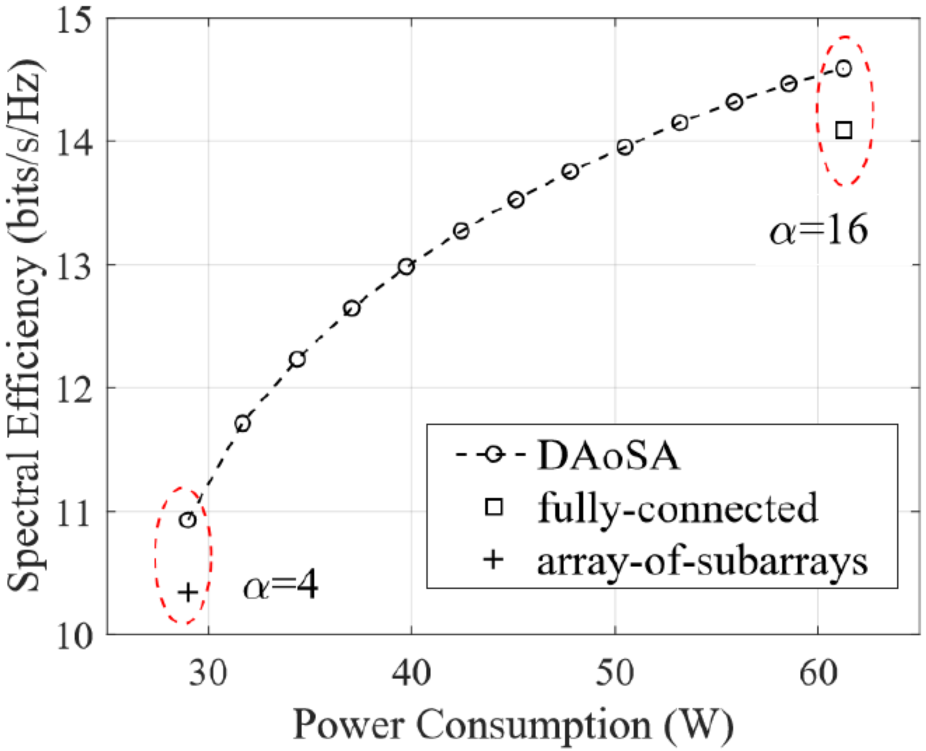


Numerical results of 256 antennas at transmitter and receiver, transmitted power is 20 dBm, $L_t = 4$.

- Both the FC and AoSA architectures are special cases when $\alpha$ = 16 and 4
- Through intelligently controlling switches, the DAoSA architecture achieves different levels of spectral efficiency and power consumption


L. Yan, C. Han and J. Yuan, **"A dynamic array-of-subarrays architecture and hybrid precoding algorithms for terahertz wireless communications,"** IEEE JSAC, 2020.

# Hybrid Beamforming with Practical Phase Shifters

- With **growing frequency** and **higher resolution**, both the **power consumption** and **hardware complexity** of phase shifters increase
- At the THz band, it is critical to **reduce the resolution** of the phase shifters
- Most architectures use infinite-resolution-adjustable phase shifter → ultra-high hardware complexity
- low-resolution-adjustable phase shifter → high hardware complexity
- Use **fixed phase shifter** → low hardware complexity

## Dynamic-subarray with fixed phase shifter (DS-FPS) hybrid beamforming design

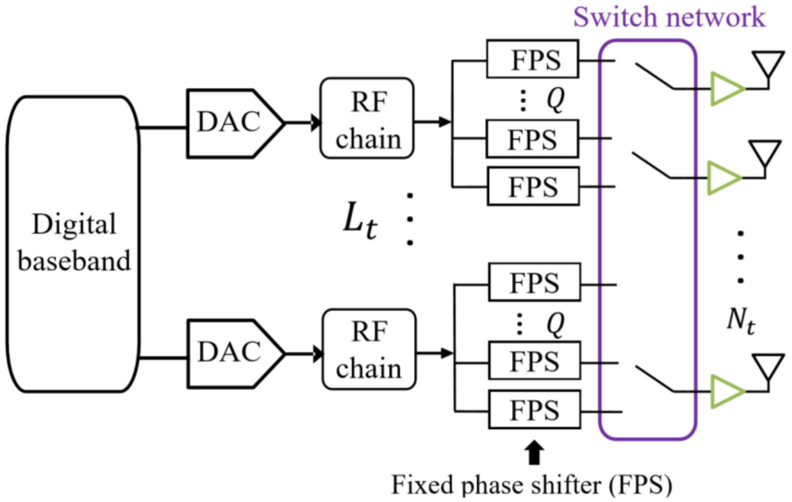


- **Fixed phase shifter (FPS)** only needs to provide a **non-adjustable and fixed phase,** which is **low-cost**
- To compensate the performance loss caused by the non-adjustable phase of FPSs, we insert a **switch network** to make each antenna select one proper FPS to connect with
- Both FPS and switch are low-cost devices → DS-FPS is an **energy- and hardware-efficient solution**

L. Yan, C. Han, N. Yang and J. Yuan, "Dynamic-subarray with Fixed Phase Shifters for Energy-efficient Terahertz Hybrid Beamforming under Partial CSI," IEEE Transactions on Wireless Communications, 2022.

# Hybrid Beamforming Under Partial CSI

- **Typical representation** of channel state information (CSI) for MIMO system at k-th subcarrier

$$\mathbf{H}[k] = \begin{bmatrix} H[k]_{11} & \cdots & H[k]_{1N_t} \\ \vdots & \ddots & \vdots \\ H[k]_{N_r 1} & \cdots & H[k]_{N_r N_t} \end{bmatrix}$$

The MIMO channel matrix is composed by $N_r N_t$ channel responses

➢ The CSI is proportional to the **square of number of antennas**

➢ Full CSI is hard to acquire for **THz UM-MIMO system**

- **Angular representation** of CSI for MIMO system

$$\mathbf{H}[k] = \sum_{i=1}^{N_p} \alpha_i[k]\mathbf{a}_{ri}[k]\mathbf{a}_{ti}[k]^H$$

$$\mathbf{a}_{ri}[k] = \left[1, \ldots, e^{j\frac{2\pi}{\lambda_k}d(L-1)\sin(\phi_{ri})\sin(\theta_{ri})}\right]^T \otimes \left[1, \ldots, e^{j\frac{2\pi}{\lambda_k}d(W-1)\cos(\theta_{ri})}\right]^T$$

The MIMO channel matrix is composed by $N_p$ multipath components

➢ The CSI is linearly related to the **number of multipath,** which is small in **sparse** THz channel

➢ **Much fewer information** than the typical representation

***Can we further simplify the CSI we needed? Of course yes!***

# Hybrid Beamforming Under Partial CSI

**Simplified partial CSI:**

- **Tx** knows the **DoD** and **amplitude of path gain** of each multipath
- **Rx** knows the **DoA** and **amplitude of path gain** of each multipath

$$\mathbf{H}[k] = \sum_{i=1}^{N_p} \alpha_i[k]\mathbf{a}_{ri}[k]\mathbf{a}_{ti}[k]^H$$

$$= \mathbf{A}_r[k]\mathbf{\Lambda}[k]\mathbf{A}_t[k]^H$$

$$= \mathbf{A}_r[k]\left(\bar{\mathbf{\Lambda}}[k] \odot e^{j*\dot{\mathbf{\Lambda}}[k]}\right)\mathbf{A}_t[k]^H$$

**Reduce the CSI feedback overhead by 50%**

DoA

Amplitude of path gain

DoD

Partial CSI at Rx

Partial CSI at Tx

**How to utilize this partial CSI to design the THz hybrid beamforming?**

L. Yan, C. Han, N. Yang and J. Yuan, **"Dynamic-subarray with Fixed Phase Shifters for Energy-efficient Terahertz Hybrid Beamforming under Partial CSI,"** IEEE Transactions on Wireless Communications, 2022.

# Hybrid Beamforming Under Partial CSI

In THz UM-MIMO systems with **ultra-massive antennas** & **sparse multipath components**, the assumption holds that the **array response vectors of different multipath are orthogonal**

$$\mathbf{A}_r[k]^H \mathbf{A}_r[k] \approx N_r \mathbf{I}_{N_p}$$

$$\frac{1}{N_r}\mathbf{a}_{ri}[k]^H \mathbf{a}_{rl}[k] \approx \mathbb{1}(i=l)$$

Spectral efficiency:

$$\frac{1}{K}\sum_{k=1}^{K} \log_2\left(\left|\mathbf{I}_{N_r} + \left(1/\sigma_k^2\right)\mathbf{H}[k]\mathbf{P}[k]\mathbf{P}[k]^H\mathbf{H}[k]^H\right|\right)$$

$$\approx \frac{1}{K}\sum_{k=1}^{K} \log_2\left(\left|\mathbf{I}_{N_p} + \left(N_r/\sigma_k^2\right)\overline{\boldsymbol{\Lambda}}[k]^2\mathbf{A}_t[k]^H\mathbf{P}[k]\mathbf{P}[k]^H\mathbf{A}_t[k]\right|\right)$$

Amplitude of path gain

DoD

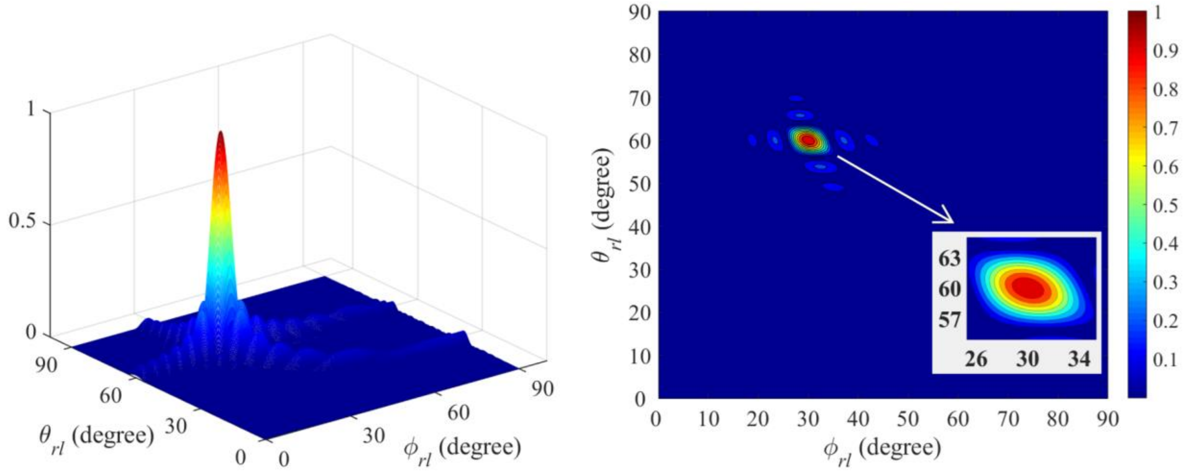


Illustration of the orthogonality of array response vectors

- For most angles of $\phi_{rl}$ and $\theta_{rl}$, which locate in the blue region, $\frac{1}{N_r}\left|\mathbf{a}_{ri}[k]^H \mathbf{a}_{rl}[k]\right| \approx 0$

**Only DoD information and amplitude of path gain is needed to design hybrid beamformer.**

L. Yan, C. Han, N. Yang and J. Yuan, **"Dynamic-subarray with Fixed Phase Shifters for Energy-efficient Terahertz Hybrid Beamforming under Partial CSI,"** IEEE Transactions on Wireless Communications, 2022.

# Error of Partial CSI

### Row-successive-decomposition (RSD) algorithm

- Design the digital beamforming matrix via **SVD method** to maximize SE
- Design **each row** of the analog matrix **successively**

### Row-by-row (RBR) algorithm

- Transform the SE maximization into Euclidean distance minimization
- Alternatively solve digital and analog beamforming matrices.
- Design **each row** of the analog matrix **in parallel**

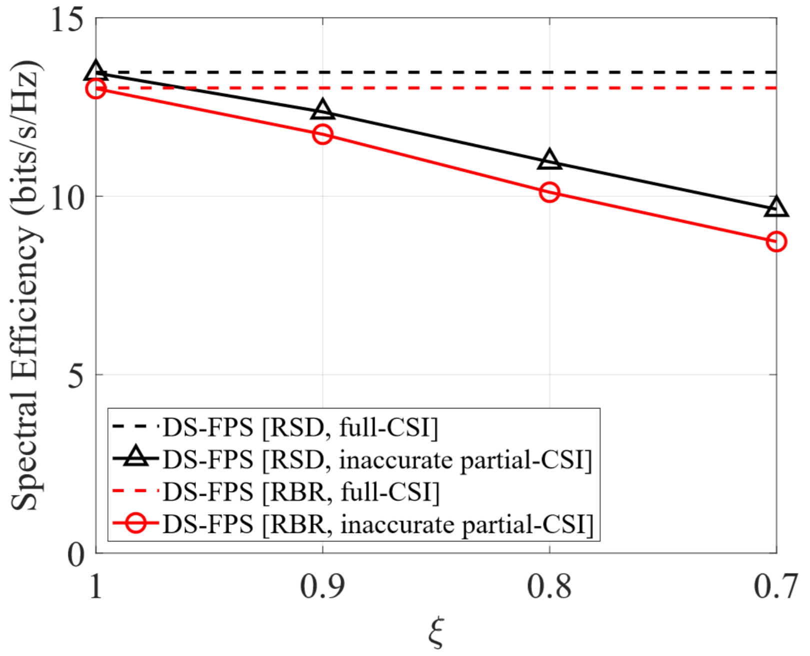


- $\xi$ represents the error of partial CSI
- The case $\xi = 1$ denotes that the partial CSI is accurate
- Full-CSI is considered as accurate and unrelated with $\xi$

- With accurate partial-CSI, both **the two algorithms achieve similar spectral efficiency** with the case of accurate full-CSI
- As the error of partial CSI increases, both the two algorithms achieves decreasing spectral efficiency

# Spectral Efficiency

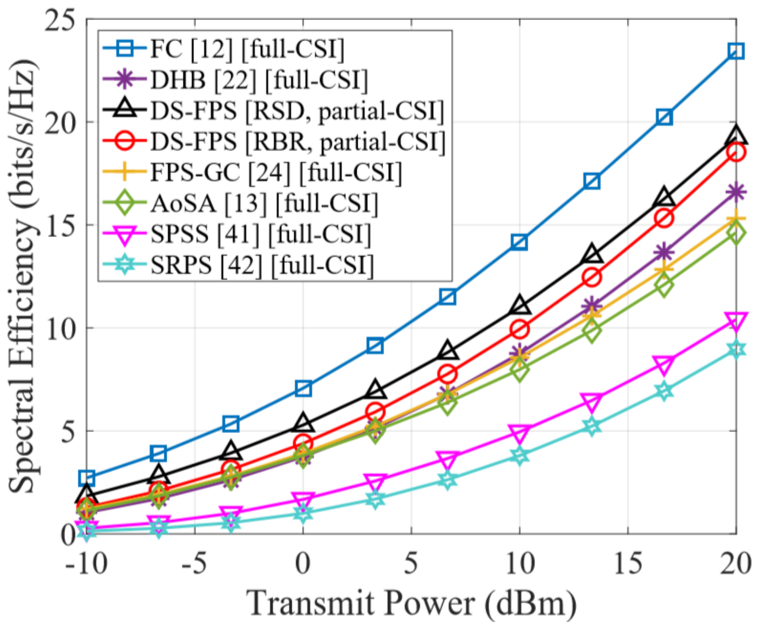


Spectral efficiency versus the transmit power $\rho$ of DS-FPS architecture. $N_t = N_r = 1024, D = 40$m. Number of FPSs is 32.

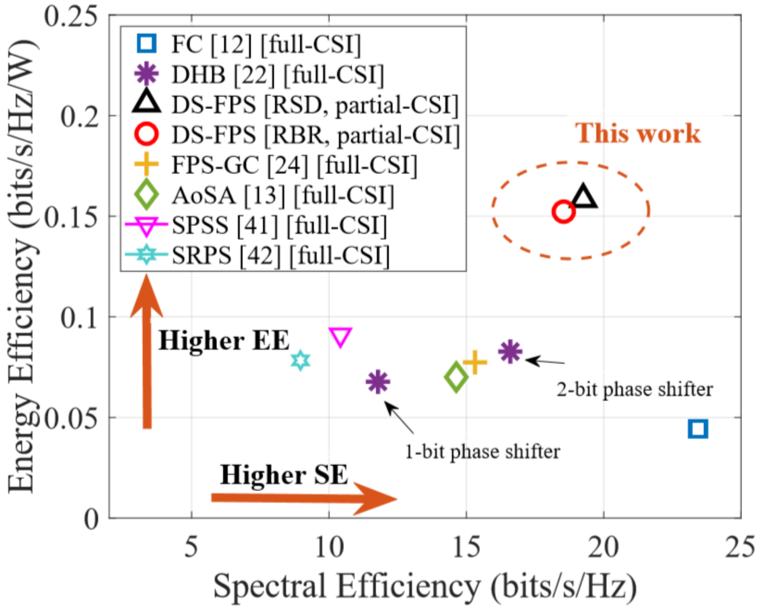


Energy efficiency versus spectral efficiency of the DS-FPS architecture. $N_t = N_r = 1024, D = 40$m, $\rho = 20$ dBm. Number of FPSs is 32.

Left figure:

- The **spectral efficiency** of DS-FPS is lower than FC and **higher** than the other architectures
- The RSD algorithm achieves higher spectral efficiency than the RBR, with higher computational complexity

Right figure:

- The **energy efficiency** of the DS-FPS architecture is **substantially higher** than the other existing schemes

# Beam Squint Problem with Phase Shifters

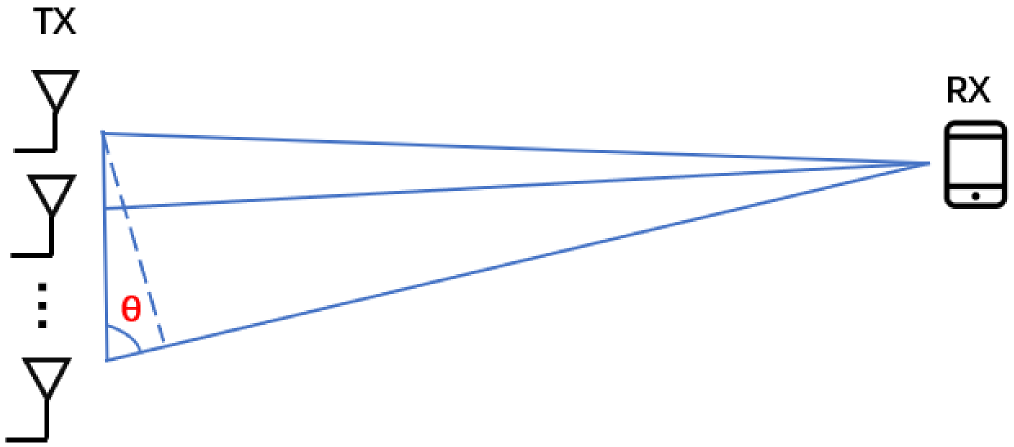


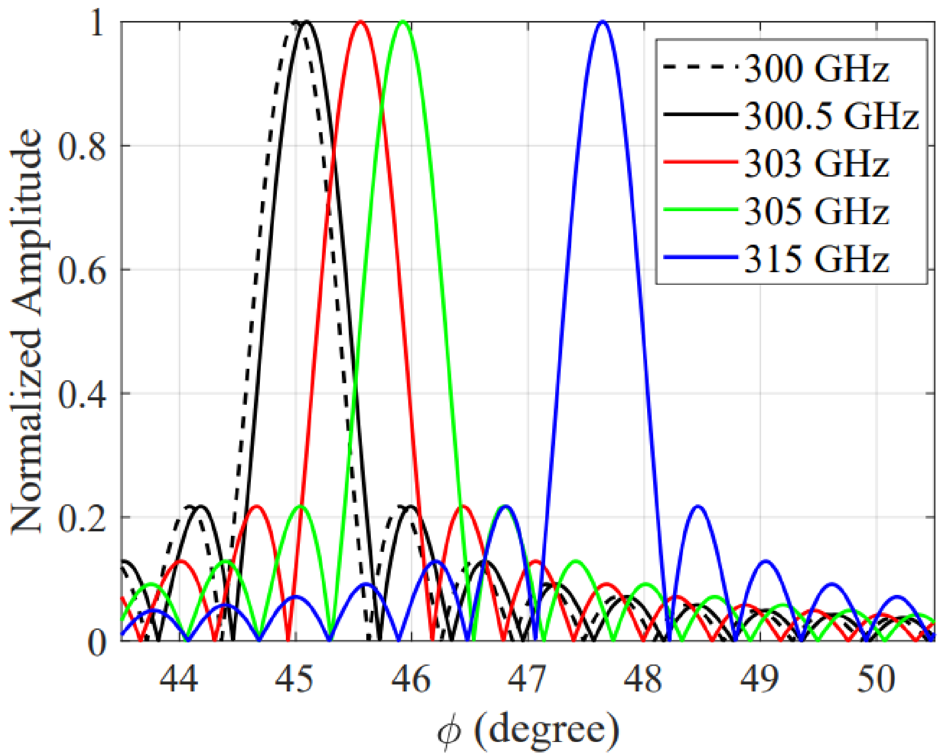


0.3 THz central frequency, 256 antennas.

For wideband multi-carrier systems, the beamforming weight of the $n^{th}$ antenna at the $m^{th}$ carrier should be

$$\frac{2\pi f_m}{c}(n-1)d\cos(\theta)$$

However, due to the ***frequency-flat*** property of phase shifter, the beamforming weight is usually designed for **central frequency** $f_c$ and is the same for all carriers.

$$\frac{2\pi f_c}{c}(n-1)d\cos(\theta)$$

With the frequency deviating from $f_c$, **the beam direction is misaligned and the array gain is reduced.**

# Dynamic Subarray with Fixed True Time Delay

- Ultra-wideband require beamforming weights are proportional to carrier frequency
  - ➢ Existing architectures use phase shifter → generate same weight for all carrier frequencies
  - ➢ Beam squint problem: error beamforming weights → reduce array gain substantially

- True-time-delay (TTD) can generate frequency-proportional beamforming weights
- However, adjustable TTD is hard to produce in THz band

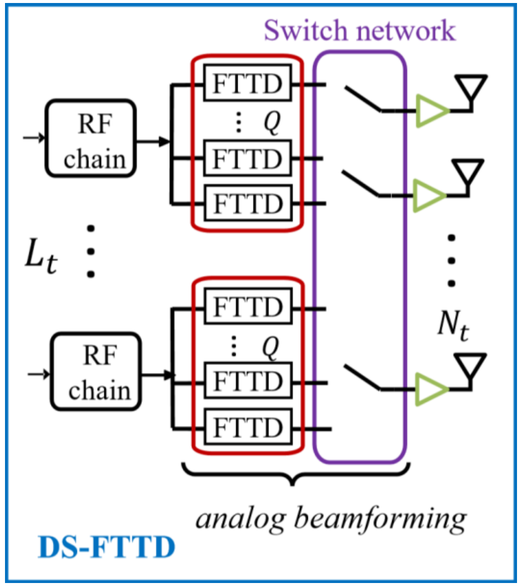


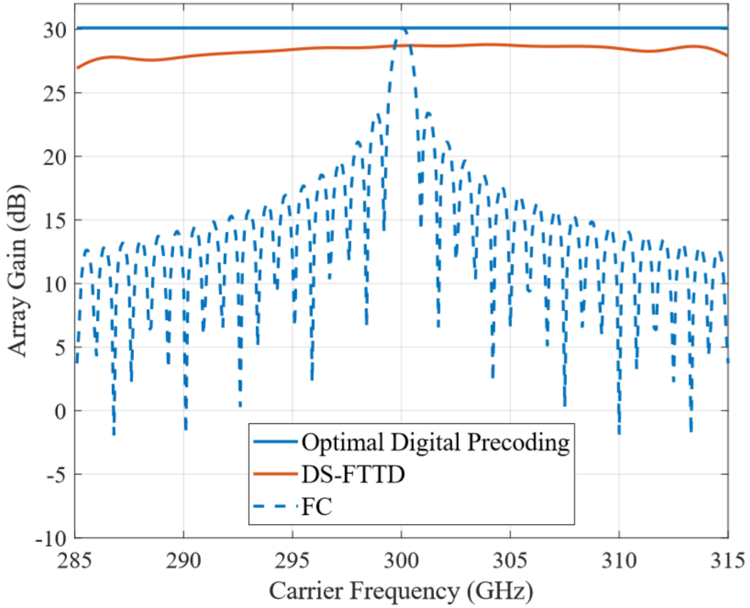


- We propose fixed TTD, with dynamic subarray architecture
  - ➢ Array gain outperforms FC substantially and approaches to optimal digital precoding
  - ➢ Substantially low hardware complexity



L. Yan, C. Han, and J. Yuan, **"Energy-efficient Dynamic-subarray with Fixed True-time-delay Design for Terahertz Wideband Hybrid Beamforming"**, IEEE Journal on Selected Areas in Communications (JSAC), 2022.

# Far-Field Beam Split Effect

- Beam split effect in wideband UM-MIMO systems
  - Beamforming is usually frequency-independent, which is accomplished by phased array
  - In wideband systems, the beams at different frequencies will split towards different angles

Prism

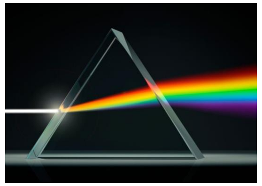

dispersion of light

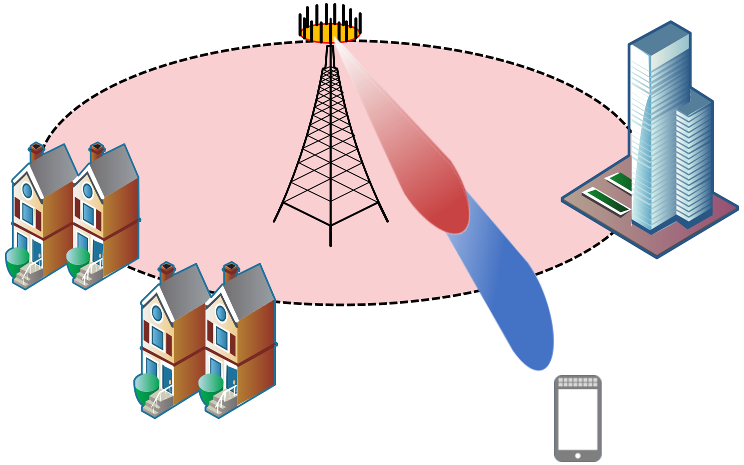

Far-field beam split

| System parameters | Beam width | Beam split | Relative split |
|---|---|---|---|
| Carrier 30 GHz, bandwidth 2 GHz, Antenna array 16×16 | 11.25° | 3° | 26% |
| Carrier 30 GHz, bandwidth 2 GHz, Antenna array 60×60 | 3° | 3° | 100% |
| Carrier 100 GHz, bandwidth 20 GHz, antenna array 16×16 | 11.25° | 9° | 80% |
| Carrier 100 GHz, bandwidth 20 GHz, antenna array 60×60 | 3° | 9° | 300% |

J. Tan and L. Dai, **"Delay-phase precoding for THz massive MIMO with beam split,"** in Proc. IEEE GLOBECOM'19, Hawaii, USA, Dec. 2019.

L. Dai, J. Tan, Z. Chen, and H. Vincent Poor, **"Delay-phase precoding for wideband THz massive MIMO,"** IEEE Trans. Wireless Commun., vol. 21, no. 9, pp. 7271-7286, Sep. 2022.

# Negative Influence of Beam Split

- Unacceptable array gain loss
  - Narrowband scheme: more than 80% array gain loss
  - Sum-rate maximization scheme: more than 50% array gain loss

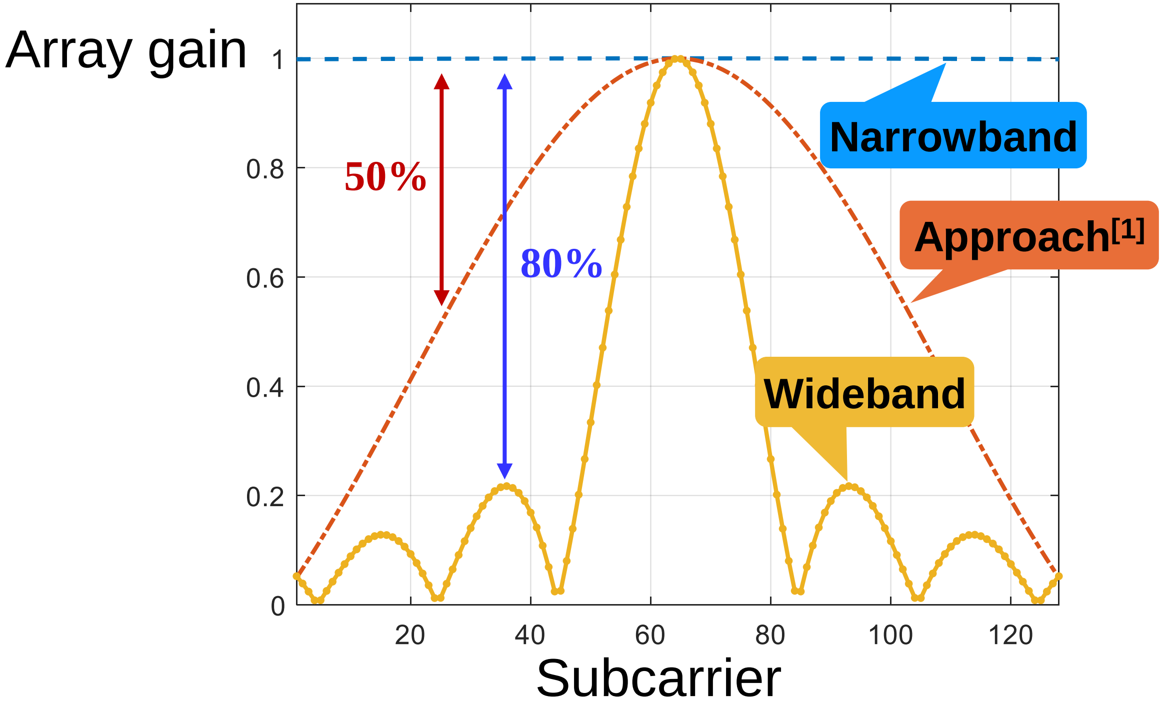


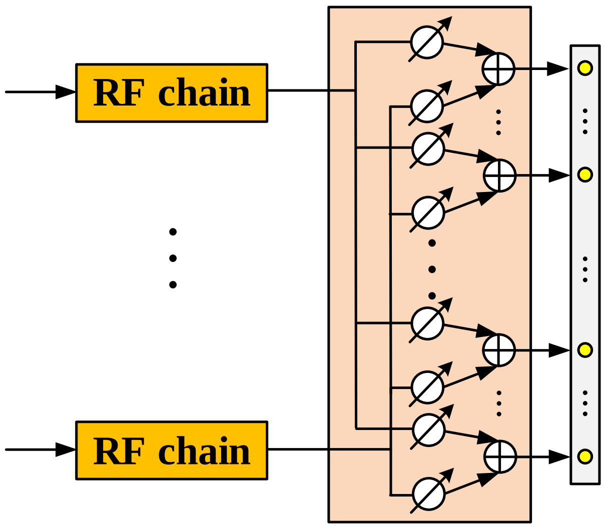


Hybrid precoding

**Classical hybrid precoding cannot mitigate the array gain loss caused by beam split**



[1] K. Venugopal, N. González-Prelcic, and R. W. Heath, **"Optimal frequency-flat precoding for frequency-selective millimeter wave channels,"** IEEE Trans. Wireless Commun., 2019.

# Idea Inspiration

- Technical problem
  - THz beam split severely aggravate the communication performance
  - Problem analogy: How to eliminate the dispersion of light?

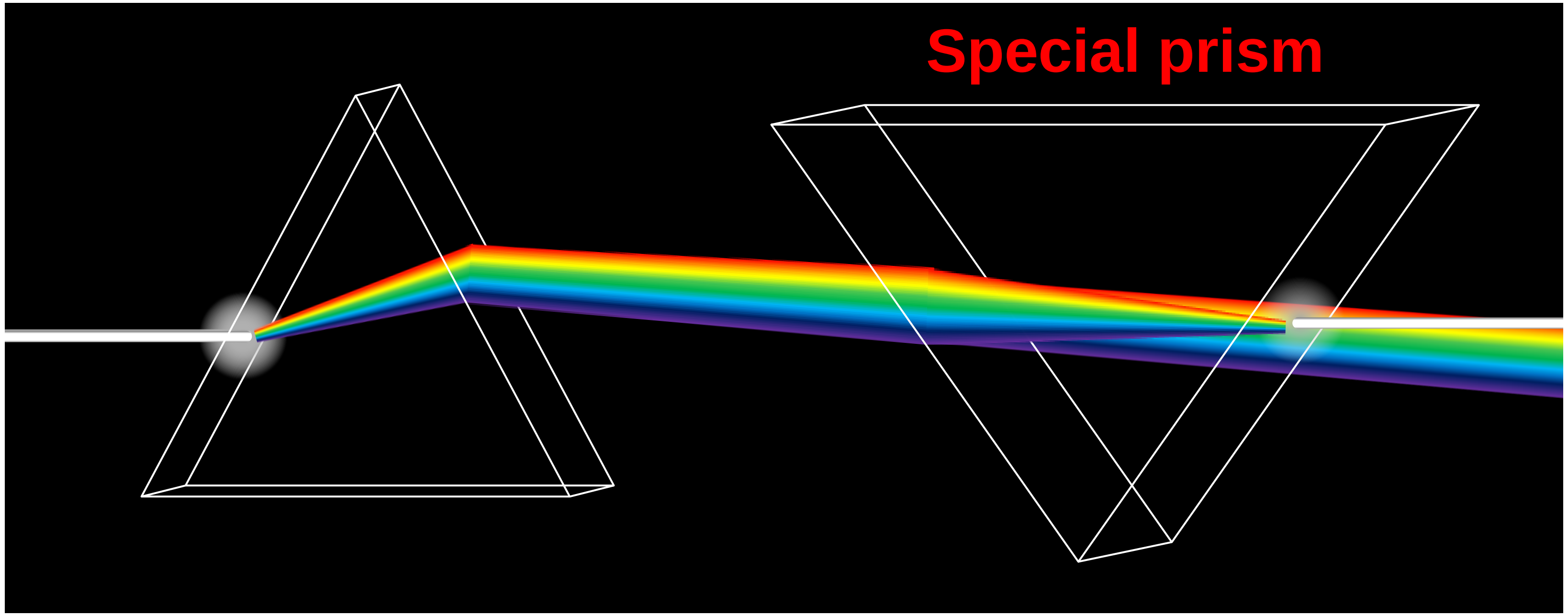


**The dispersion of light can be eliminated via a special prism**

# Delay-Phase Precoding

- Propose the delay phase precoding (DPP) architecture
- Introduce the time-delay module to realize frequency-dependent phase shift

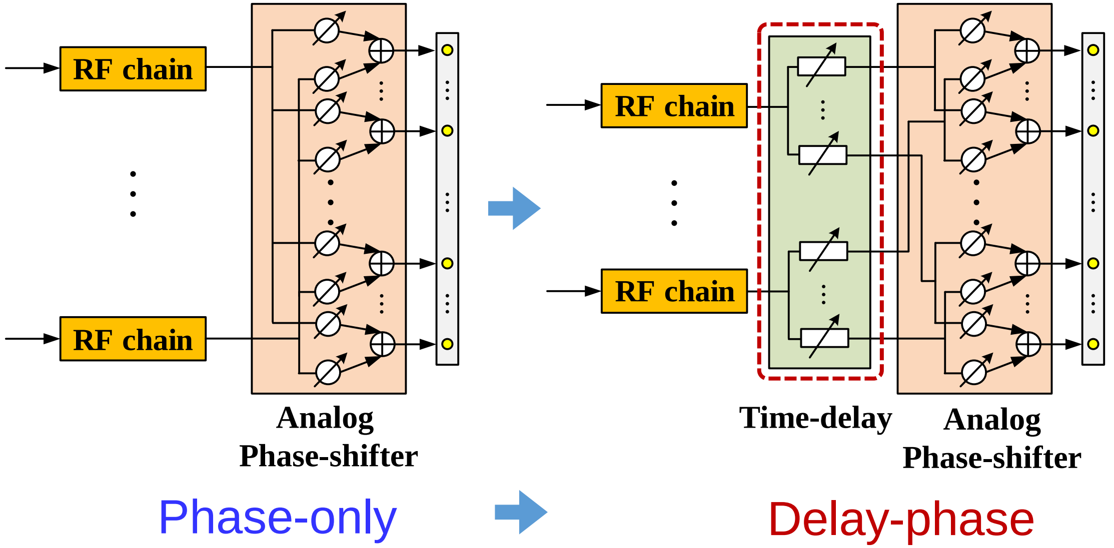


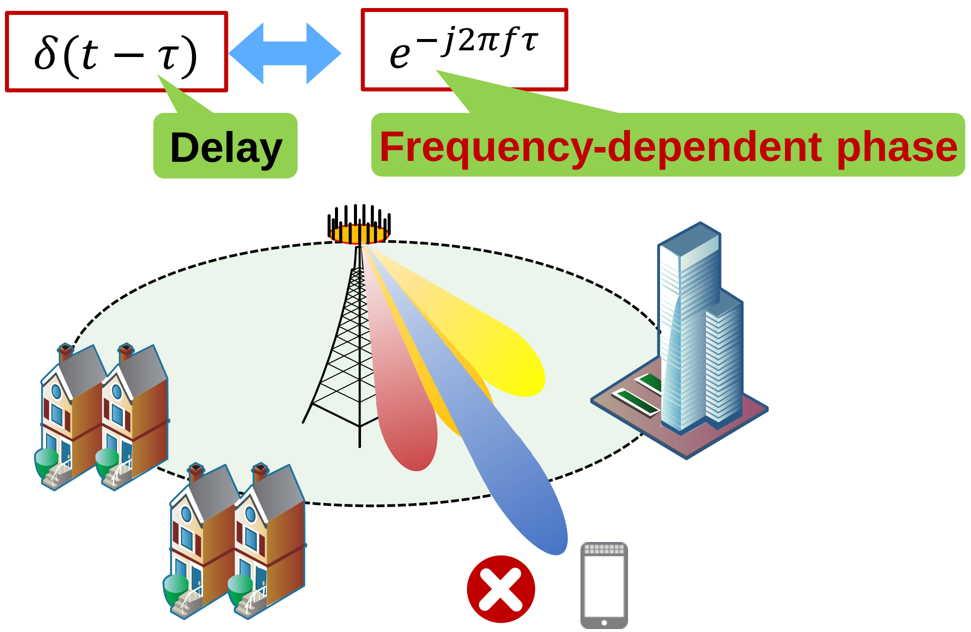


Chong Han, Linglong Dai, and Zhi Chen ©

L. Dai, J. Tan, Z. Chen, and H. Vincent Poor, **"Delay-phase precoding for wideband THz massive MIMO,"** IEEE Trans. Wireless Commun., vol. 21, no. 9, pp. 7271-7286, Sep. 2022.

# Simulation Result

- Precoding performance
  - Parameters: 256 antennas, 0.1 THz carrier frequency, 5 GHz bandwidth

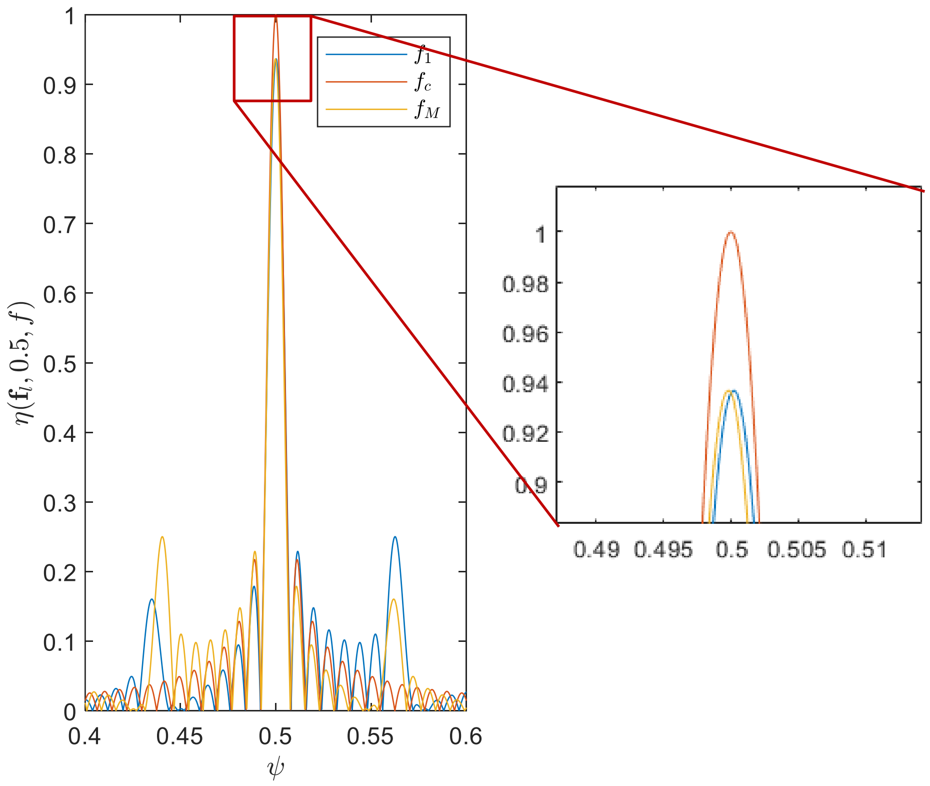


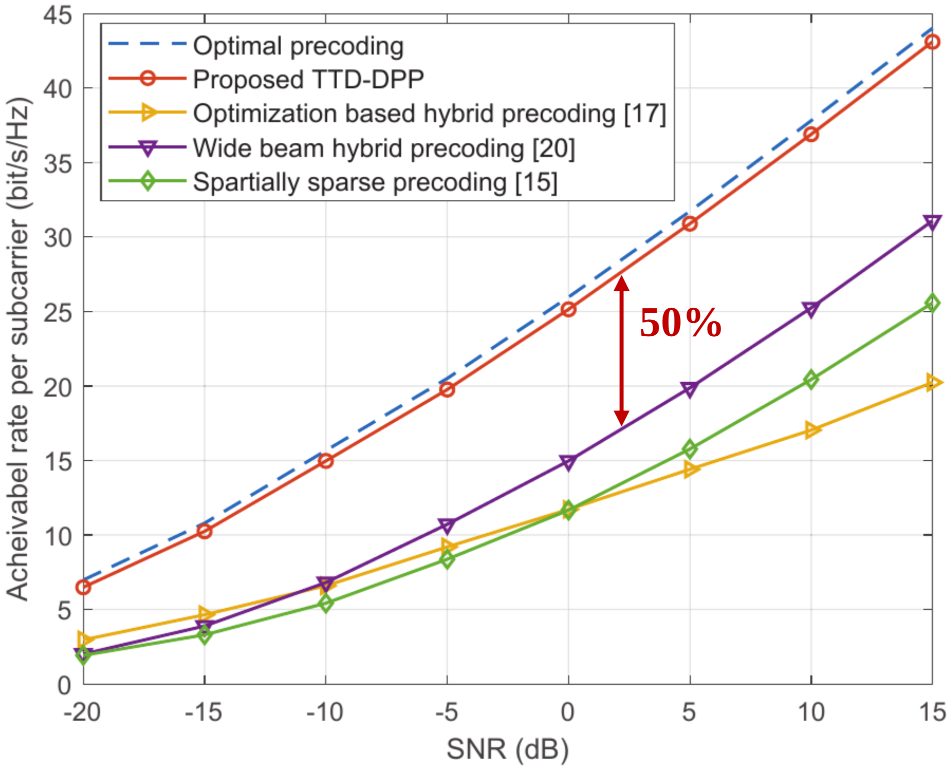


**DPP could achieve near-optimal transmission rate on all considered subcarriers**



L. Dai, J. Tan, Z. Chen, and H. Vincent Poor, **"Delay-phase precoding for wideband THz massive MIMO,"** IEEE Trans. Wireless Commun., vol. 21, no. 9, pp. 7271-7286, Sep. 2022.

# Outline

# From Far-field to Near-field

- Can we still use far-field beamforming algorithm in the near-field?
- Far-field channel model: $\mathbf{H}_{\mathrm{P}} = \Sigma_{p=1}^{N_p} \left|\alpha_p^{11}\right| e^{-j\frac{2\pi}{\lambda}D_p^{11}} \mathbf{a}_{rp}\left(\theta_{rp}^{11}, \phi_{rp}^{11}\right) \mathbf{a}_{tp}^{\mathrm{H}}\left(\theta_{tp}^{11}, \phi_{tp}^{11}\right)$ → linear phase
- Near-field channel model: $\mathbf{H}_{\mathrm{S}}[i,l] = \Sigma_{p=1}^{N_p} \left|\alpha_p^{il}\right| e^{-j\frac{2\pi}{\lambda}D_p^{il}}$ → non-linear phase

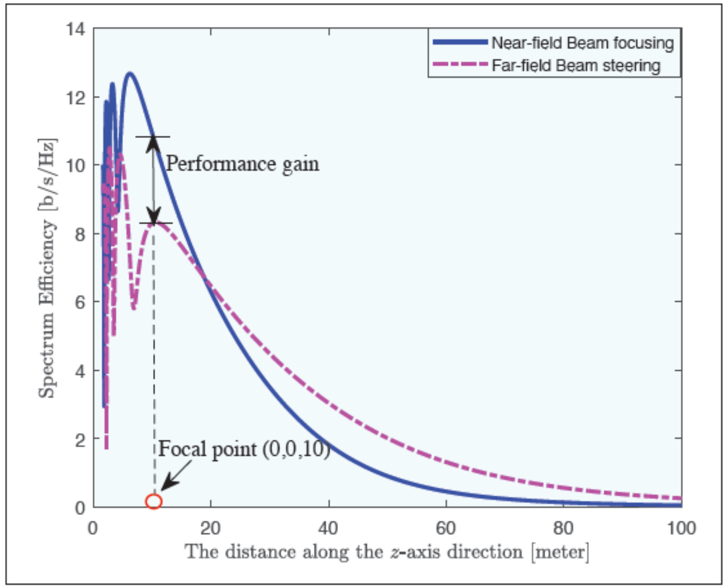


Near-field focusing and far-field beam steering

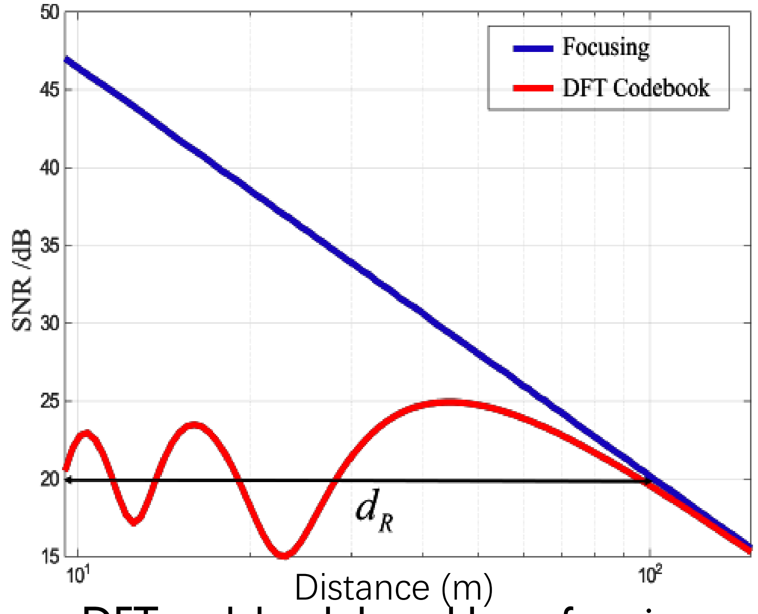


DFT codebook-based beamforming

Large performance gap

**Far-field beamforming, e.g., beam steering & DFT codebook, cannot be used in near-field**

F. Wang et al., **"Ring-type Codebook Design for Reconfigurable Intelligent Surface Near-field Beamforming,"** 2022 IEEE 33rd Annual International Symposium on Personal, Indoor and Mobile Radio Communications (PIMRC), Kyoto, Japan, 2022, pp. 391-396.

H. Zhang, N. Shlezinger, F. Guidi, D. Dardari and Y. C. Eldar, **"6G Wireless Communications: From Far-Field Beam Steering to Near-Field Beam Focusing,"** in IEEE Communications Magazine, vol. 61, no. 4, pp. 72-77, April 2023.

# Spatial Multiplexing under Extreme Sparsity

- *Do we really "hate" near-field?*
- THz channel: extreme sparse (LoS only) → poor inter-path multiplexing → limited data rate

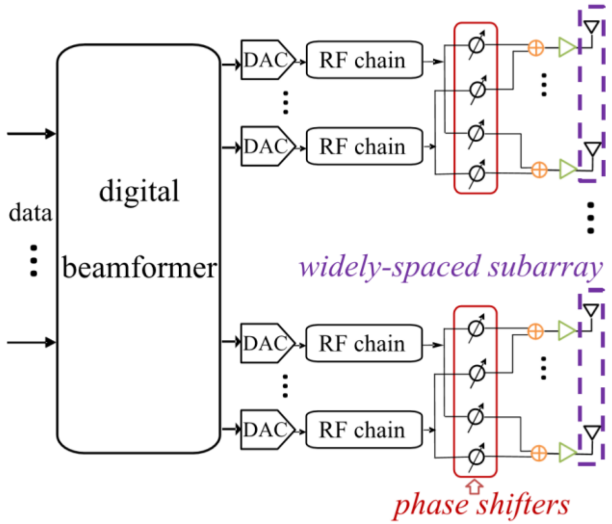


Widely-spaced multi-subarray (WSMS) architecture

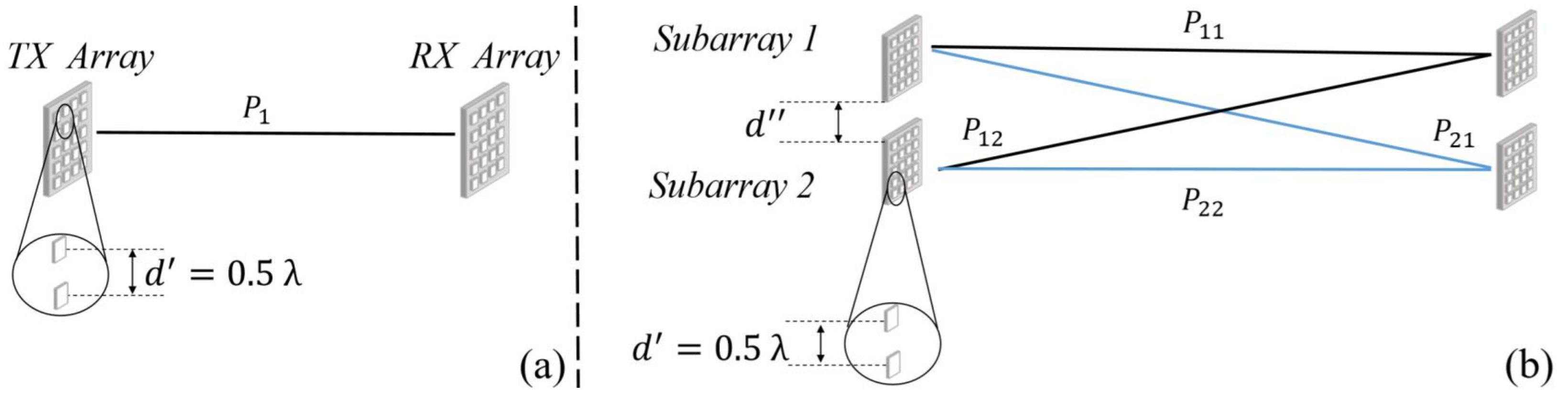


- Widely-spaced subarrays
  - ➢ The utilization of the widely-spaced subarrays at Tx **enlarges the range of near-field**
  - ➢ Near-field propagation → spherical-wave model → intra-path multiplexing
- Half wavelength antenna in subarray → far-field propagation → planar-wave propagation → inter-path multiplexing

L. Yan, Y.-H. Chen, C. Han, and J. Yuan, **"Joint Inter-path and Intra-path Multiplexing for Terahertz Widely-spaced Multi-subarray Hybrid Beamforming Systems"**, IEEE Transactions on Communications, 2022

# Beamforming for Single-user WSMS System

## Single-user Architecture

➢ Tx & Rx: *k* widely-spaced compact subarrays

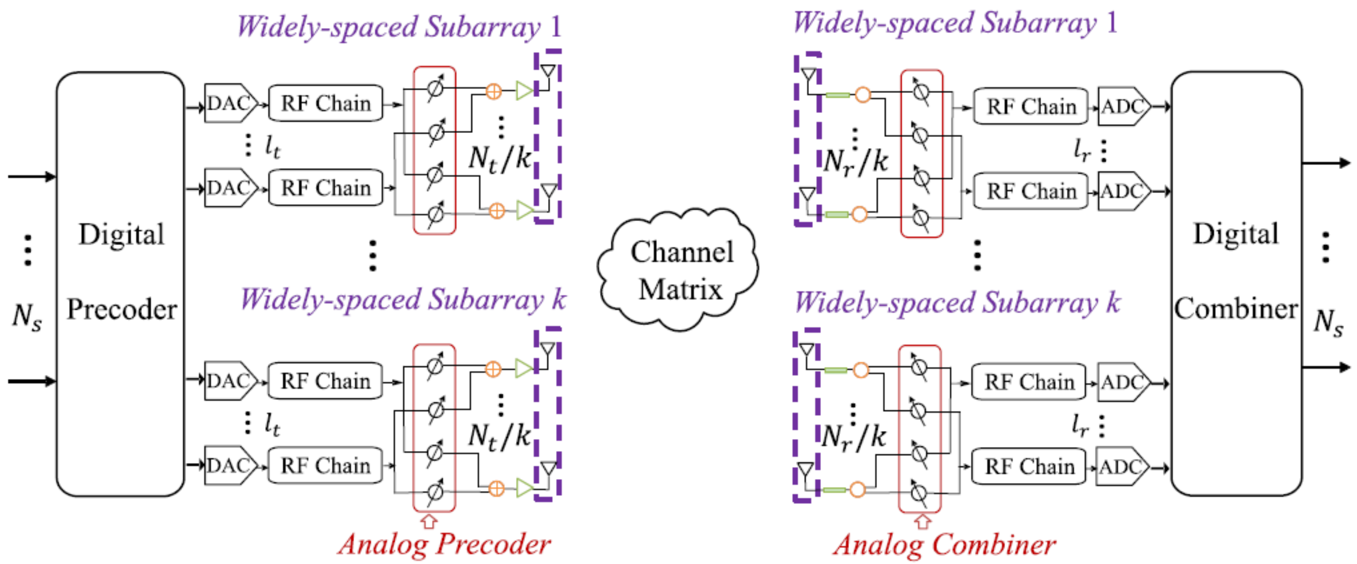


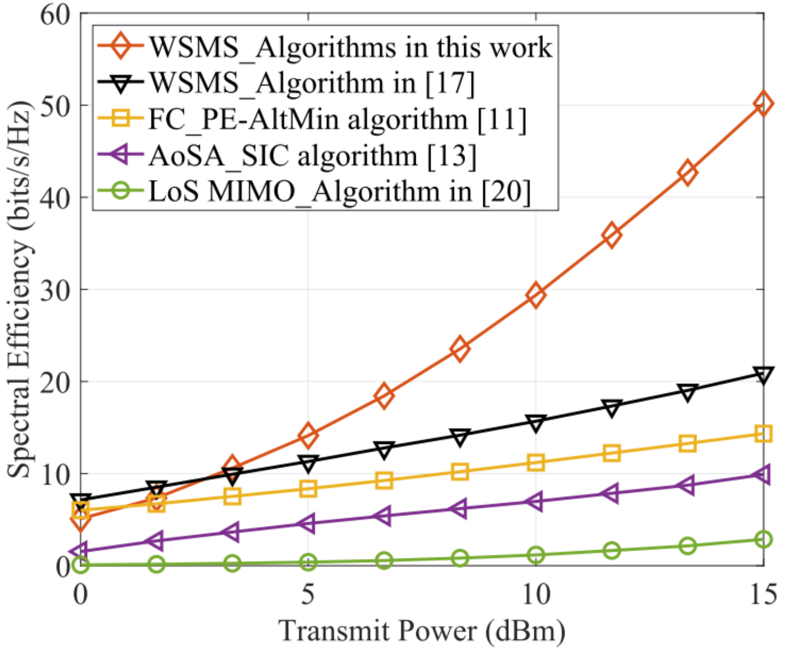


➢ WSMS architecture achieves 35 bits/s/Hz and 40 bits/s/Hz higher spectral efficiency than FC and AoSA

➢ The spatial multiplexing gain of WSMS is substantially improved to ***k*** times!

➢ Using **spherical-wave propagation** to exploit **intra-path multiplexing**, in addition to **inter-path multiplexing**


L. Yan, Y.-H. Chen, C. Han, and J. Yuan, **"Joint Inter-path and Intra-path Multiplexing for Terahertz Widely-spaced Multi-subarray Hybrid Beamforming Systems"**, IEEE Transactions on Communications, 2022

# Beamforming for Multi-user WSMS System

## Multi-user Architecture

- Base station (BS): *k* widely-spaced compact subarrays
- Each user: a compact array

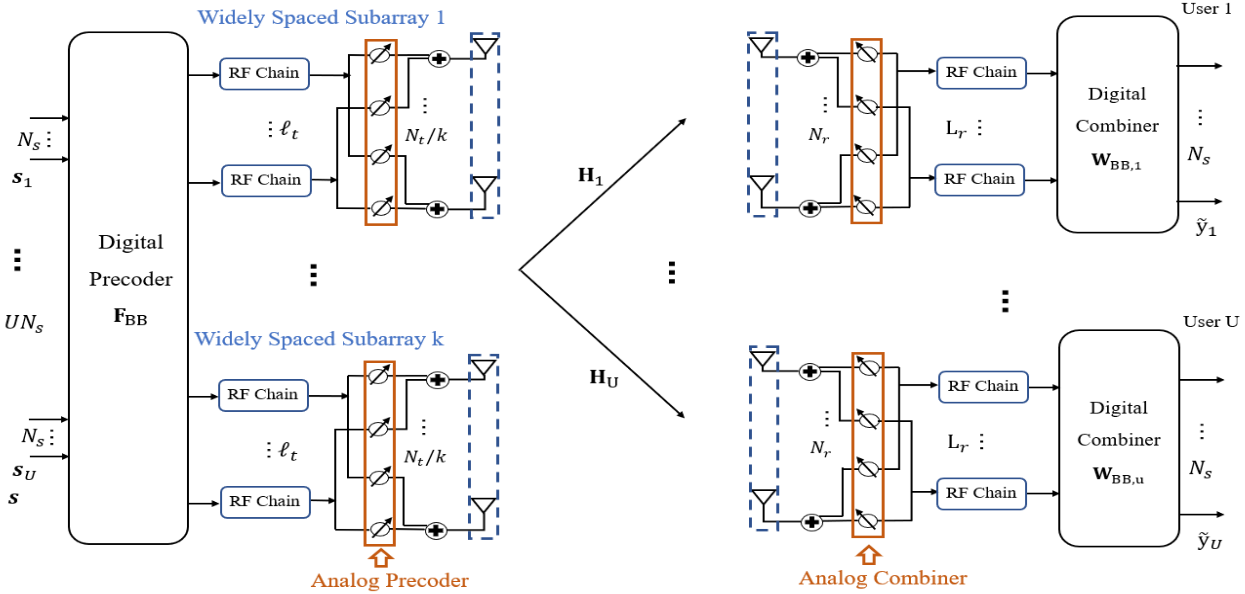


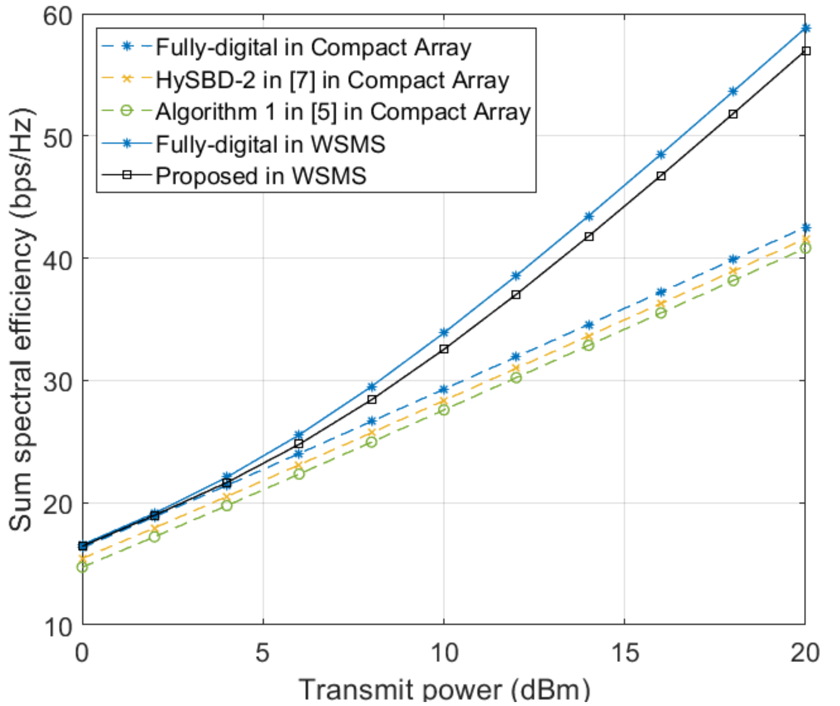


- Proposed algorithm in multi-user WSMS architecture achieves enhanced sum spectral efficiency compared to the compact array architectures

H.-Y. Shen, L. Yan, C. Han, and H. Liu (NokiaBell), **"Alternating Optimization Based Hybrid Beamforming in Terahertz Widely-spaced Multi-subarray Systems"**, in Proc. of IEEE GLOBECOM Workshop on Terahertz Communications, 2022.

Chong Han, Linglong Dai, and Zhi Chen ©

# Near-field Beamforming for MU-WSMS System

- UPA with 1024 antenna (0.3 THz): $d_R \approx 1\ m$ → mostly far field → only angle domain
- WSMS with 0.5 m array size: $d_R$ over $180\ m$ → enlarged near field → additional distance domain

| 2D scenario: azimuth angle only | | 3D scenario: azimuth and elevation angles | |
|---|---|---|---|
| Compact | WSMS | Compact | WSMS |
| 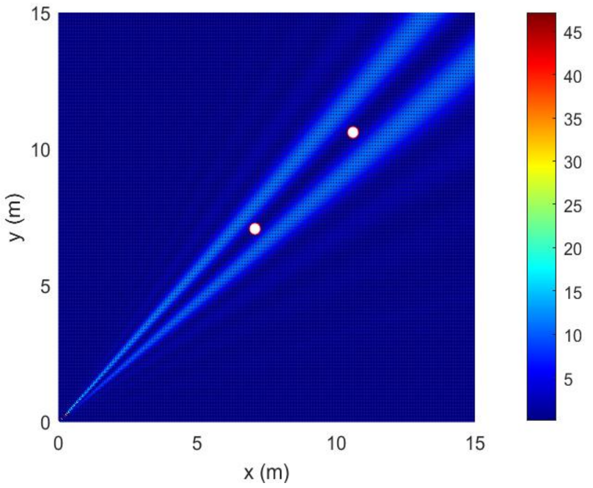 | 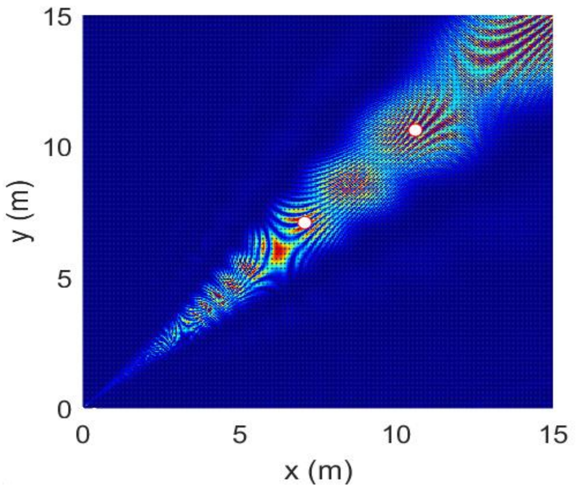 | 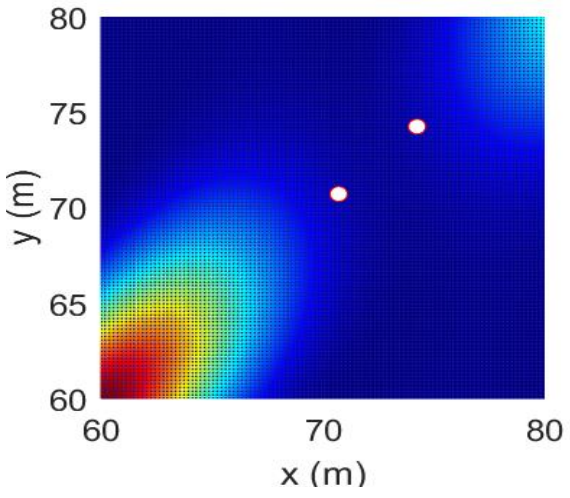 | 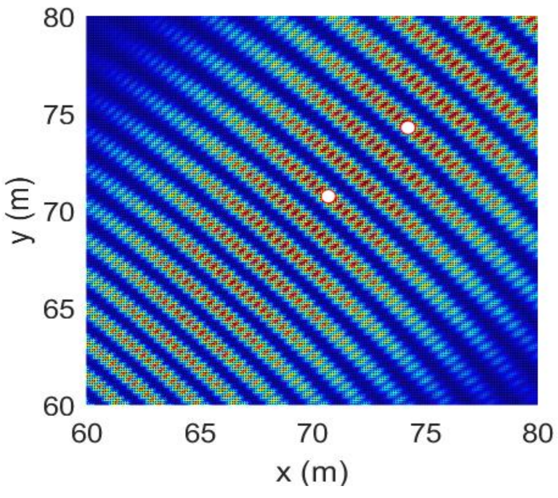 |

Beamforming algorithm based on user interference cancellation

# From Far-field to Near-field

- UPA with 1024 antenna (0.3 THz): $d_R \approx 1\ m$ → mostly far field → only angle domain
- WSMS with 0.5 m array size: $d_R$ over $180\ m$ → enlarged near field → additional distance domain

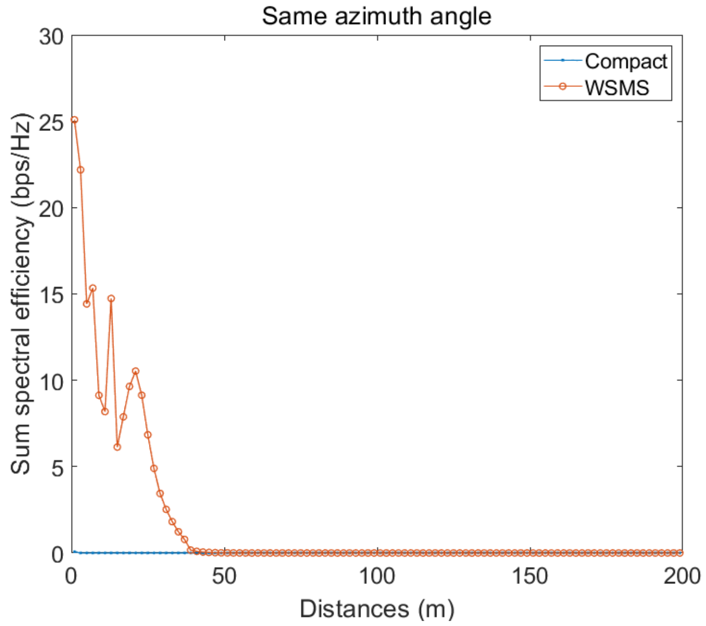


2D scenario for users at the same azimuth angle

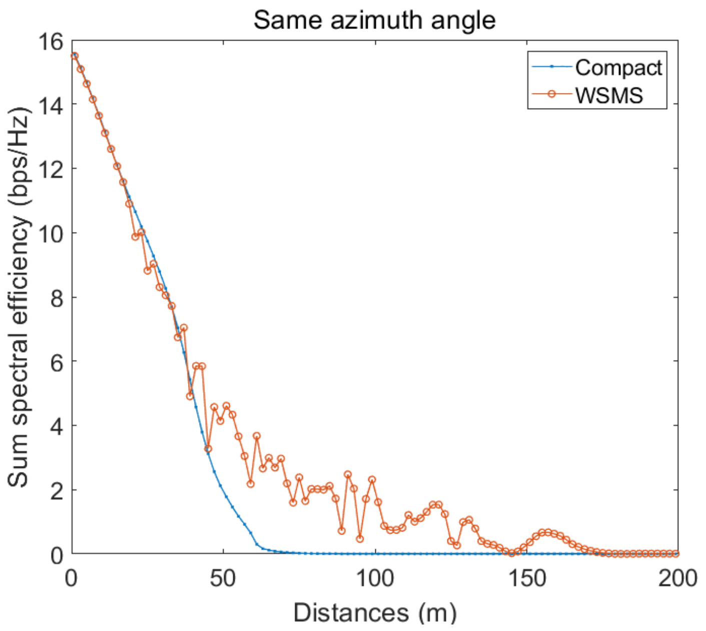


3D scenario for users at the same azimuth angle

→ Large performance gap

**Neglecting near-field effect in multi-user causes noticeable performance degradation**

# Near-Field Beam Split Effect

- Far-field beam split: beams at different frequencies be steered to different angles
- Near-field beam split: beams at different frequencies be focused on different locations

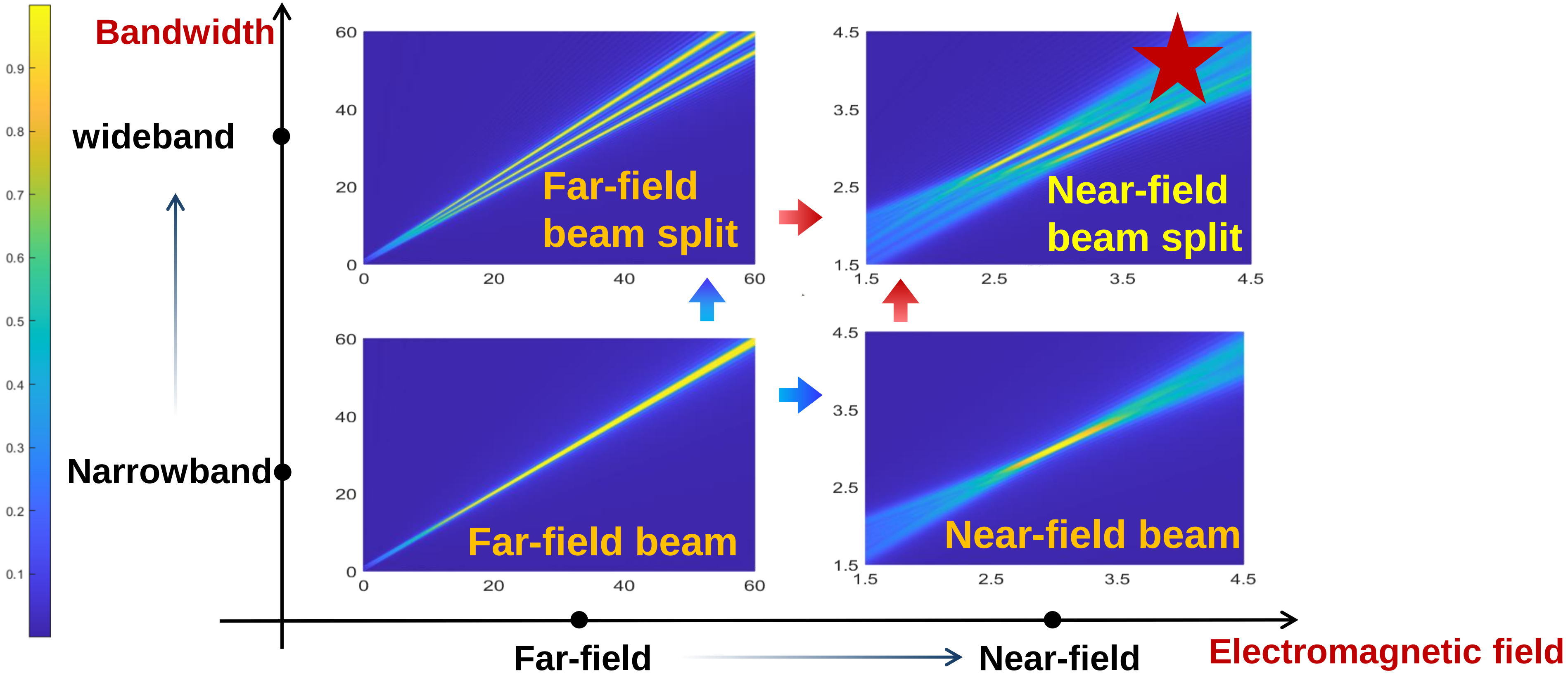


**The near-field beam split effect has not been well studied**



M. Cui, L. Dai, R. Schober, and L. Hanzo, **"Near-field wideband beamforming for extremely large antenna array,"** arXiv:2109.10054, Sep. 2021.

# Challenge in Near-Field Wideband Systems

- Existing beamforming technologies suffer from a severe performance loss due to the near-field beam split effect

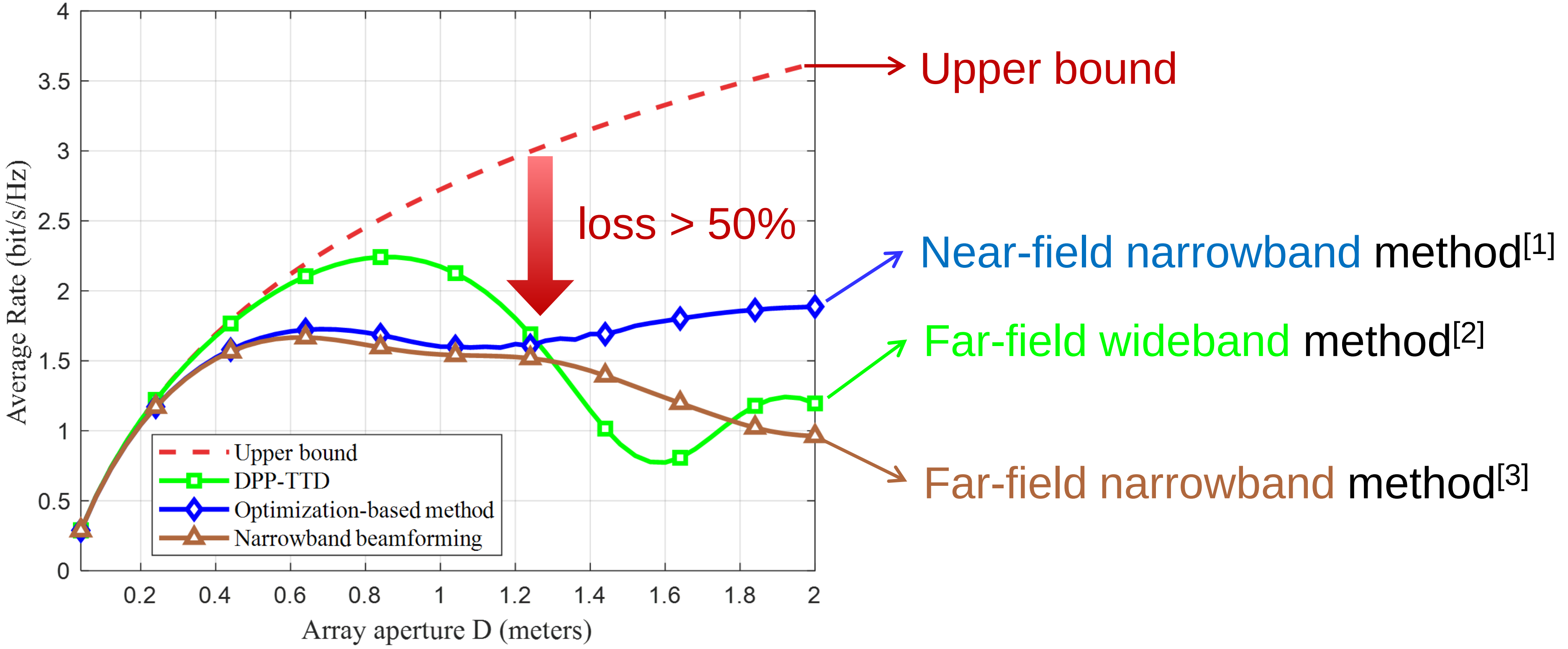



[1] N. J. Myers and R. W. Heath, **"InFocus: A spatial coding technique to mitigate misfocus in near-field LoS beamforming,"** IEEE Trans. Wireless Commun., vol. 21, no. 4, pp. 2193-2209, Apr, 2022.

[2] L. Dai, J. Tan, Z. Chen, and H. Vincent Poor, **"Delay-phase precoding for wideband THz massive MIMO,"** IEEE Trans. Wireless Commun., vol. 21, no. 9, pp. 7271-7286, Sep. 2022.

[3] X. Yu, J. Shen, J. Zhang, and K. B. Letaief, **"Alternating minimization algorithms for hybrid precoding in millimeter wave MIMO systems,"** IEEE J. Sel. Topics Signal Process., vol. 10, no. 3, pp. 485-500, Mar. 2016.

# Partitioned-Far-Field Model

- **The partitioned-far-field approximation of the near-field channel**
  - Partition the entire large array into $Q$ small sub-arrays

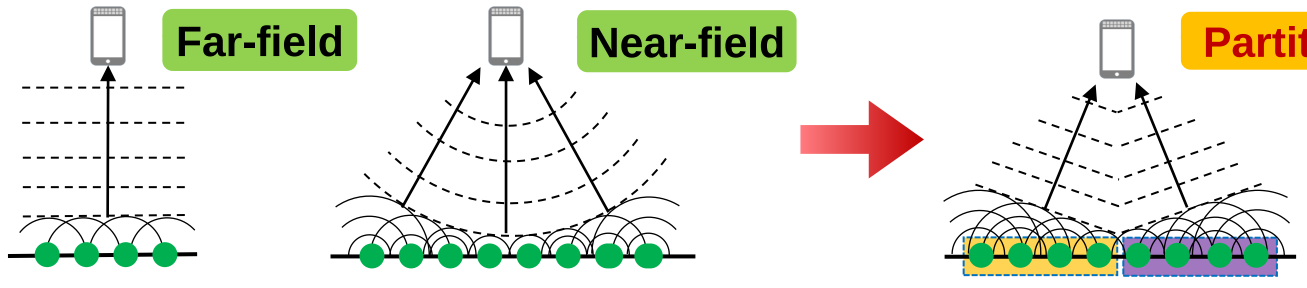


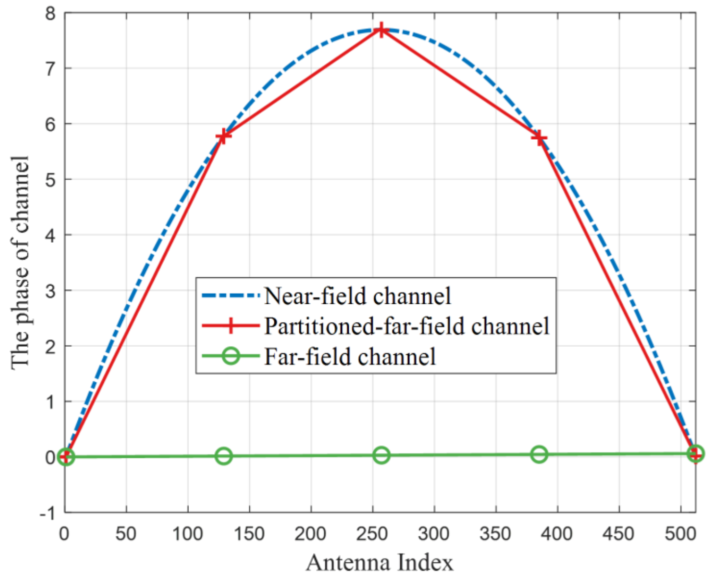


  - The user is located in the far-field region of each small subarray
    - ✓ For the $p$-th antenna of the $q$-th subarray

Distance: $r_q^{(p)} \approx r_q + pd\theta_q$

Phase: $\phi_q^{(p)} = \frac{2\pi}{\lambda} r_q^{(p)} = \frac{2\pi}{\lambda} r_q + \frac{2\pi}{\lambda} pd\theta_q$

**Subarray-wise near-field phase** | **Antenna-wise far-field phase**

**The near-field channel is decoupled to multiple far-field channels across different subarrays**

# Phase-Delay Focusing (PDF)

- Steer beams from different sub-array towards different directions by phase shifters
- Compensate for the subarray-wise near-field phase discrepancies by time delayers

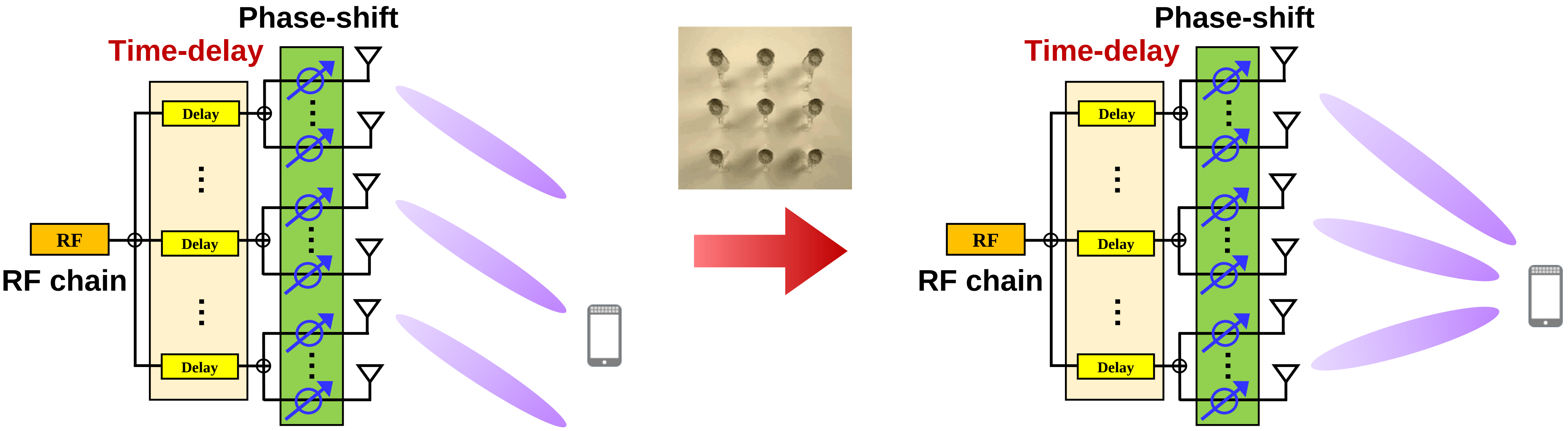


(a) Far-field beam split solution

(b) Proposed phase-delay focusing (PDF)

**The proposed PDF can overcome the near-field beam split effect**



M. Cui, L. Dai, R. Schober, and L. Hanzo, "Near-field wideband beamforming for extremely large antenna array," arXiv:2109.10054, Sep. 2021.

# Simulation Results

- **Achievable average rate vs. array aperture**

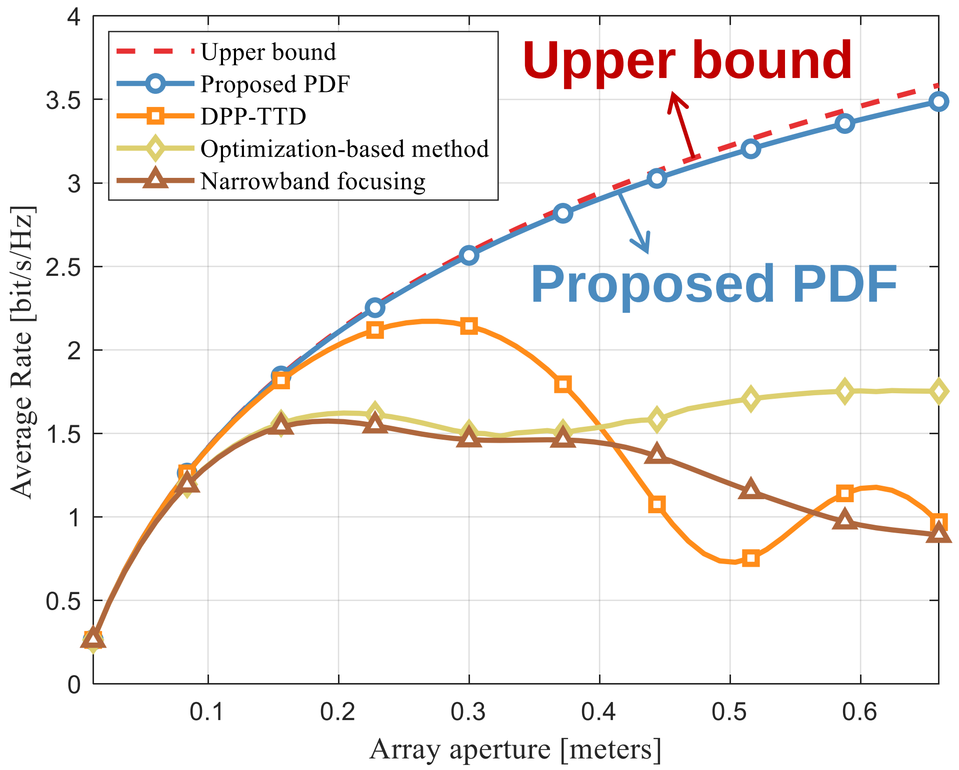


| Parameter | Value |
|---|---|
| Carrier | 100 GHz |
| Bandwidth | 5 GHz |
| Number of subcarriers | 1024 |
| Number of antennas | 512 |
| SNR | 10 dB |

**Phase-delay focusing (PDF) can achieve more than 95% of the optimal rate**



M. Cui, L. Dai, R. Schober, and L. Hanzo, **"Near-field wideband beamforming for extremely large antenna array,"** arXiv:2109.10054, Sep. 2021.

# Outline

# Beam Management

- Beam training/alignment
  - ➢ Align the beam with a certain user
- Beam tracking
  - ➢ Keep track of the mobile user
- Beam-guided medium access
  - ➢ Serve multiple users

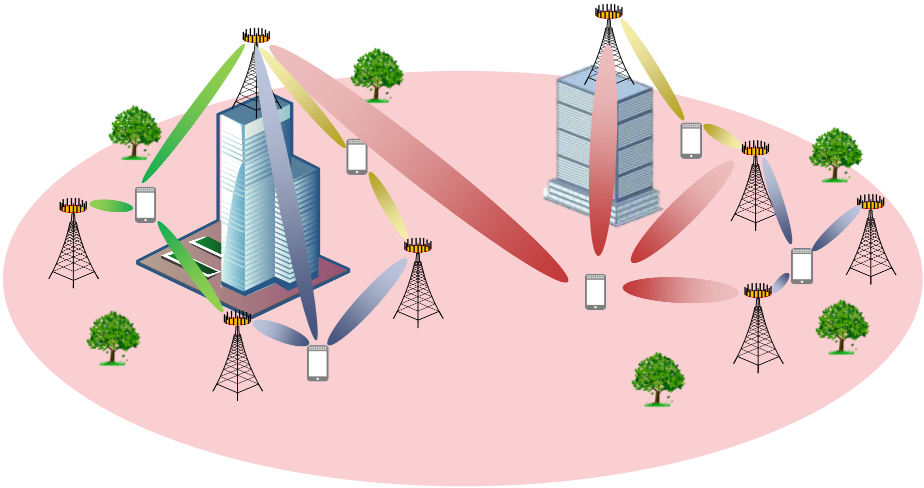

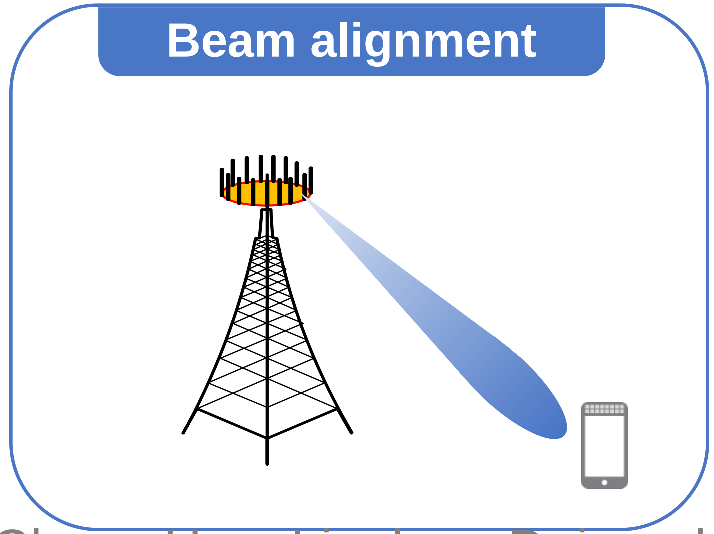


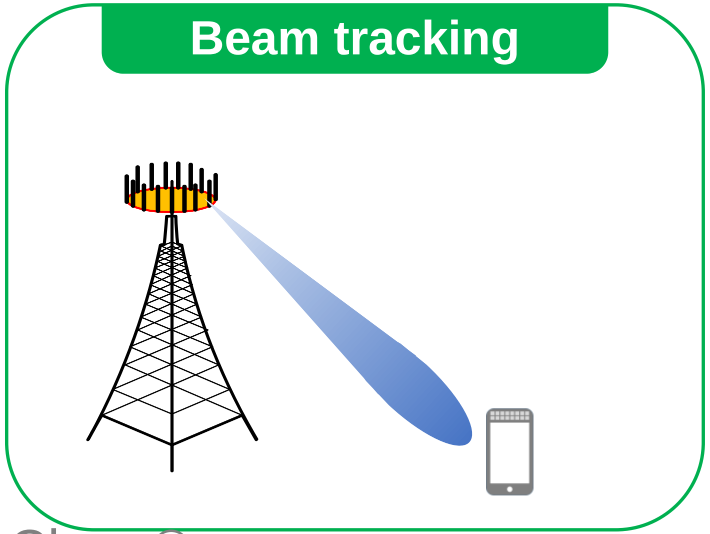


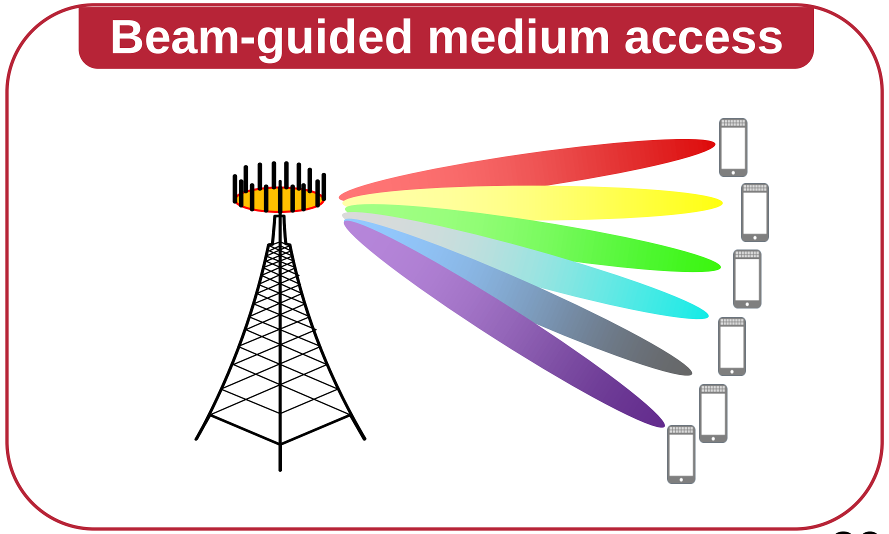

# Challenges on Beam Management

- The cost of beam management is high due to the large number of antennas
- The electromagnetic field structure changes fundamentally due to the near field communication
- The array gain decreases due to the beam split effect caused by large bandwidth

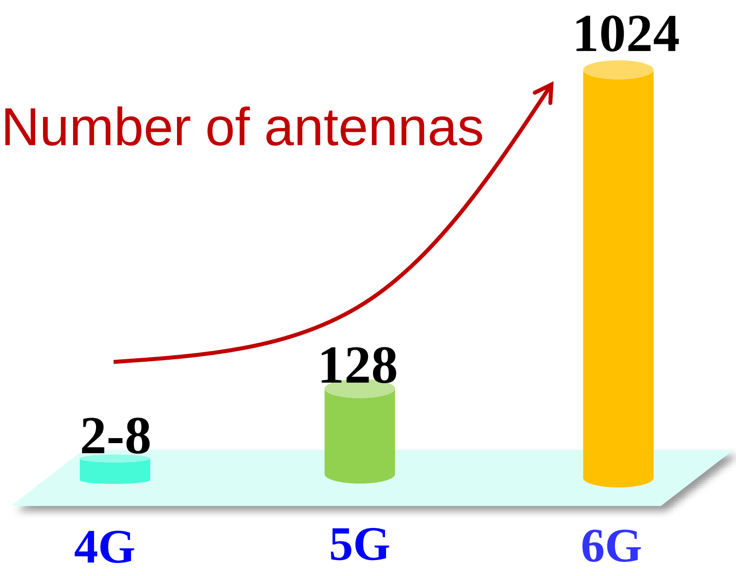


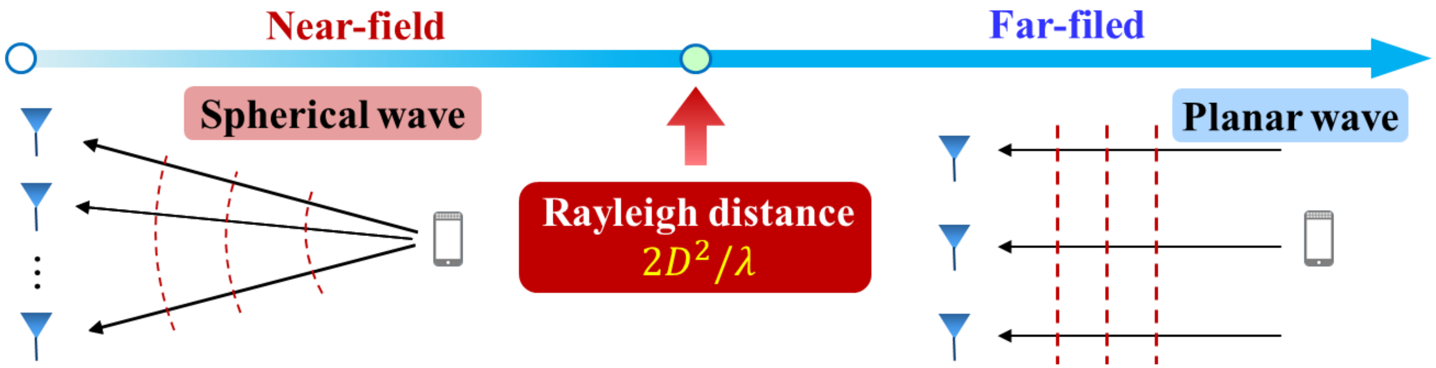


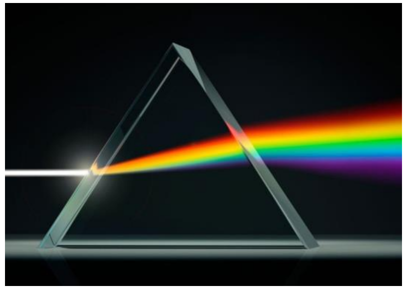

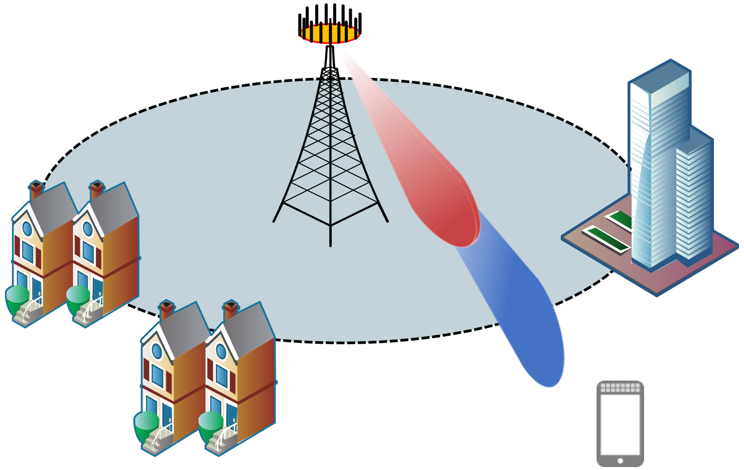

# Beam Training

## What is beam training?

$$\{\mathbf{w}^{\text{opt}}, \mathbf{f}^{\text{opt}}\} = \arg\max \left|\mathbf{w}^H \mathbf{a}_r \mathbf{a}_t^H \mathbf{f}\right|^2,$$

$\mathbf{a}_t$ and $\mathbf{a}_r$ are unknown

Beam training is the process of seeking the solutions of the beamformer and combiner, by testing beam pairs, without requiring any CSI.

**Beam Training**
- **Training Protocol**: The training protocol determines the training reliability and complexity.
- **Codebook Design**: Codebook design aims to optimize the weights of each codeword to make its beam pattern cover the zone specified by the protocol.

# Beam Training Protocol

- **Exhaustive search** is the simplest protocol, that is, exhaustively testing the narrow beam pairs of the transmitter and the receiver.

- Compared to the exhaustive search, some **other training protocols** are more appealing owing to their lower training complexity.

TABLE IX
COMPARISON OF THE BEAM TRAINING PROTOCOLS.

| Training Protocol | Training complexity |
|---|---|
| Exhaustive search | $N^2$ |
| One-side search | $2N$ |
| Adaptive search | $4\log_2 N$ |
| Parallel search | $N^2/N_{RF}$ |
| Two-stage search | $N^2/Q + Q$ |
| One-side $M$-Tree search | $2M\log_M N$ |
| Both-side $M$-Tree search | $M^2\log_M N$ |

B. Ning, Z. Tian, W. Mei, Z. Chen, C. Han, S. Li, J. Yuan, and R. Zhang, **"Beamforming technologies for ultra-massive MIMO in terahertz communications,"** IEEE O. J. ComSoc., 2023.

# Beam Training Protocol

## Hierarchical Search

The most efficient protocol is M-tree search, which is a multi-stage hierarchical protocol.

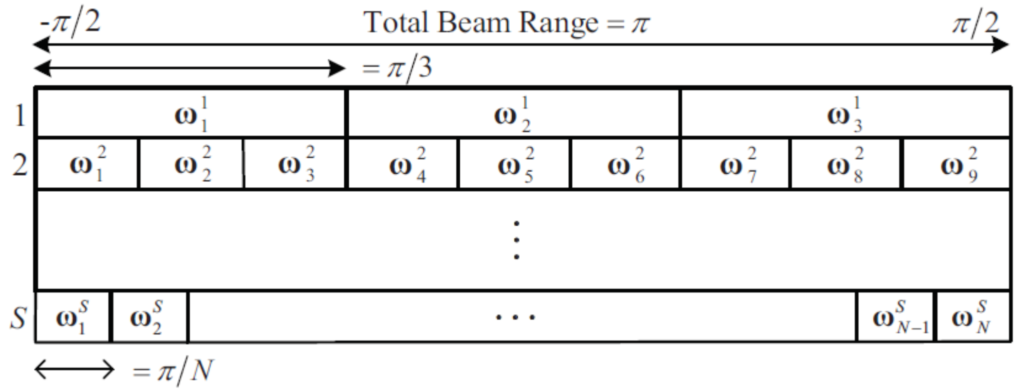


Zone Division

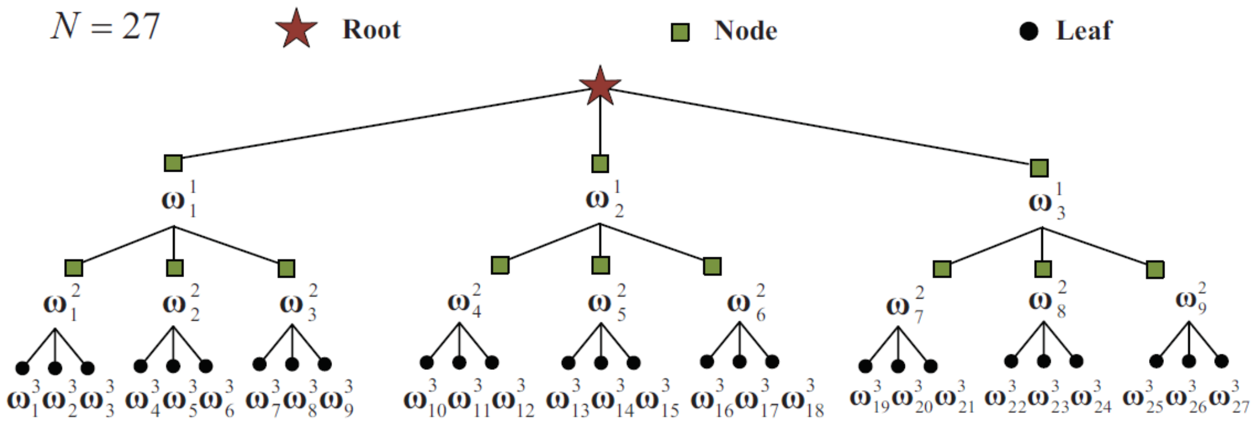


Search Manner

We start with using an omnidirectional beam (root) for initial detection. Then, in each stage of the M-tree search, we find and follow the best beam (node) for the next stage search, until the best narrow beam (leaf) is found.

B. Ning, Z. Tian, W. Mei, Z. Chen, C. Han, S. Li, J. Yuan, and R. Zhang, **"Beamforming technologies for ultra-massive MIMO in terahertz communications,"** IEEE O. J. ComSoc., 2023.

# Beam Training Protocol

M-tree search can be classified as **one-side** M-tree search and **both-side** M-tree search.

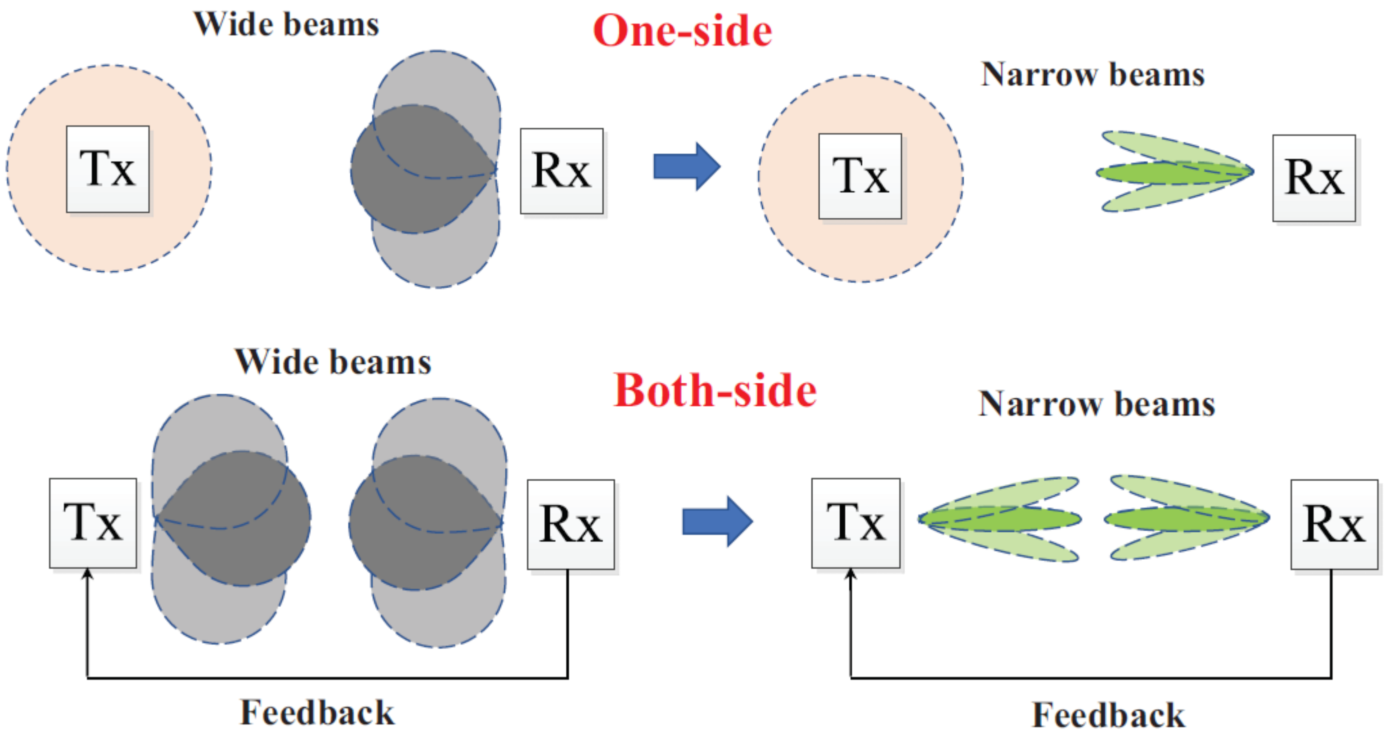


The training complexity is given by

$$T_{\text{one}} = 2M \log_M N.$$

$$T_{\text{both}} = M^2 \log_M N.$$



B. Ning, Z. Tian, W. Mei, Z. Chen, C. Han, S. Li, J. Yuan, and R. Zhang, **"Beamforming technologies for ultra-massive MIMO in terahertz communications,"** IEEE O. J. ComSoc., 2023.

# Beam Training Protocol

- Training Protocol Design is an **open problem**, which is quite different for different scenarios.

- Training Protocol Design includes the zone division (for each beam) and the search manner.

- Training Protocol Design is related to the antenna geometries, serving range, and power constraint.

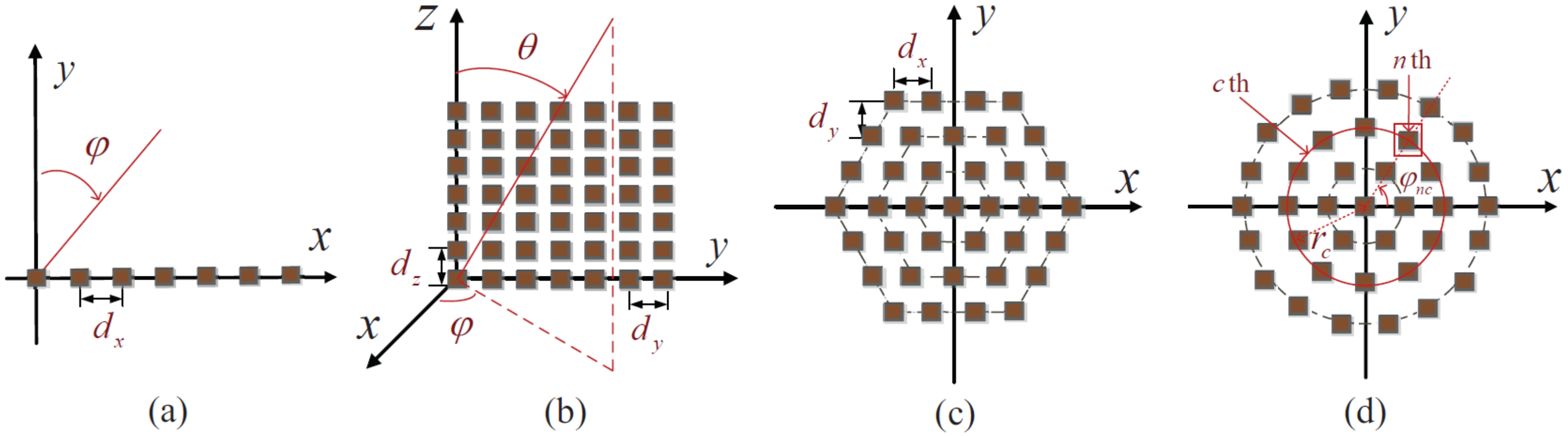



B. Ning, Z. Tian, W. Mei, Z. Chen, C. Han, S. Li, J. Yuan, and R. Zhang, **"Beamforming technologies for ultra-massive MIMO in terahertz communications,"** IEEE O. J. ComSoc., 2023.

# Beam Training Protocol

## Protocol for 3D Beams

- For THz UM-MIMO system with QUPA architecture, we proposed a grid-based (GB) training protocol.

**Define** $\Theta(\theta) = -\cos\theta$ and $\Phi(\phi) = \sin(\phi - \frac{\pi(k-1)}{2}) + \sqrt{2}(k-1).$

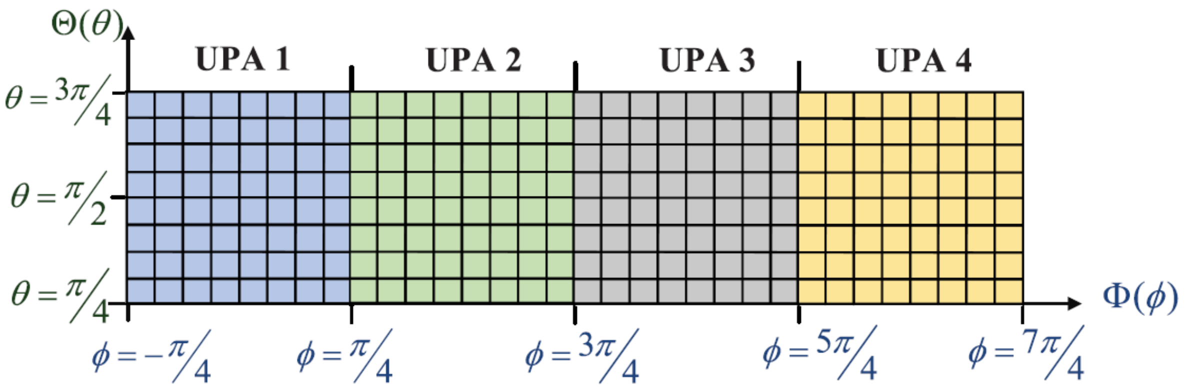


Narrow Beams

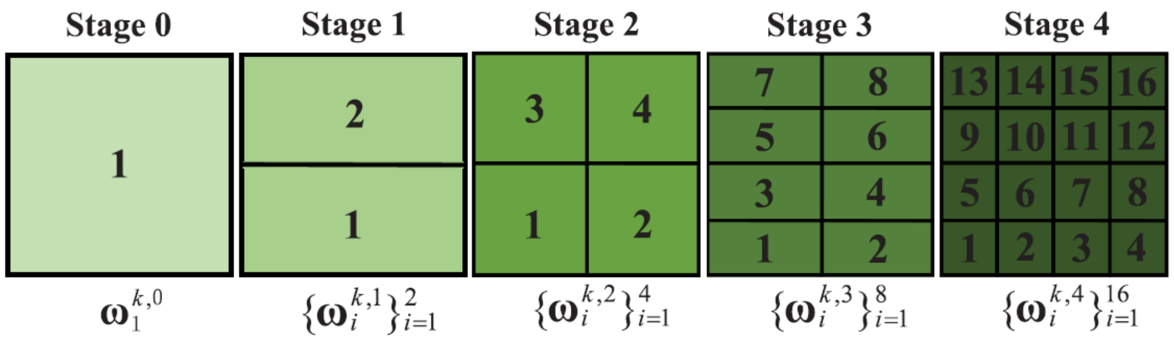


Wide Beams



B. Ning, Z. Chen, Z. Tian, C. Han, and S. Li, "A unified 3D beam training and tracking procedure for terahertz communication," IEEE Trans. Wireless Commun., Sep. 2021.

# Beam Training

## Protocol for 3D Beams

- For THz UM-MIMO system with QUPA architecture, we proposed a grid-based (GB) training protocol.

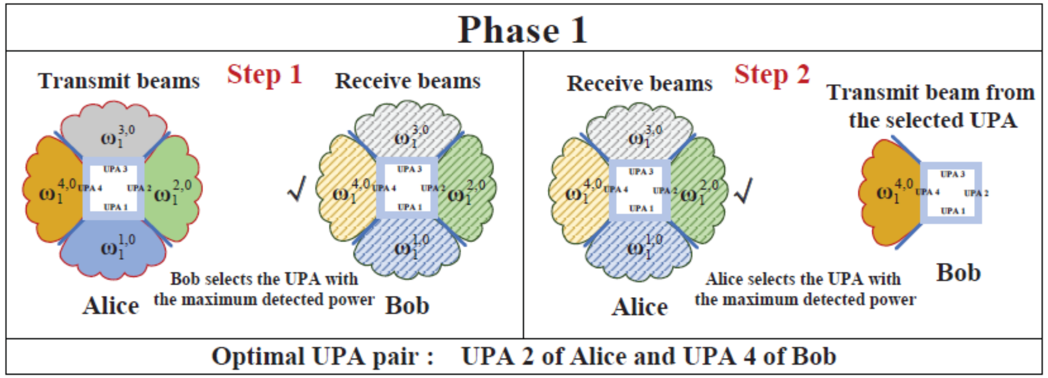


### Phase 1: Find the optimal array pair

The proposed beam training has a time complexity of $4\log_2 N^2 + 4$.

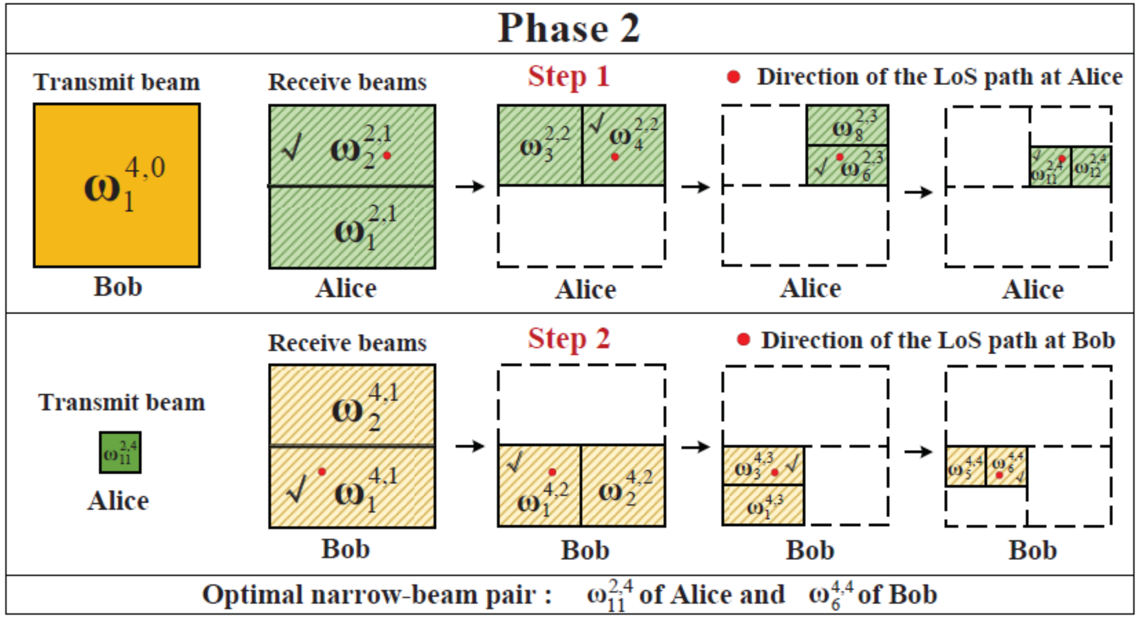


### Phase 2: Find the optimal narrow beam pair



B. Ning, Z. Chen, Z. Tian, C. Han, and S. Li, "A unified 3D beam training and tracking procedure for terahertz communication," IEEE Trans. Wireless Commun., Sep. 2021.

## Beam Training and Tracking

After a successful beam alignment by training protocol, we can apply the tracking protocol by leveraging the prior information of aligned beams, which helps to reduce the training overhead.

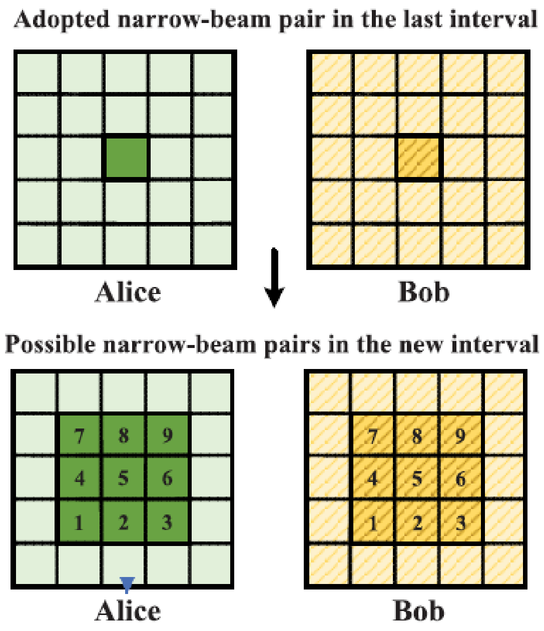


Tracking Mode 1

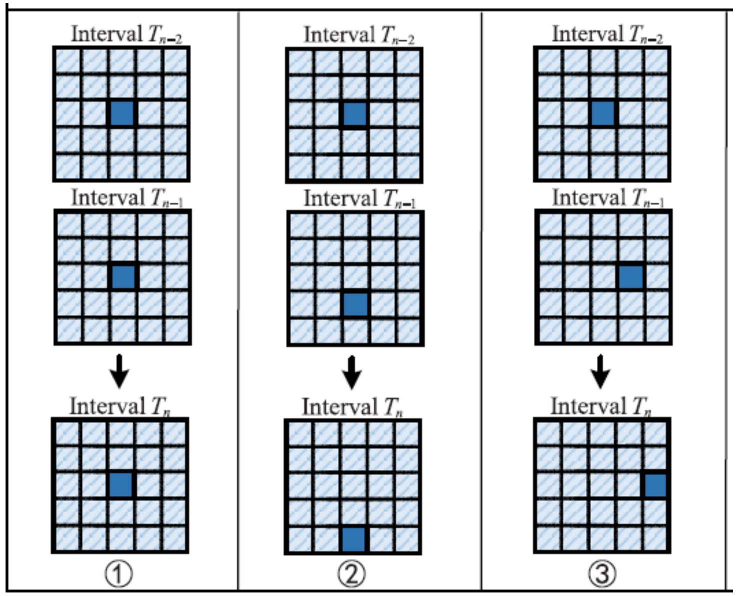


Tracking Mode 2

**Mode 1: Only know the last beam pair**

**We need 12 beam tests to find the beam pair in the 9x9 pairs.**

**Mode 2: know the last two beam pairs**

**We only need one beam test, but not stable.**

**Mode 1 is stable  Mode 2 is faster.**

Chong Han, Linglong Dai, and Zhi Chen ©

B. Ning, Z. Chen, Z. Tian, C. Han, and S. Li, "A unified 3D beam training and tracking procedure for terahertz communication," IEEE Trans. Wireless Commun., Sep. 2021.

# Unified Procedure for Training and Tracking

## A unified procedure combines the training and tracking protocols.

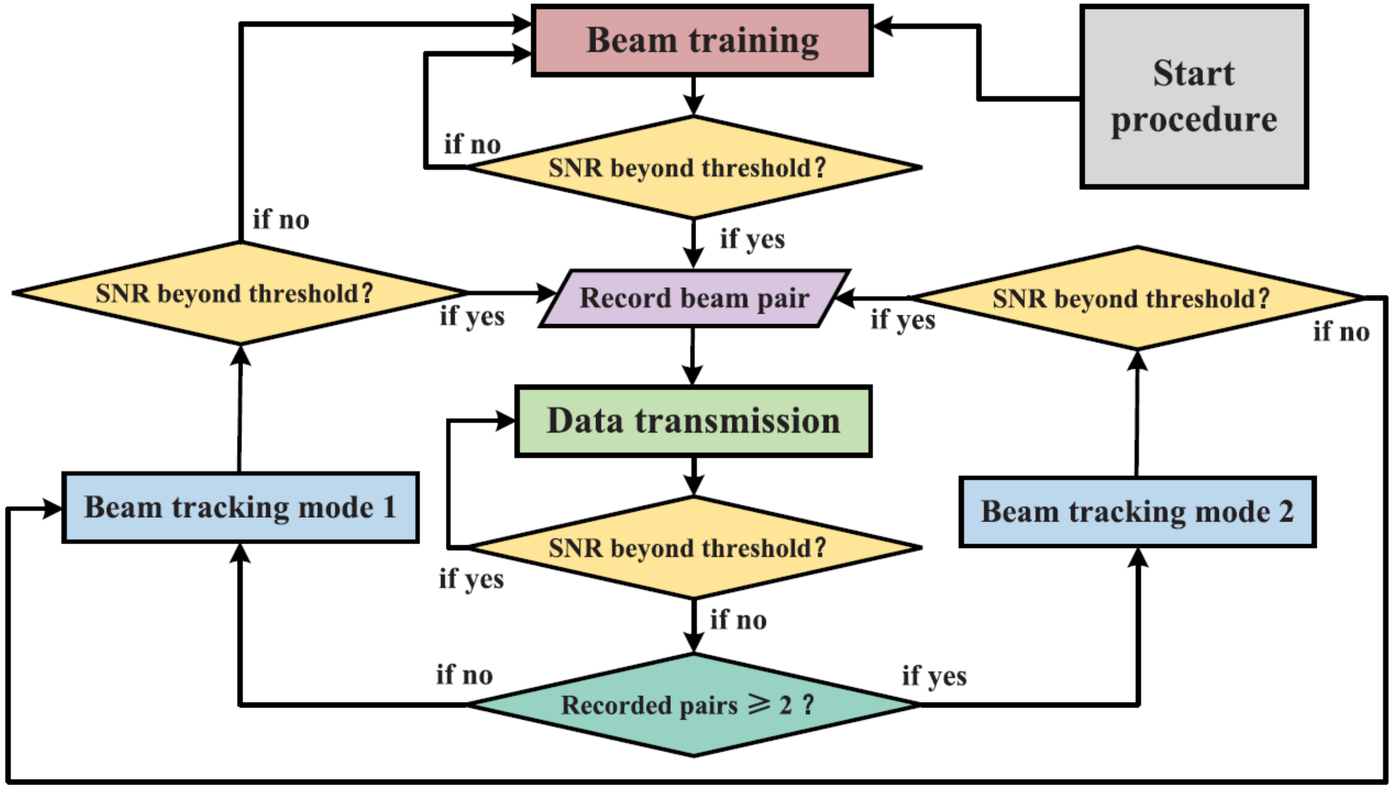


- Our proposed procedure adopts dynamic on-demand beam training/tracking depending on the real-time quality of service.
- If tracking mode 2 failed, this procedure subsequently applies tracking mode 1.



B. Ning, Z. Chen, Z. Tian, C. Han, and S. Li, **"A unified 3D beam training and tracking procedure for terahertz communication,"** IEEE Trans. Wireless Commun., Sep. 2021.

# Beam Training Codebook

## Codebook Design

Codebook design aims to optimize the weights of each codeword to make its **beam pattern** cover the zone specified by the protocol.

## Beam pattern:

Beam pattern is characterized by the magnitude (or power) of the array factor, i.e.,

$$g(\phi, \mathbf{w}) = \left| \mathbf{w}^H \mathbf{a}(\phi) \right|, \quad \phi \in \left[ -\frac{\pi}{2}, \frac{\pi}{2} \right]$$

- In the training protocol, the narrow beams in the bottom stage can be set as array response vectors whereas the **wide-beam design** is an **open problem**.



B. Ning, Z. Tian, W. Mei, Z. Chen, C. Han, S. Li, J. Yuan, and R. Zhang, **"Beamforming technologies for ultra-massive MIMO in terahertz communications,"** IEEE O. J. ComSoc., 2023.

# Beam Training Codebook

## Codebook Design

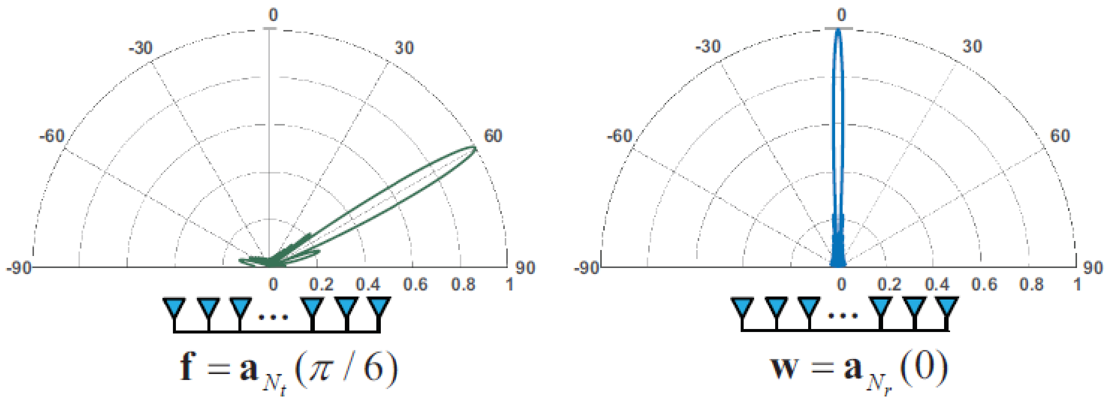


**Narrow Beam Patterns**

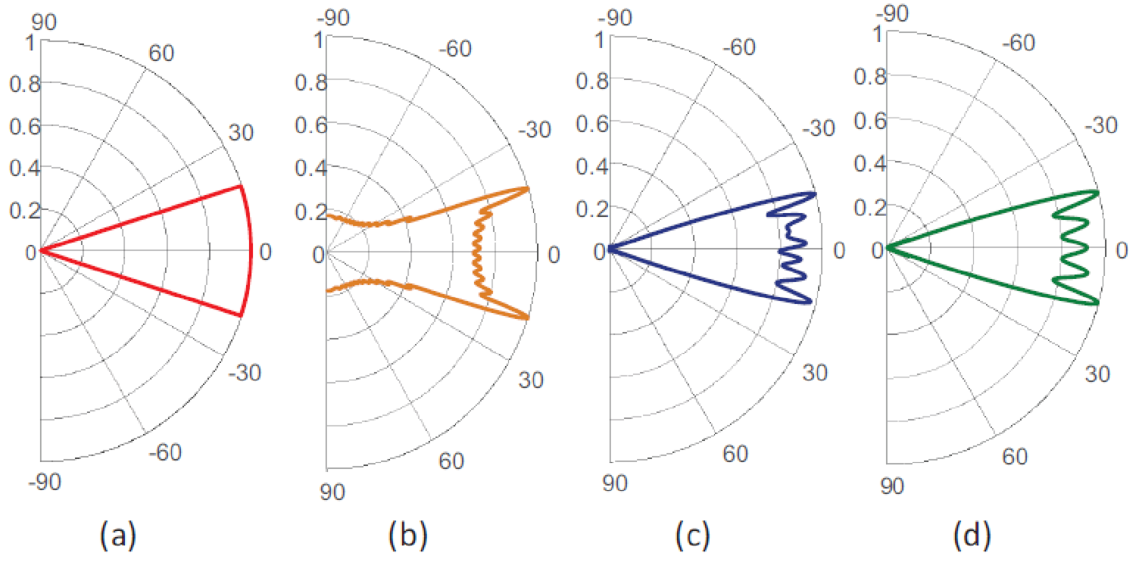


**Wide Beam Patterns**

Nt=32: (a) ideal beam pattern. (b) beam pattern by ROP. (c) beam pattern in COP. (d) beam pattern by SNB-GP


(b) A. Alkhateeb, O. E. Ayach, G. Leus, and R. W. Heath, **"Channel estimation and hybrid precoding for millimeter wave cellular systems,"** **IEEE J. Sel. Topic Signal Process., vol. 8, no. 5, pp. 831–846, Oct. 2014.**

(c) K. Chen, C. Qi, and G. Y. Li, **"Two-step codeword design for millimeter wave massive MIMO systems with quantized phase shifters,"** **IEEE Trans. Signal Process., vol. 68, pp. 170–180, 2020.**

(d) S. Noh, M. D. Zoltowski, and D. J. Love, **"Multi-resolution codebook and adaptive beamforming sequence design for millimeter wave beam alignment,"** **IEEE Trans. Wireless Commun., vol. 16, no. 9, pp. 5689–5701, Sep. 2017.**

# Codebook Optimization

Existing approaches are heuristic, we proposed a optimization-based method, which is referred to as successive convex approximation (SCA)-based auxiliary target pursuit (SCA-ATP).

To tackle this problem, we propose a BPE metric to characterize the gap between the practical beam pattern and the ideal one. Specifically, given a codeword $\boldsymbol{\omega}(\theta^-, \theta^+)$, its BPE can be expressed as

$$\begin{aligned}
&\varepsilon\left\{\boldsymbol{\omega}(\theta^-, \theta^+)\right\} \\
&\triangleq \int_{\varphi\in[\theta^-,\theta^+]} \left|\gamma - \left|\mathbf{a}_{N_t}(\varphi)^H \boldsymbol{\omega}(\theta^-, \theta^+)\right|\right|^2 d\varphi \\
&+ \int_{\varphi\in[\theta_*^-,\theta^-]\cup[\theta^+,\theta_*^+]} \left|\mu(\varphi) - \left|\mathbf{a}_{N_t}(\varphi)^H \boldsymbol{\omega}(\theta^-, \theta^+)\right|\right|^2 d\varphi \\
&+ \int_{\varphi\in[-\frac{\pi}{2},\theta_*^-]\cup[\theta_*^+,\frac{\pi}{2}]} \left|\mathbf{a}_{N_t}(\varphi)^H \boldsymbol{\omega}(\theta^-, \theta^+)\right|^2 d\varphi,
\end{aligned}$$

where $\mu(\varphi) \in \mathbb{R}$ is an arbitrary real variable with $0 \leq \mu(\varphi) \leq \gamma$. Hence, the wide-beam realization problem can be formulated as

$$\begin{aligned}
(\mathrm{P1}):\quad &\min_{\boldsymbol{\omega}(\theta^-,\theta^+),\ \mu(\varphi)} \quad \varepsilon\left\{\boldsymbol{\omega}(\theta^-, \theta^+)\right\} \\
&\text{s.t.}\quad 0 \leq \mu(\varphi) \leq \gamma, \quad \varphi \in [\theta_*^-, \theta^-] \cup [\theta^+, \theta_*^+].
\end{aligned}$$

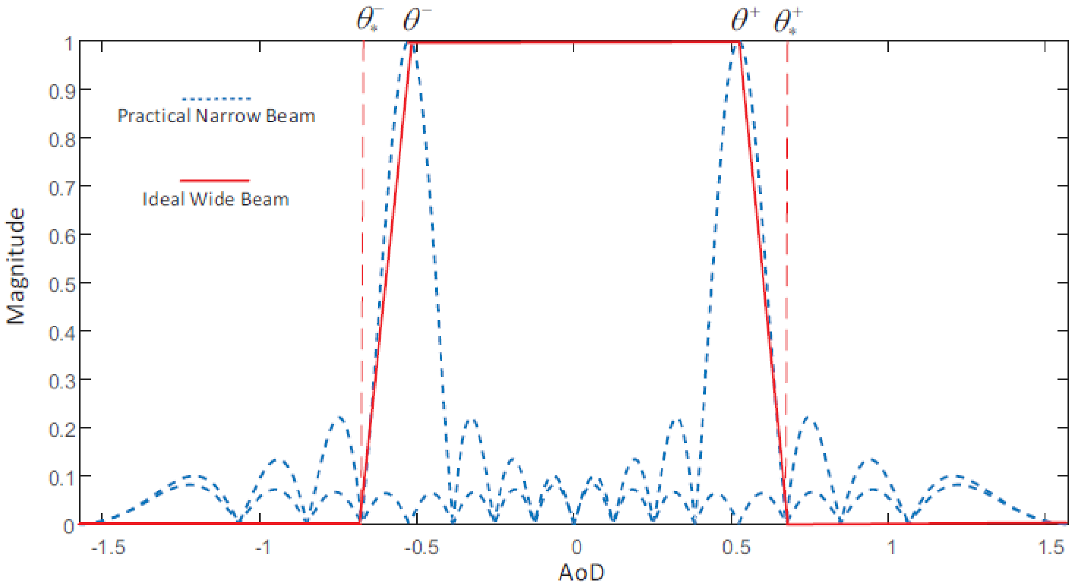

## Codebook Design

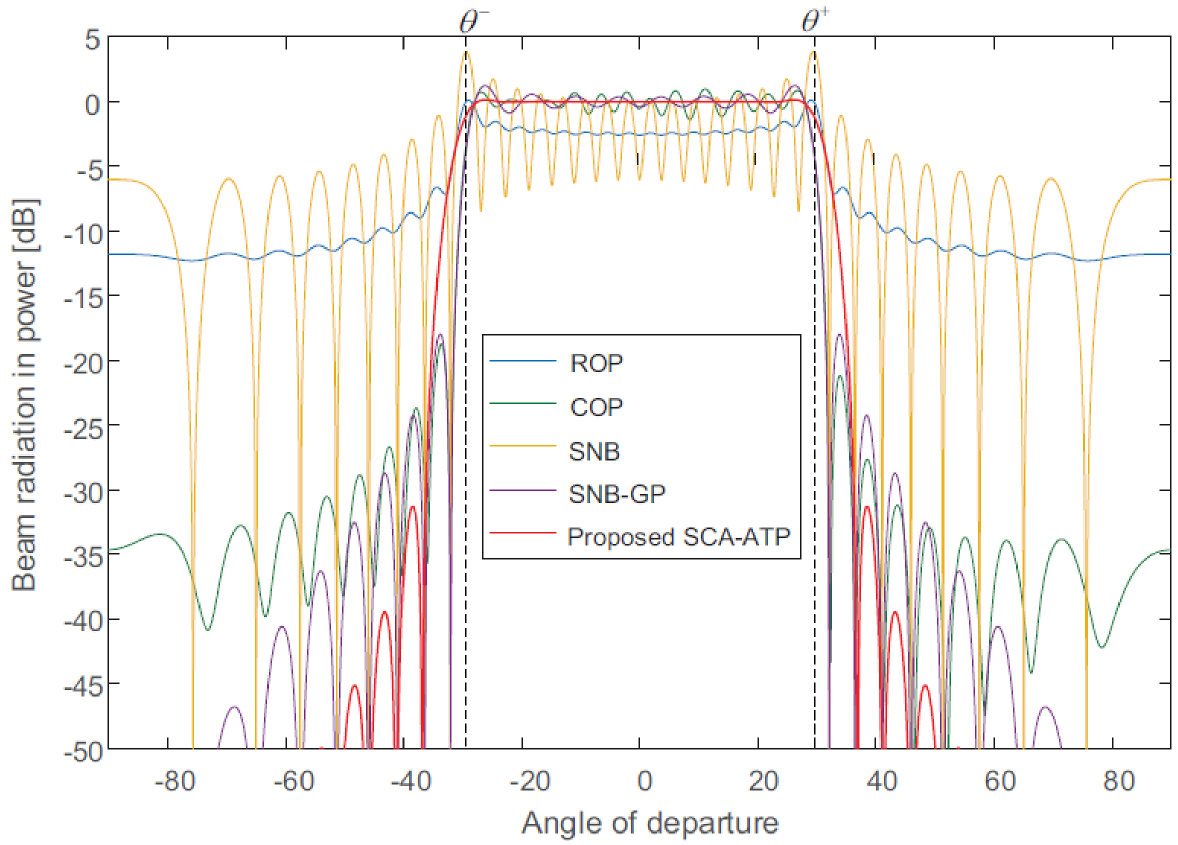


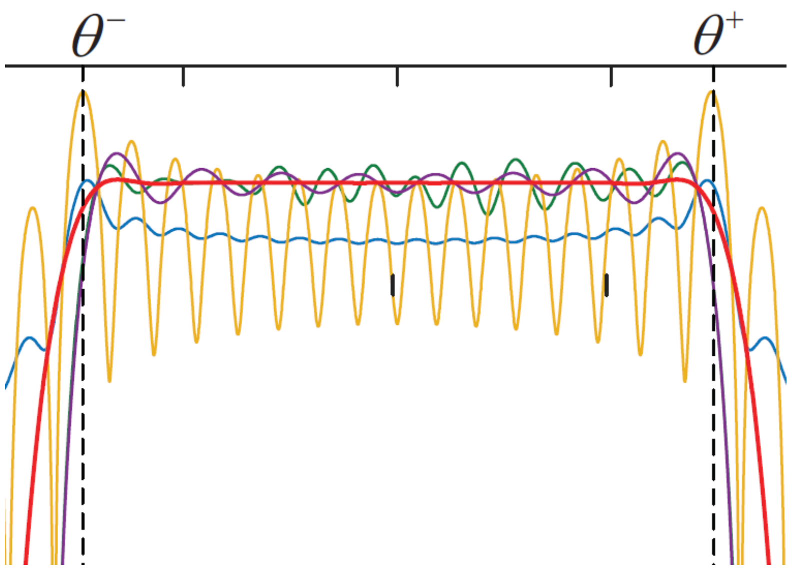


The beam pattern via SCA-ATP has a flatter main lobe and decent side-lobe suppression



B. Ning and Z. Chen, **"An optimization-based wide-beam design for THz MIMO,"** in **IEEE Global Commun. Conf., Rio de Janeiro, Brazil, 2022.**

# Codebook Optimization

## Codebook Design

Although **SCA-ATP** yields a good performance, it cannot be used for real-time design due to the high complexity. In sight of this, we further propose an **S-SARV** method for the real-time design as a low-complexity solution.

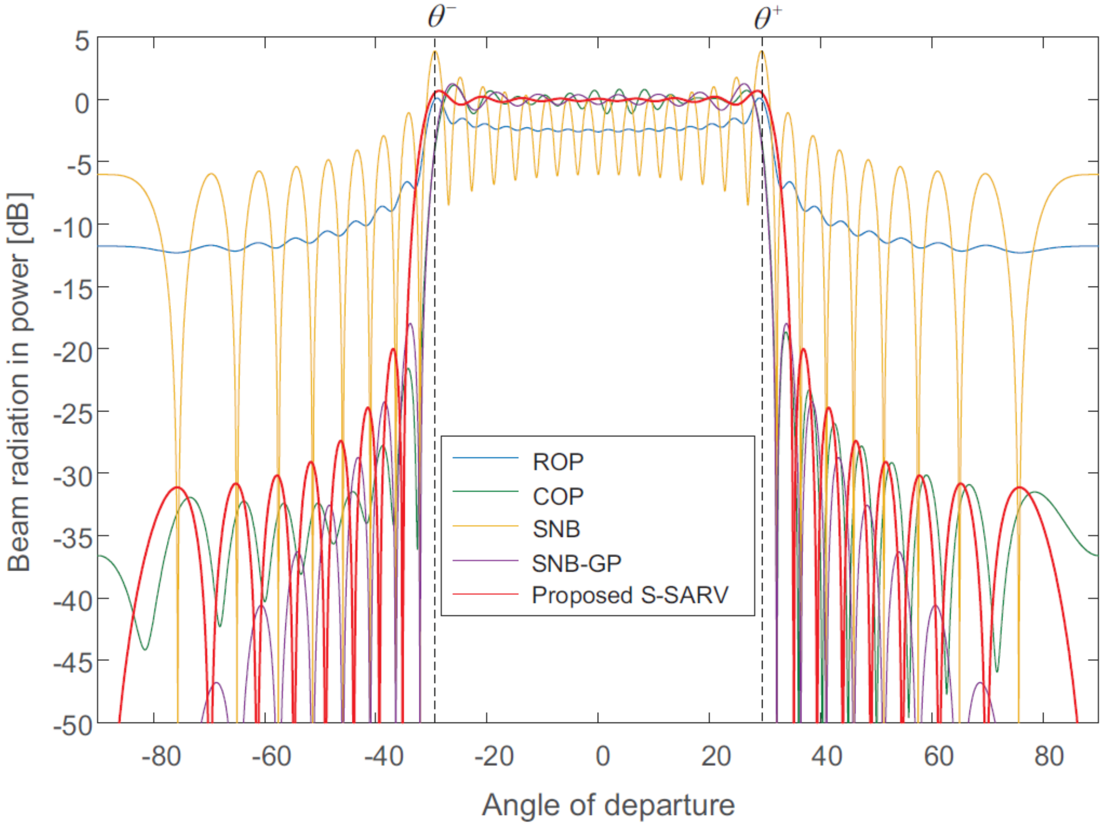


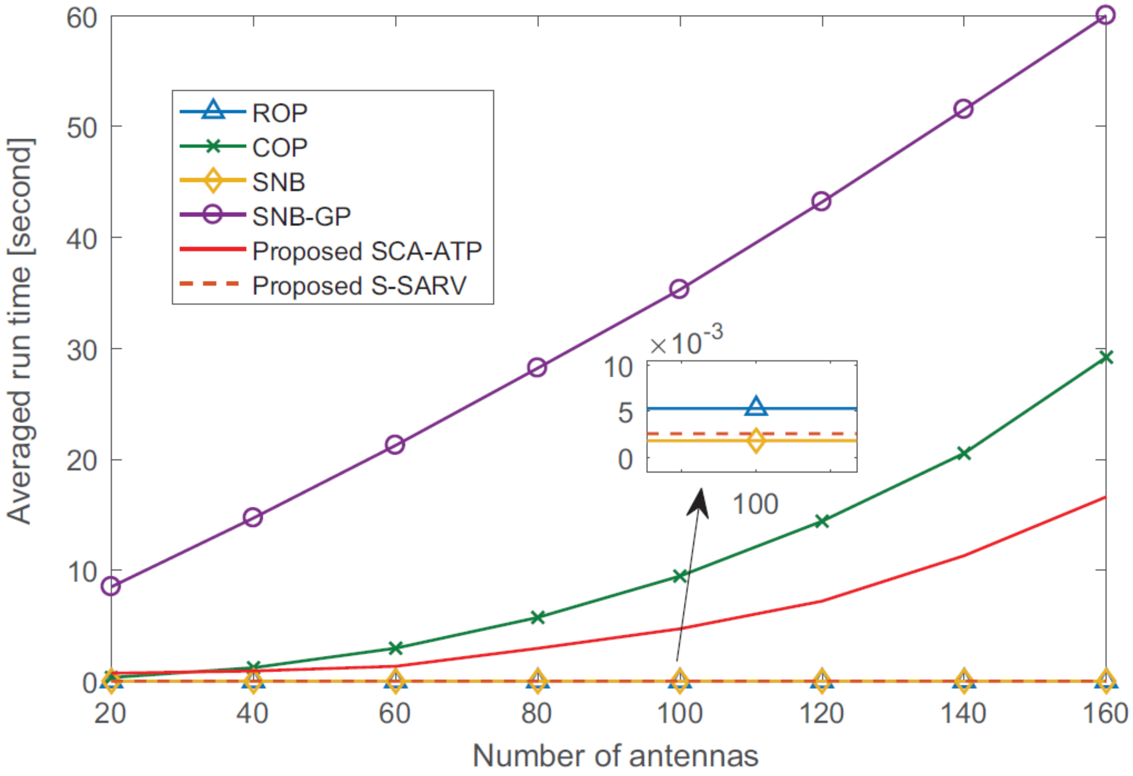




B. Ning, T. Wang, C. Huang, Y. Zhang, and Z. Chen, **"Wide-beam designs for terahertz massive MIMO: SCAATP and S-SARV,"** IEEE Internet of Things J., **2023.**

# Codebook Optimization

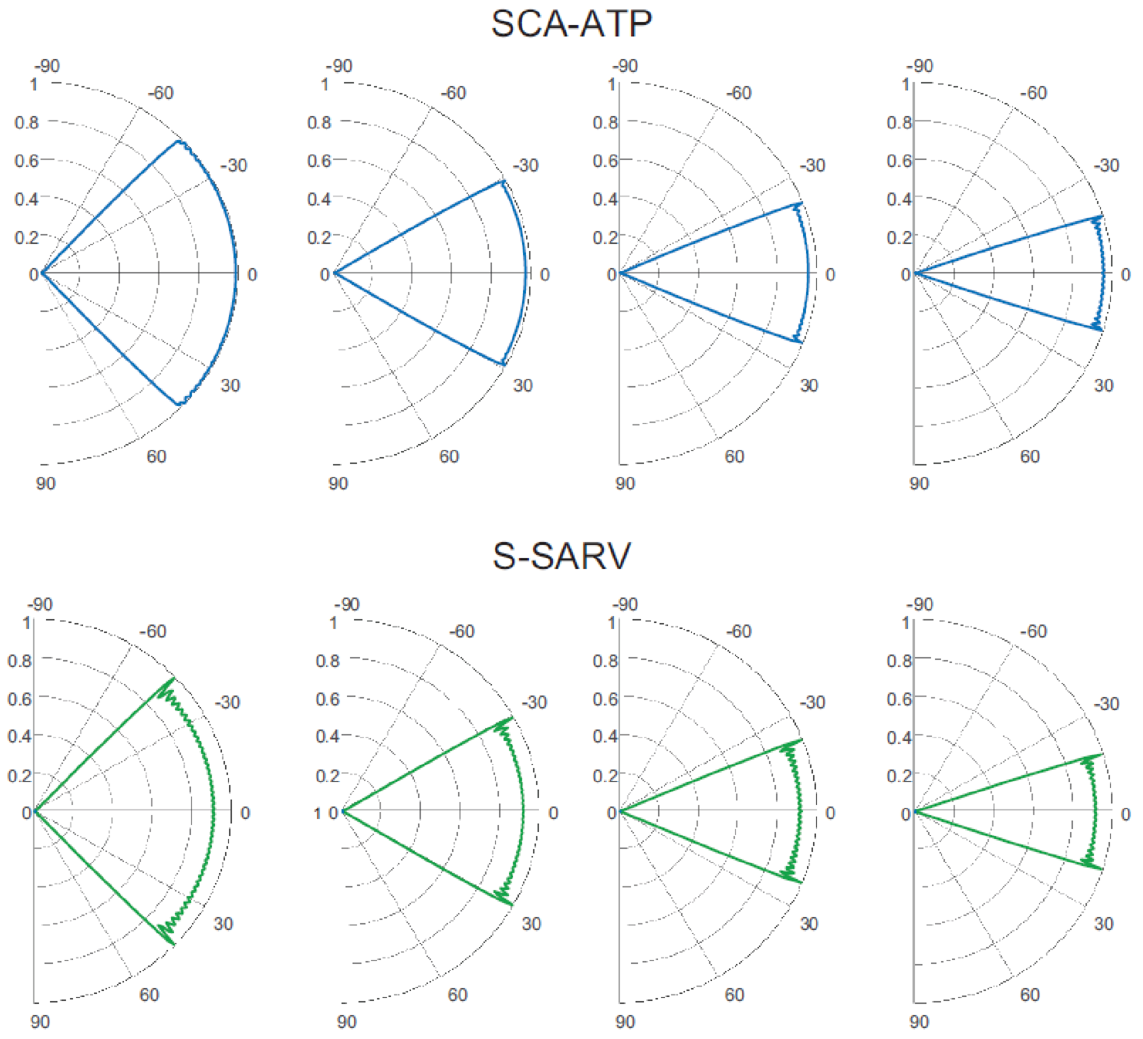


TABLE X
COMPARISON OF THE WIDE-BEAM APPROACHES.
MORE ⋆ REPRESENTS LOWER COMPLEXITY OR HIGHER PERFORMANCE

| Wide-beam approaches | Complexity | Performance |
|---|---|---|
| ROP [135] | ⋆⋆⋆⋆⋆ | ⋆⋆ |
| COP [136] | ⋆⋆ | ⋆⋆⋆⋆ |
| SNB [137] | ⋆⋆⋆⋆⋆ | ⋆ |
| SNB-GP [119] | ⋆ | ⋆⋆⋆⋆ |
| SCA-ATP [138] | ⋆⋆⋆ | ⋆⋆⋆⋆⋆ |
| S-SARV [139] | ⋆⋆⋆⋆⋆ | ⋆⋆⋆⋆ |

To the best of our knowledge, the beam pattern of the SCA-ATP is closest to the ideal one, and the S-SARV is the best approach to balance the performance and computational complexity.

B. Ning, T. Wang, C. Huang, Y. Zhang, and Z. Chen, **"Wide-beam designs for terahertz massive MIMO: SCAATP and S-SARV,"** IEEE Internet of Things J., **2023**.

Chong Han, Linglong Dai, and Zhi Chen ©

# Beam Estimation

Process the received signal after beam training to obtain the accurate estimated beam direction

## Target

Millidegree-level DoA estimation
Millisecond-level DoA tracking

## Existing solutions

On-grid: estimation accuracy restricted by the grid resolution ✘
Off-grid: cannot be directly applied to different hybrid beamforming architectures ✘

Received signal: $\mathbf{y} = \mathbf{W}^{\mathrm{H}}\mathbf{H}[f,r,k]\mathbf{F}\mathbf{s} + \mathbf{W}^{\mathrm{H}}\mathbf{n},$

THz channel: $\mathbf{H}[f,r,k] = \sum_{\ell=1}^{L} \alpha_\ell[f,r,k]\mathbf{a}_r(\theta_{\ell,r}[k],\phi_{\ell,r}[k])\mathbf{a}_t(\theta_{\ell,t}[k],\phi_{\ell,t}[k])^H = \mathbf{A}_r[k]\mathbf{\Lambda}[k]\mathbf{A}_t^H[k]$

Combining matrix: When $N_{RF} = 16, N_r = 1024,$ Compression rate is 16/1024=1.56

# DAoSA-MUSIC Beam Estimation and Tracking

## DAoSA-MUSIC estimation

Design two stage coarse and refine training and signal reconstruction to handle the combining matrix

## DAoSA-MUSIC-T tracking

Deploy correlations among tracking time slots with fifty-percent reduced training overhead

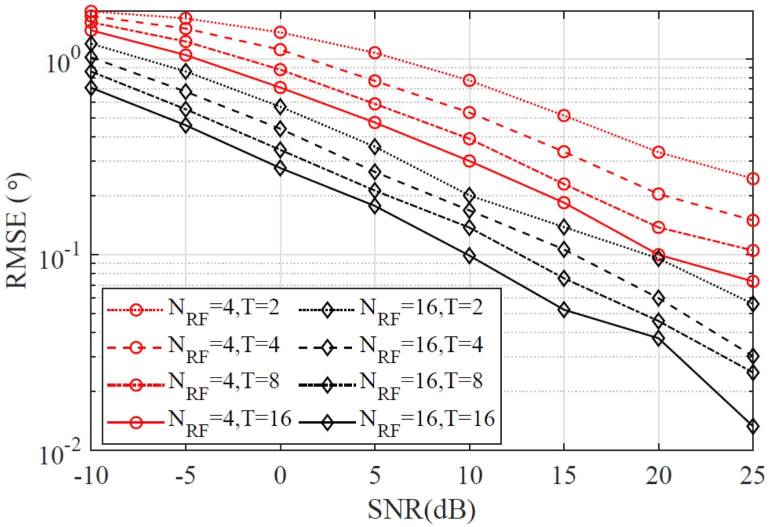


Millidegree-level estimation precision when SNR = 10 dB and $N_{RF}$=16

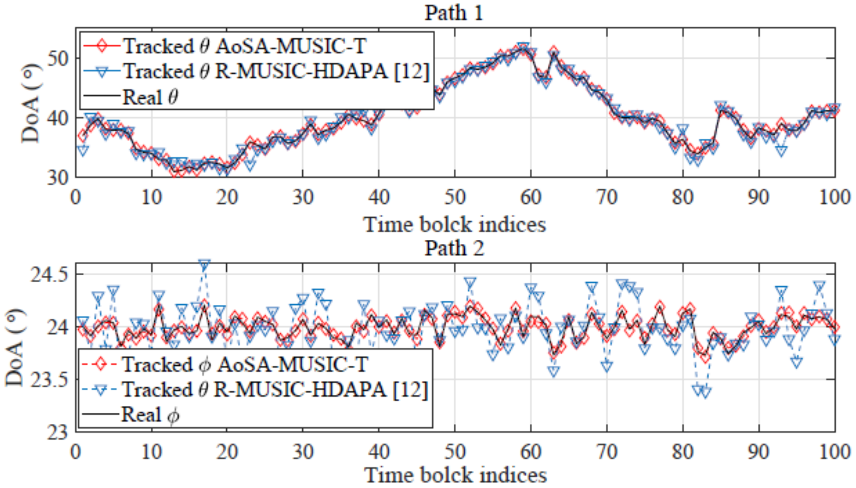




Y.-H. Chen, L. Yan, C. Han, and M. Tao, **"Millidegree-Level Direction-of-Arrival Estimation and Tracking for Terahertz Ultra-Massive MIMO Systems,"** IEEE Trans. Wireless Commun., 2022.

# DL Beam Estimation

## DCNN estimation

Design a DCNN network for DoA estimation, input the channel observation

Require coarse training only

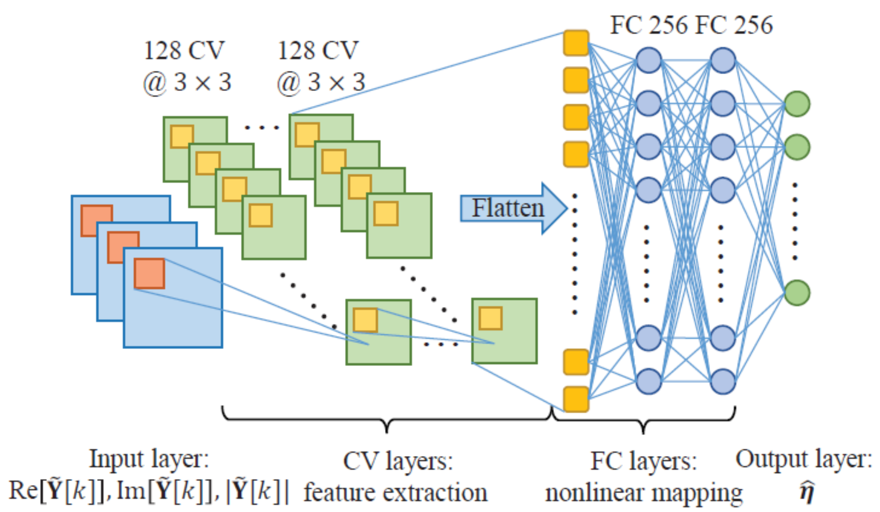


DCNN network structure

0.1° estimation precision in milliseconds with course training only

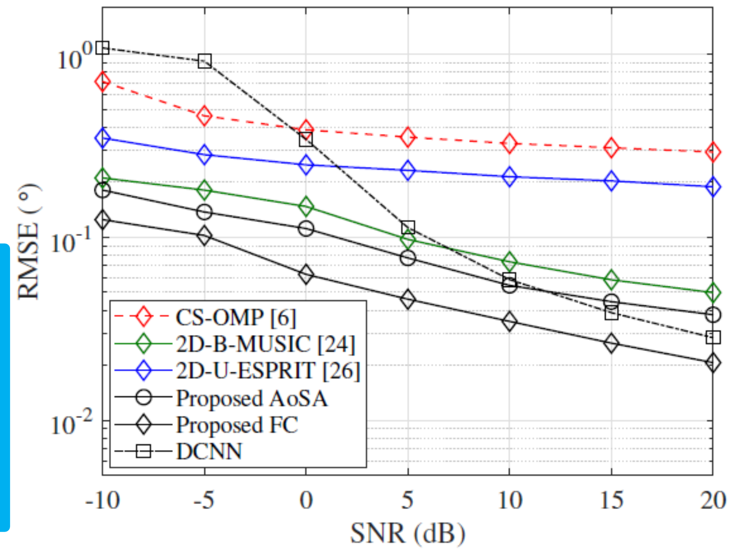


Estimation RMSE comparison



Y.-H. Chen, L. Yan, C. Han and M. Tao, **"Millidegree-Level Direction-of-Arrival Estimation and Tracking for Terahertz Ultra-Massive MIMO Systems"**, IEEE Trans. Wireless Commun., 2022.

## ConvLSTM tracking

Design a ConvLSTM network for DoA tracking

Convolution layers: extract spatial correlations

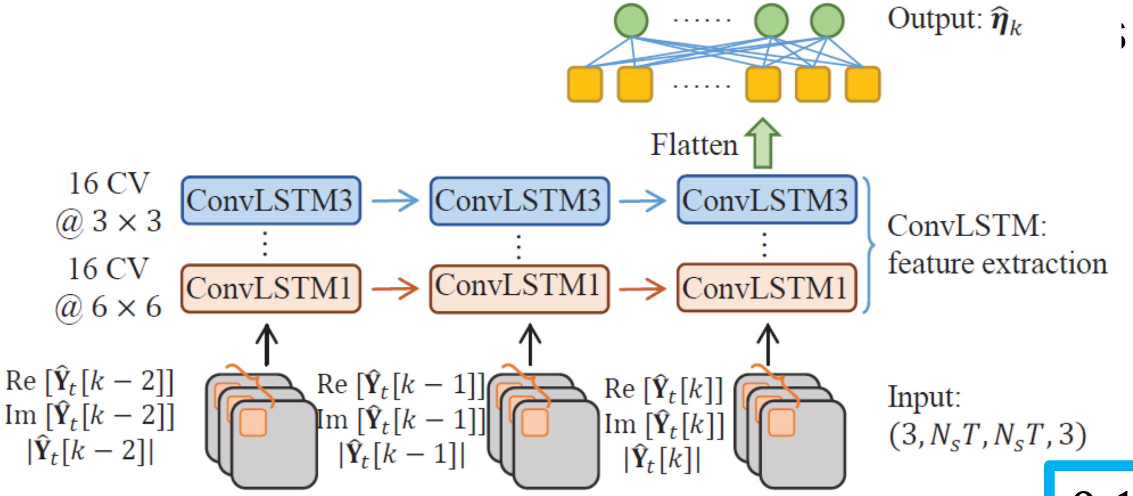


ConvLSTM network structure

0.1° tracking precision with 50% reduced training overhead in ms

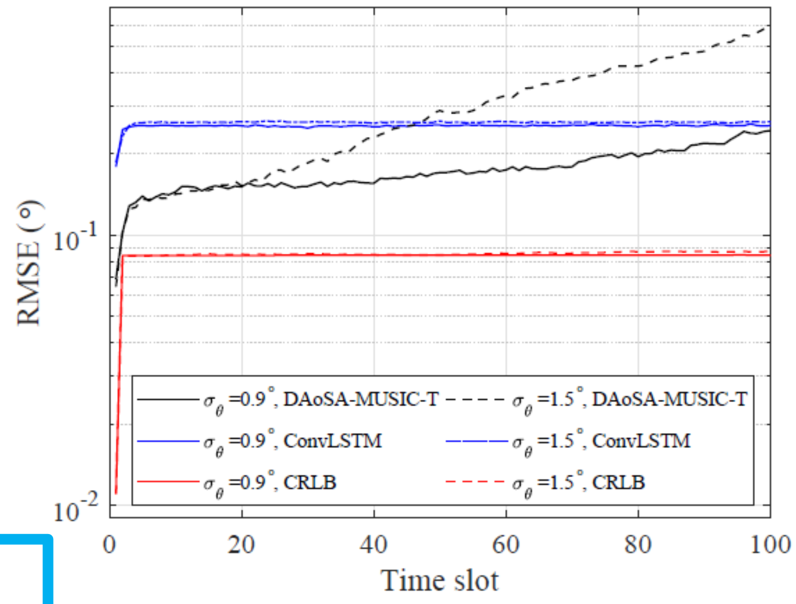


Tracking RMSE over time

Y.-H. Chen, L. Yan, C. Han and M. Tao, **"Millidegree-Level Direction-of-Arrival Estimation and Tracking for Terahertz Ultra-Massive MIMO Systems"**, IEEE Trans. Wireless Commun., 2022.

# Challenge of THz Near-Field Beam Estimation

- Existing far-field beam estimation relies on the angle-domain sparsity exploited by the orthogonal angle-domain codebook, i.e., the DFT codebook
- The near-field angle-domain channels suffer from a severe energy spread problem

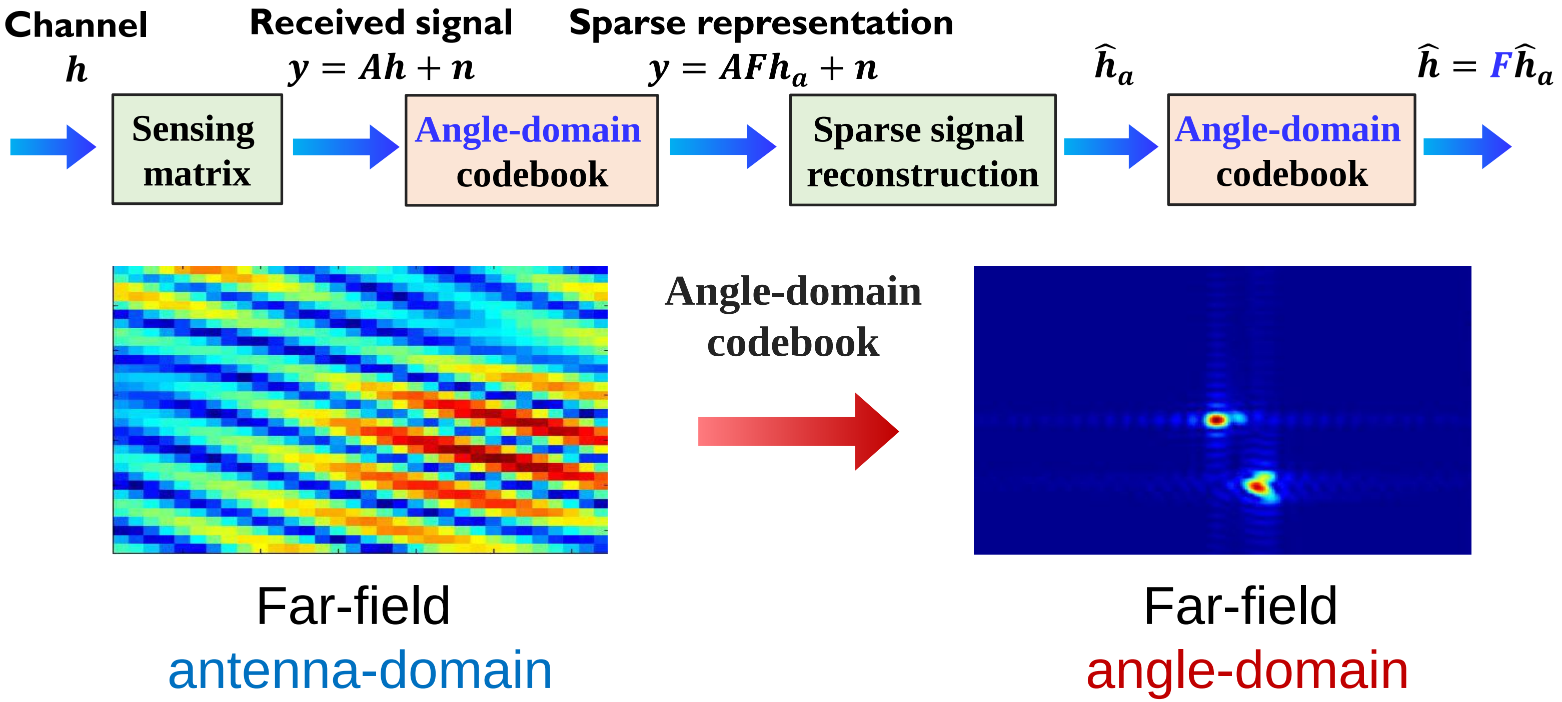


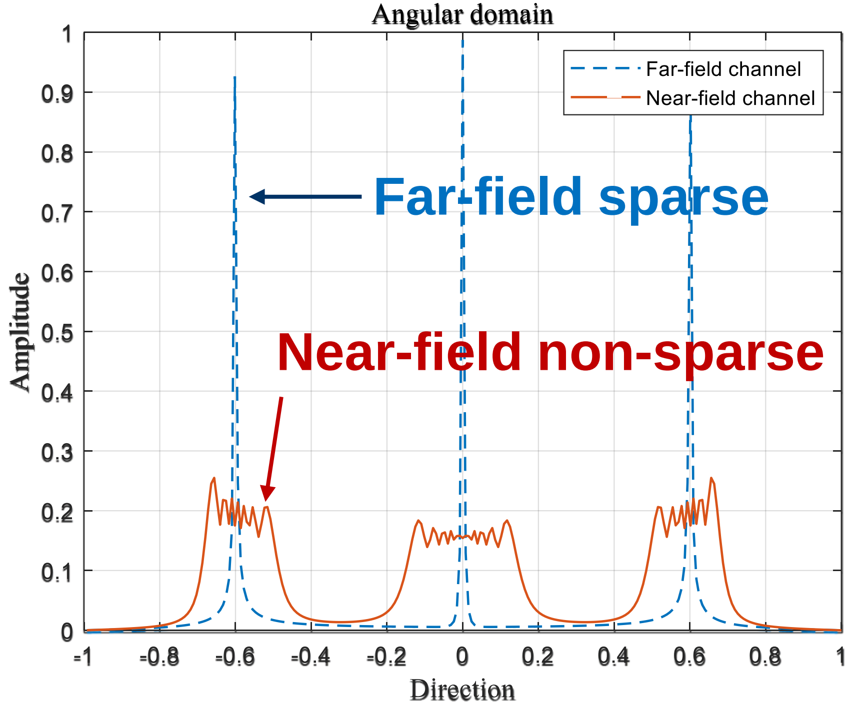


**The angle-domain codebook is not appropriate for near-field beam estimation**

# Near-Field Beam Codebook Design

- Far-field codebook: samples multiple angle grids in the angle domain
- Near-field codebook: samples multiple “angle-distance” grids in the polar domain

Angle-domain codeword $\boldsymbol{a}(\theta) = \left[e^{jn\pi\theta}\right]_{n=-N}^{N}$

Polar-domain codeword $\boldsymbol{a}(\theta, r) = \left[e^{jk\sqrt{r+n^2d^2-2rnd\theta}}\right]_{n=-N}^{N}$

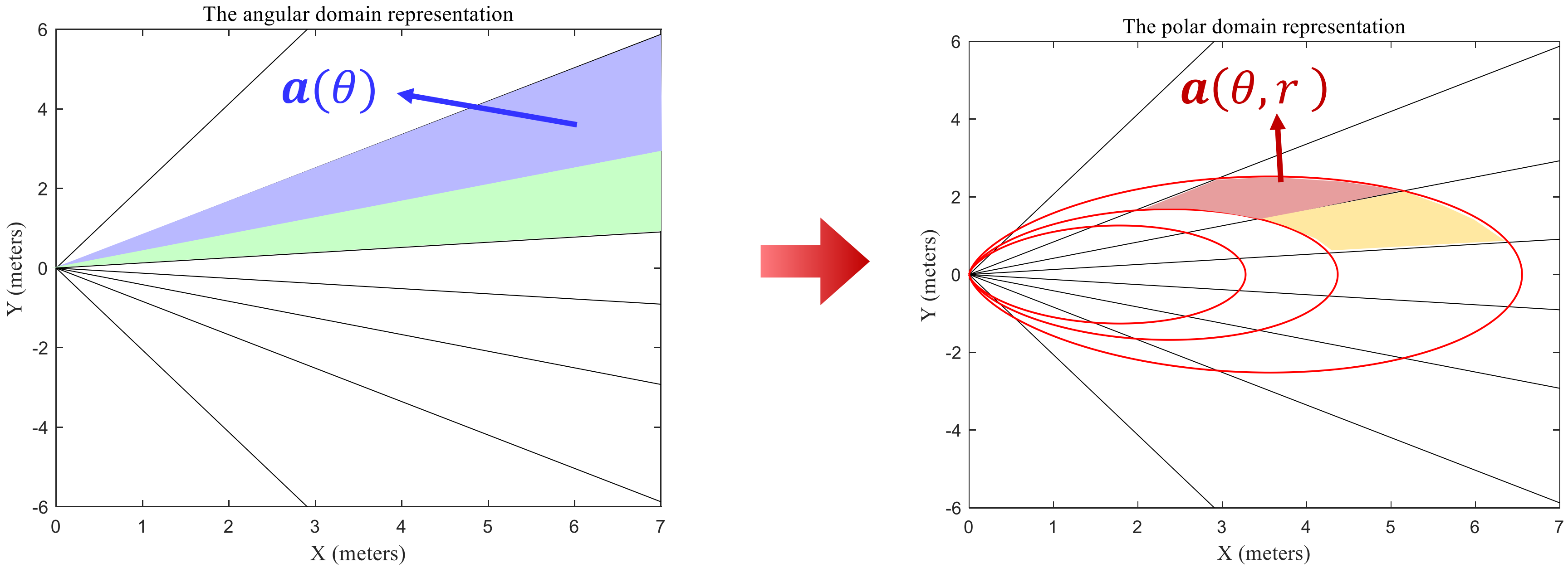


**How to design the additional distance sampling criterion in polar-domain**

Chong Han, Linglong Dai, and Zhi Chen ©

M. Cui and L. Dai, **“Channel estimation for extremely large-scale MIMO: Far-field or near-field?,”** IEEE Trans. Commun., **2022.**

# The Distance-Sampling Criterion

- With the decrease of distance, the near-field effect becomes obvious and the distance information gradually becomes significant
- To exploit the near-field information, the grids can be sampled sparsely far away from ELAA, but should be sampled densely near the ELAA

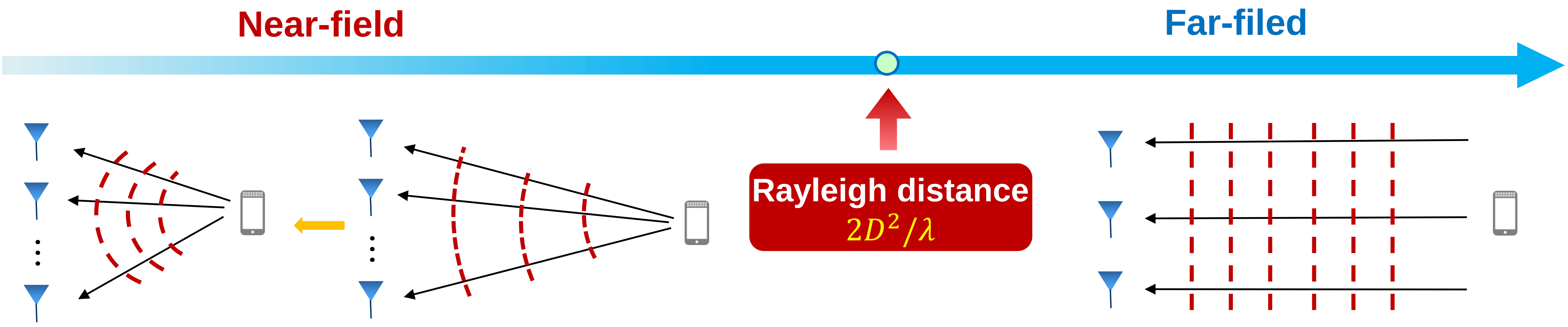


**A non-uniform distance-sampling criterion is preferred**



M. Cui and L. Dai, "Channel estimation for extremely large-scale MIMO: Far-field or near-field?," IEEE Trans. Commun., 2022.

# Polar-Domain Codebook Based Beam Estimation

- Codebook design method: minimizing the largest mutual coherence of the codebook
- Based on the Fresnel approximation, we prove the following sampling criteria

**Uniform angle sampling:** $\theta_n = \frac{2n}{N} - \frac{N+1}{N}, \qquad n = \{1,2,\cdots,N\}$

**Non-uniform distance sampling:** $r_{n,s} = \frac{1}{s}(1-\theta_n^2)Z_\Gamma, \ s = \{1,2,\cdots,S\}, \ Z_\Gamma = \frac{M^2 d^2}{2\lambda\beta_\Gamma^2}$

The number of sampled distances

- The polar-domain codebook can be constructed as

$$\boldsymbol{P}_n = [\boldsymbol{a}(\theta_n, r_{n,1}), \boldsymbol{a}(\theta_n, r_{n,2}), \cdots, \boldsymbol{a}(\theta_n, r_{n,S})] \qquad \boldsymbol{P} = [\boldsymbol{P}_1, \boldsymbol{P}_2, \cdots, \boldsymbol{P}_N]$$

- Polar-domain codebook based near-field beam estimation

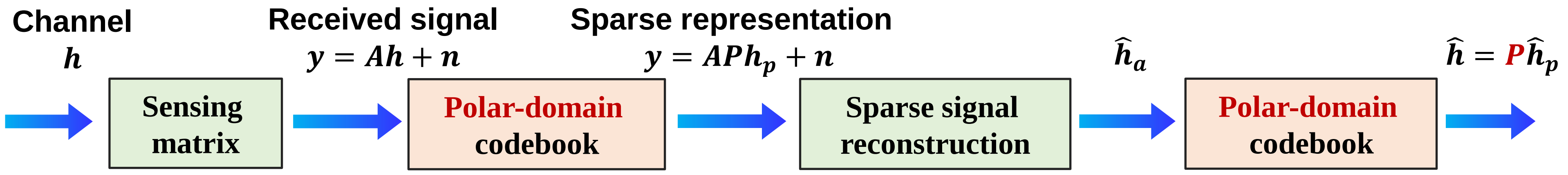




M. Cui and L. Dai, "Channel estimation for extremely large-scale MIMO: Far-field or near-field?," IEEE Trans. Commun., 2022.

# Simulation Result

- NMSE vs. Distance

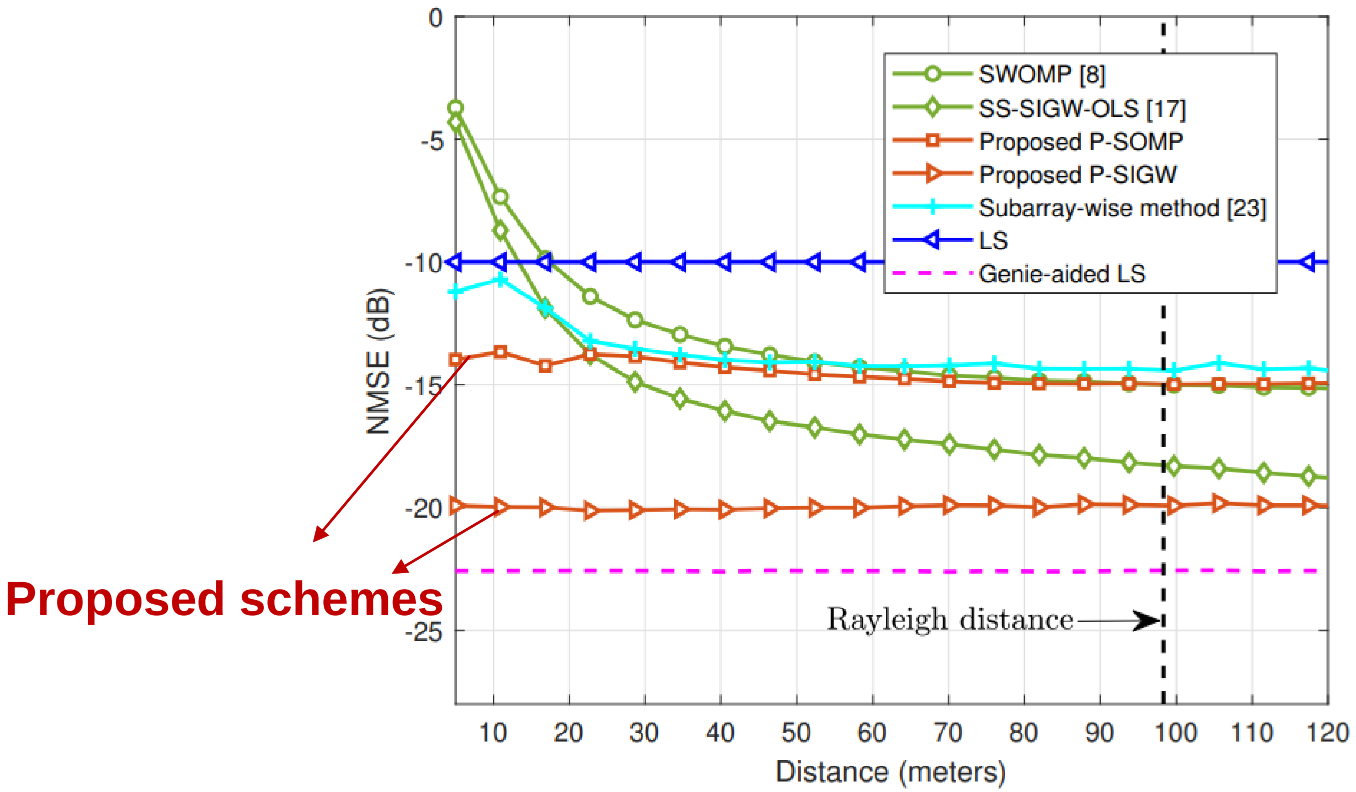


| Parameter | Value |
| --- | --- |
| Carrier | 100 GHz |
| Bandwidth | 400 MHz |
| Number of carriers | 1024 |
| Array Aperture | 0.4 m |
| SNR | 10 dB |
| Pilot overhead | 0.5 |

**Polar-domain codebook considerably improves the estimation accuracy in near-field**



M. Cui and L. Dai, "Channel estimation for extremely large-scale MIMO: Far-field or near-field?," IEEE Trans. Commun., 2022.

# Challenge of THz Cross-field Beam Alignment

- **Far-field beam alignment only in angle domain**

$$\mathbf{w}(\theta) = exp\left(-j\frac{2\pi}{\lambda}ndsin\theta\right)\Big|_{n=0}^{N-1}$$

  - $\theta$: angle

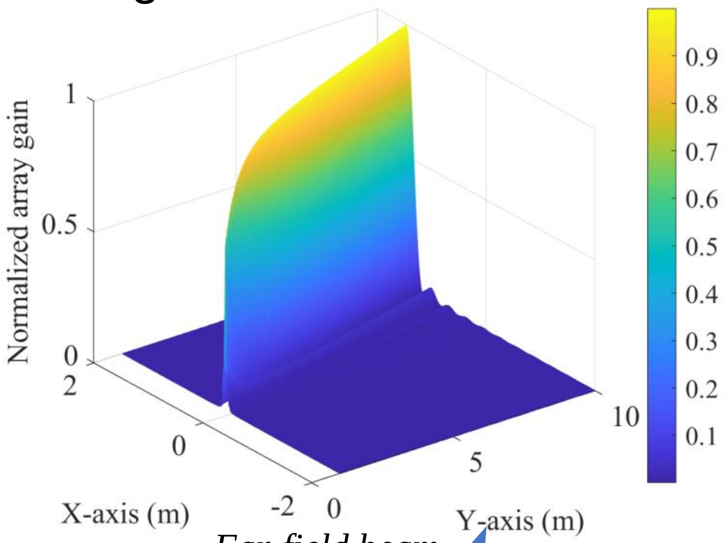


*Far-field beam*

**$N^2$ dimensional angle search**

- **Near-field beam alignment in both angle and distance domains**

$$\mathbf{w}(r,\theta) = exp\left(-j\frac{2\pi}{\lambda}\sqrt{r + n^2d^2 - 2rndsin\theta}\right)\Big|_{n=0}^{N-1}$$

  - $\theta$: angle
  - $r$: distance

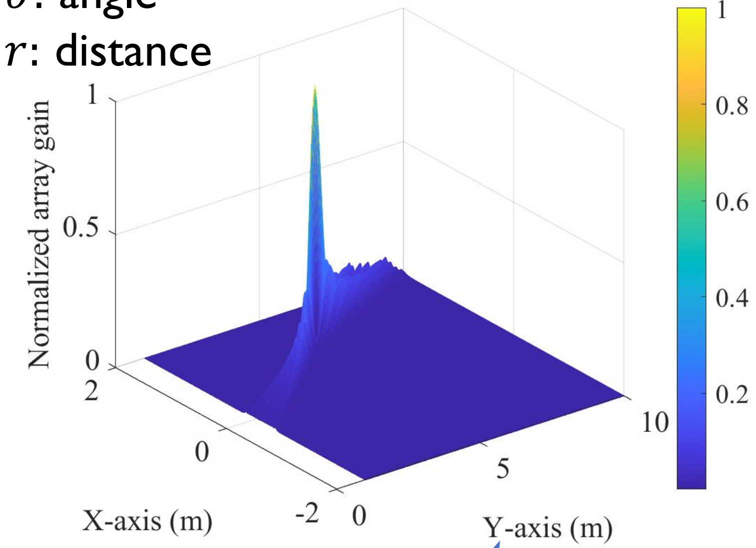


*Near-field beam*

**$N^2D^2$ dimensional angle and distance search**

*N, D: number of beams in the angle and distance domains*

**Require efficient cross-field beam management method with high accuracy**



C. Han et al., **"Cross Far- and Near-field Wireless Communications in Terahertz Ultra-large Antenna Array Systems,"** IEEE Wireless Commun., 2023.

# Far-field Training with Estimation

- **Far-field training**
  - Aim of beam training: create directional beam with enhanced SNR to scan the spatial domain
    - Large propagation losses in THz band, the SNR is low without directional beams
  - Although without distance alignment, far-field beam for training can be used in near-field as well, with sufficient SNR
- **Beam estimation**
  - At short distance: exist SNR gap by using far-field and near-field beams due to distance domain beam misalignment
  - Require low overhead beam management for precise distance and angle alignment

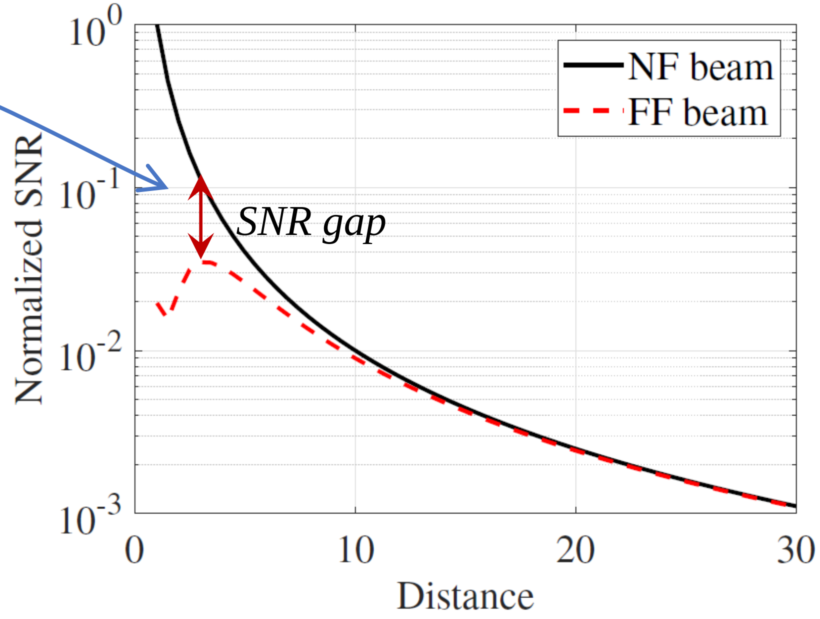


*Compared to near-field (NF) beams, far-field (FF) beams enable enough SNR for training in near- and far-field*


Y. Chen, C. Han, H. Liu, and E. Bjornson, **"Far-Field Training With Estimation for Cross-Field Beam Alignment in Terahertz UM-MIMO Systems,"** IEEE GLOBECOM, 2023.

# Performance Evaluation

- **Alignment performance**
  - TPBE achieves near-perfect spectral efficiency, 0.1 bps/Hz lower than alignment with true channel at SNR = 0 dB

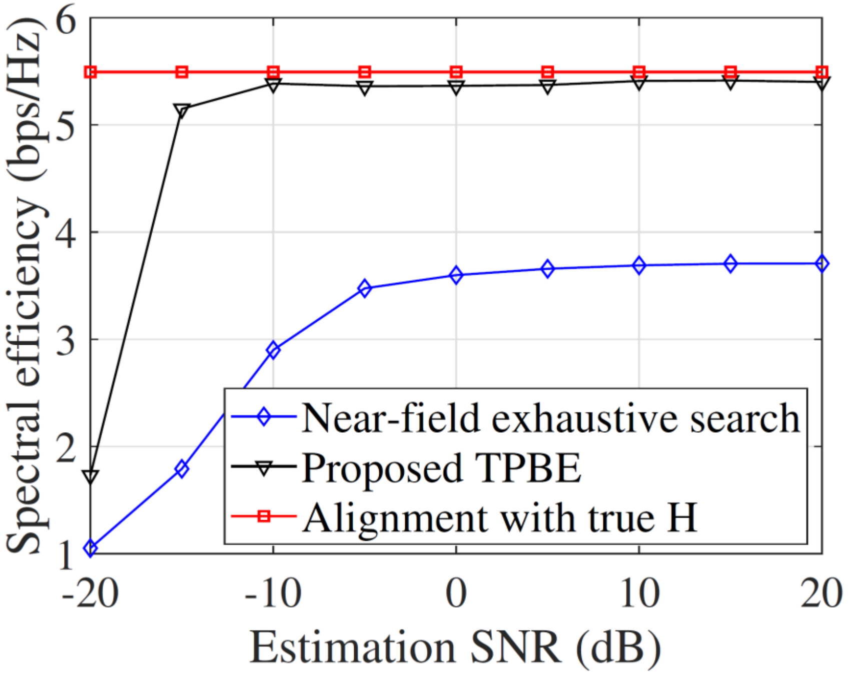


- **Training overhead**
  - 30 times reduced training overhead

| Method | **Near-field exhaustive search** | Far-field exhaustive search | **Proposed TPBE** |
|---|---|---|---|
| Training overhead | $\boldsymbol{N_b N_u C_d}$ | $N_b N_u$ | $\boldsymbol{N_b N_u}$ |

$C_d$ = 30 times reduced



Y. Chen, C. Han, H. Liu, and E. Bjornson, **"Far-Field Training With Estimation for Cross-Field Beam Alignment in Terahertz UM-MIMO Systems,"** IEEE GLOBECOM, 2023.

# Challenge of THz Beam Tracking

- Beam tracking:
  - ➢ Align the beam with a mobile user
- Technical challenge
  - ➢ The extremely narrow beam makes the pilot overhead of classical THz beam training unaffordable

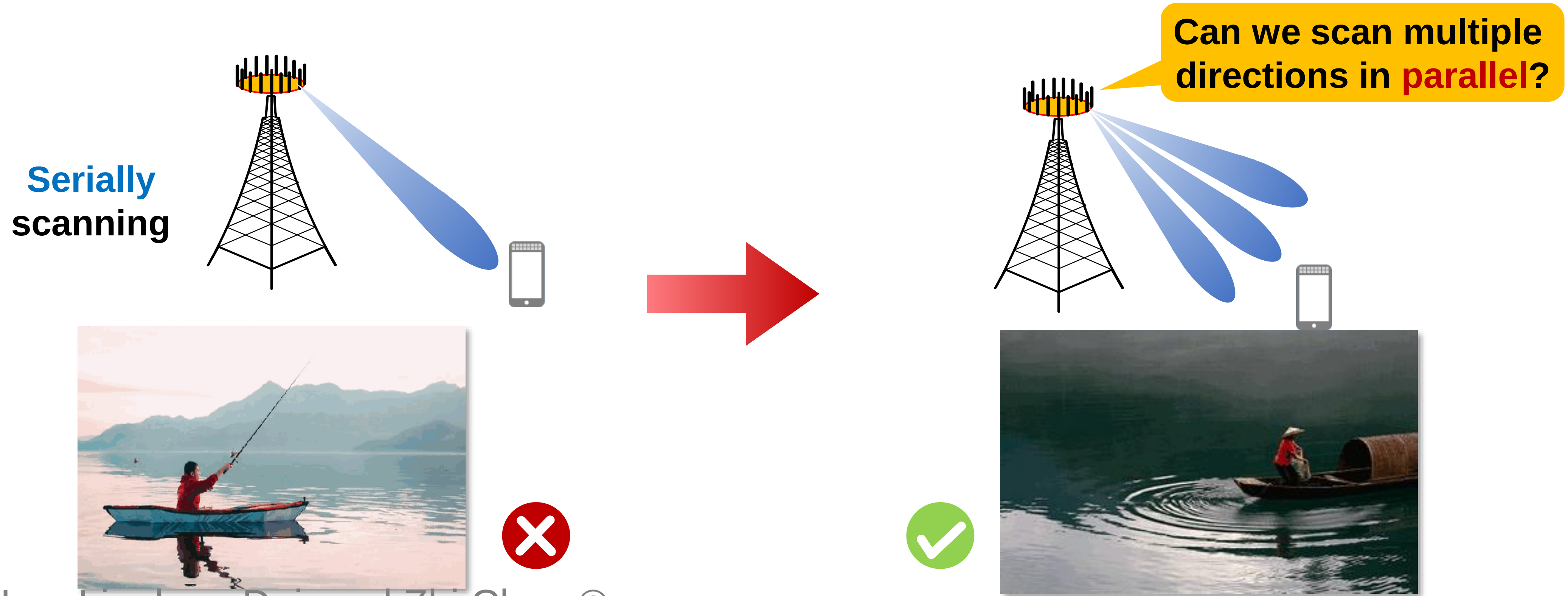

# Beam Zooming based THz Beam Tracking

- Technical challenge
  - ➢ The extremely narrow beam makes the pilot overhead of classical THz beam training unaffordable
- Beam Zooming technology
  - ➢ Redirect the vision from mitigating beam split to benefiting from it
  - ➢ Elaborately design time delays in the delay-phase precoding structure.
  - ➢ Flexibly Control the angular coverage of frequency-dependent beams over the whole bandwidth

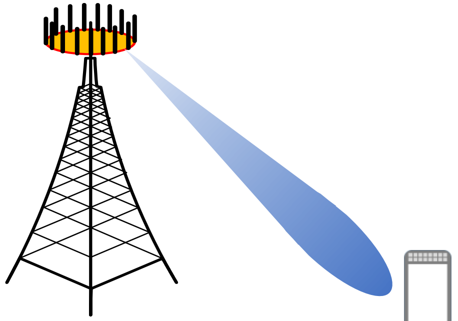

**Searching one angle per time slot**

**Beam zooming**

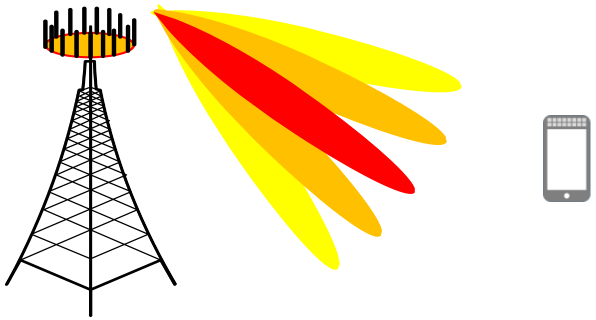

**Searching multiple angles per time slot**

Chong Han, Linglong Dai, and Zhi Chen ©

J. Tan and L. Dai, **"Wideband beam tracking in THz massive MIMO systems,"** **IEEE J. Sel. Areas Commun., 2021.**

# Simulation Result

- Performance of Beam Tracking

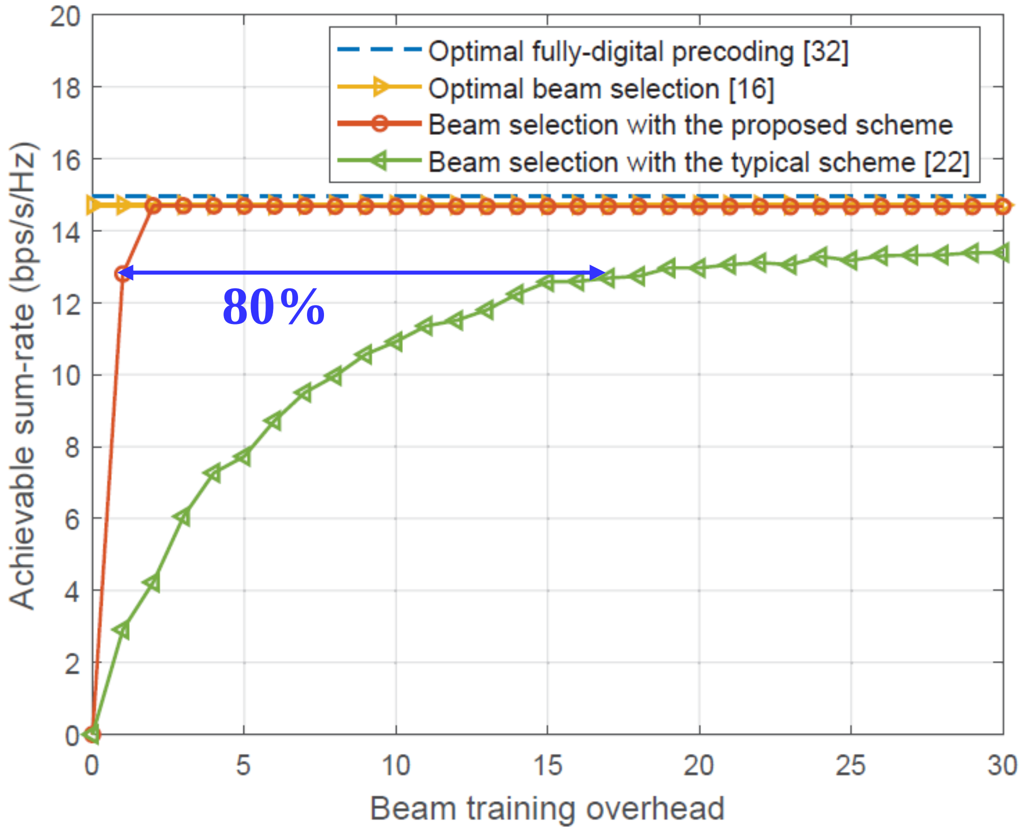


| Parameter | Value |
|---|---|
| Carrier | 100 GHz |
| Bandwidth | 5 GHz |
| Number of carriers | 1024 |
| Number of antennas | 256 |
| SNR | 10 dB |

**Remarkably reducing the pilot overhead by 80%**



J. Tan and L. Dai, "Wideband beam tracking in THz massive MIMO systems," IEEE J. Sel. Areas Commun., 2021.

# Challenge of Near-Field Beam Training

- Polar-domain codebook requires extra grids on the distance domain, leading to a substantial scaling of codebook size

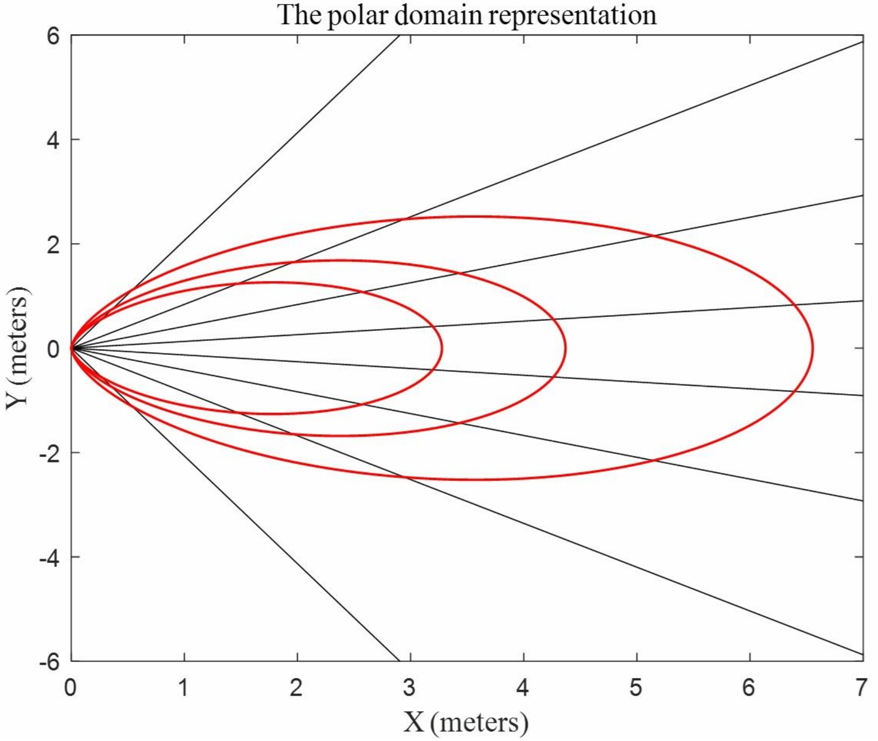


Exhaustive Search

| Parameter | Far-field codebook | Near-field codebook |
| --- | --- | --- |
| Number of antennas | 512 | 512 |
| Carriers | 100 GHz | 100 GHz |
| Number of angle grids | 512 | 512 |
| Number of distance grids | 1 | 20 |
| Codebook size | 512 | 10240 |

**The overhead of near-field exhaustive beam training is unaffordable**

# Near-field Rainbow based Beam Tracking

- Time-delay circuits are able to control the degree of the near-field beam split effect
  - The optimal distance is searched in a time division manner
  - The optimal angle is searched in a frequency division manner

$f_2$

Prism

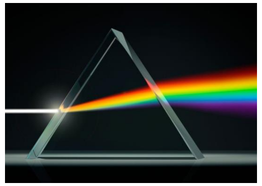

$f_2$

frequencies

$f_1$
$f_2$
$f_3$
$f_4$
$f_5$
$f_6$
$f_7$

**Exhaustive training**

**Near-field rainbow based training**

**The pilot overhead is determined by the search of distance**

# Simulation Result

- Average achievable rate vs. training overhead

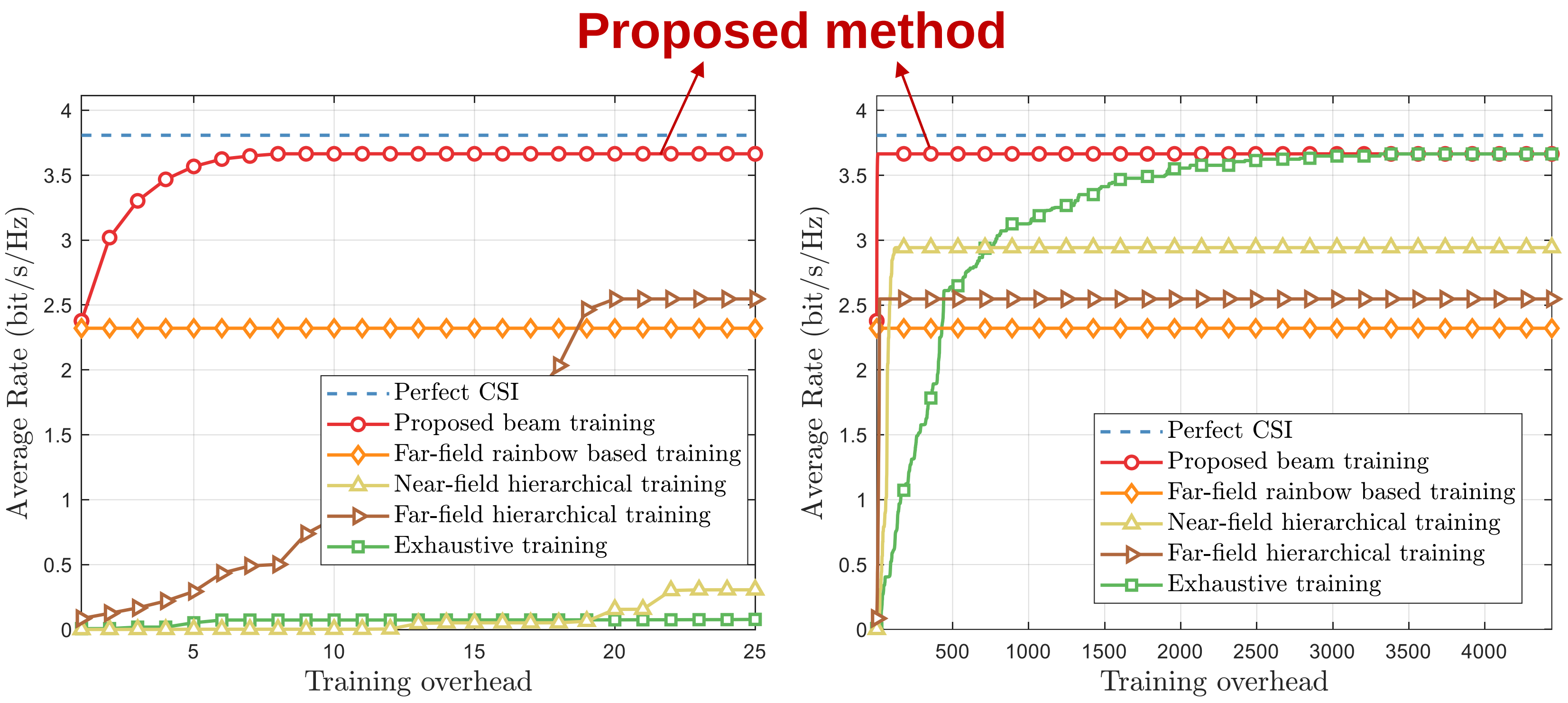


| Parameter | Value |
|---|---|
| Carrier | 60 GHz |
| Bandwidth | 3 GHz |
| Antenna number | 256 |
| Distance | $U(3\ \mathrm{m},\ 40\ \mathrm{m})$ |
| Angle | $U(-\sin\frac{\pi}{3}, \sin\frac{\pi}{3})$ |

**Our scheme achieves a near-optimal average rate with 8 training overhead**

Chong Han, Linglong Dai, and Zhi Chen ©

M. Cui, L. Dai, Z. Wang, S. Zhou, and N. Ge, **"Near-field rainbow: Wideband beam training for XL-MIMO,"** IEEE Trans. Wireless Commun., 2023.

# Comparison of far-field and near-field

- Far-field: The EM waves impinging on the antenna array can be approximately modeled as planar waves, where the phase of the EM wave is a linear function of the antenna index $n$
- Near-field: The EM waves have to be accurately modeled as spherical waves, where the phase of the EM wave is a non-linear function of the antenna index $n$

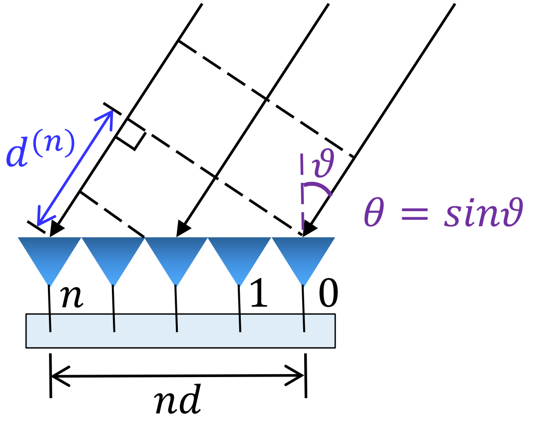


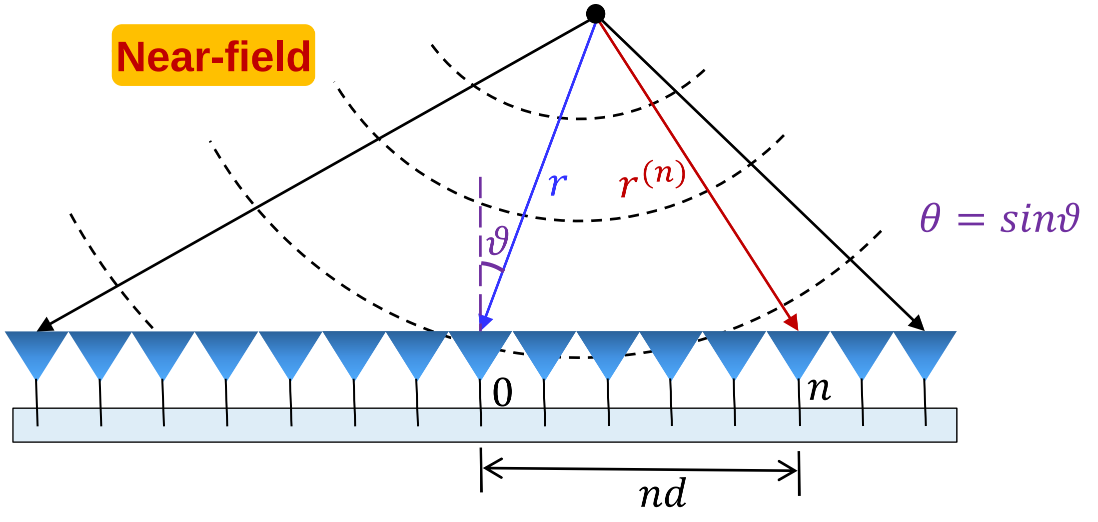


Distance: $d^{(n)} = nd\theta$ Linear

Phase: $\phi_n^{far} = -\frac{2\pi d^{(n)}}{\lambda} = -\frac{2\pi}{\lambda} nd\theta$

Distance: $r^{(n)} = \sqrt{r^2 + n^2 d^2 - 2ndr\theta}$ Non-linear

Phase: $\phi_n = \frac{2\pi(r^{(n)} - r)}{\lambda} = \frac{2\pi}{\lambda}\left(\sqrt{r^2 + n^2 d^2 - 2ndr\theta} - r\right)$

$\approx -\frac{2\pi}{\lambda} nd\theta + \frac{1-\theta^2}{\lambda r}\pi n^2 d^2$ Near-field term

# Challenge of SDMA for Far-Field Communication

- Spatial division multiple access (SDMA) is employed by massive MIMO to serve multiple users, but it fails to simultaneously serve users at the same angle
- Unlike far-field beam steering which focus on specific angles, near-field beam focusing is able to focus on specific location

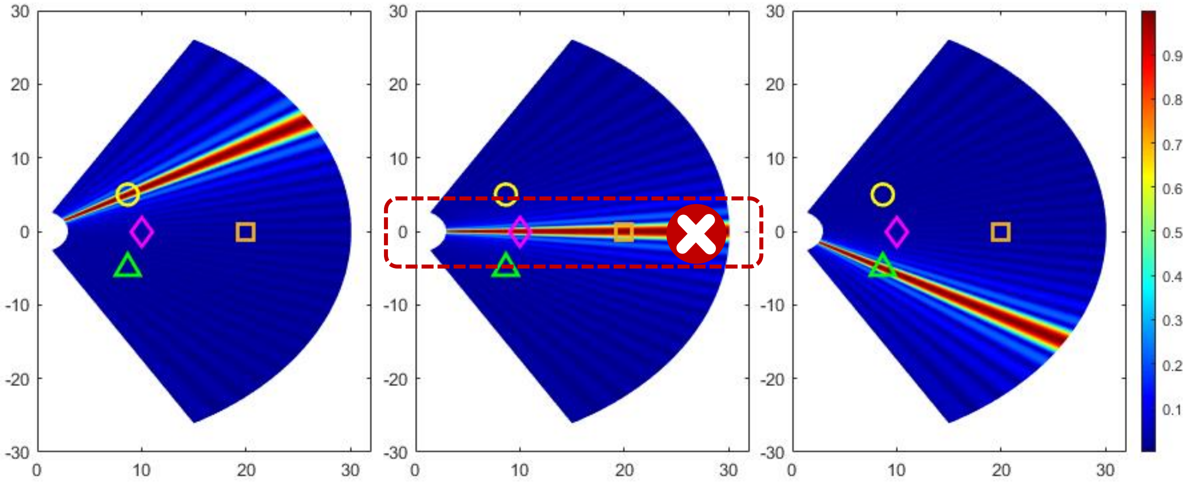

Far-field beamsteering

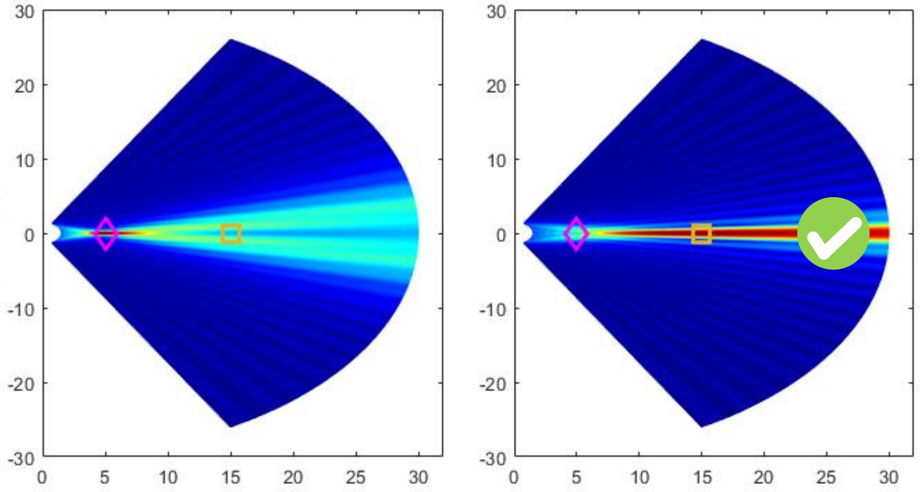

Near-field beamfocusing

**Near-field beamfocusing has the potential to serve users at the same spatial angle**

Chong Han, Linglong Dai, and Zhi Chen ©

M. Cui, Z. Wu, Y. Lu, X. Wei, and L. Dai, "Near-field MIMO communications for 6G: Fundamentals, challenges, potentials, and future directions," IEEE Commun. Mag., 2023.

# Multiple Access in Near-Field: SDMA or LDMA?

- Far-field SDMA: Users at different angles are served by orthogonal far-field beams
- Near-field location division multiple access (LDMA): Users at different locations can be simultaneously served due to property of near-field beam focusing

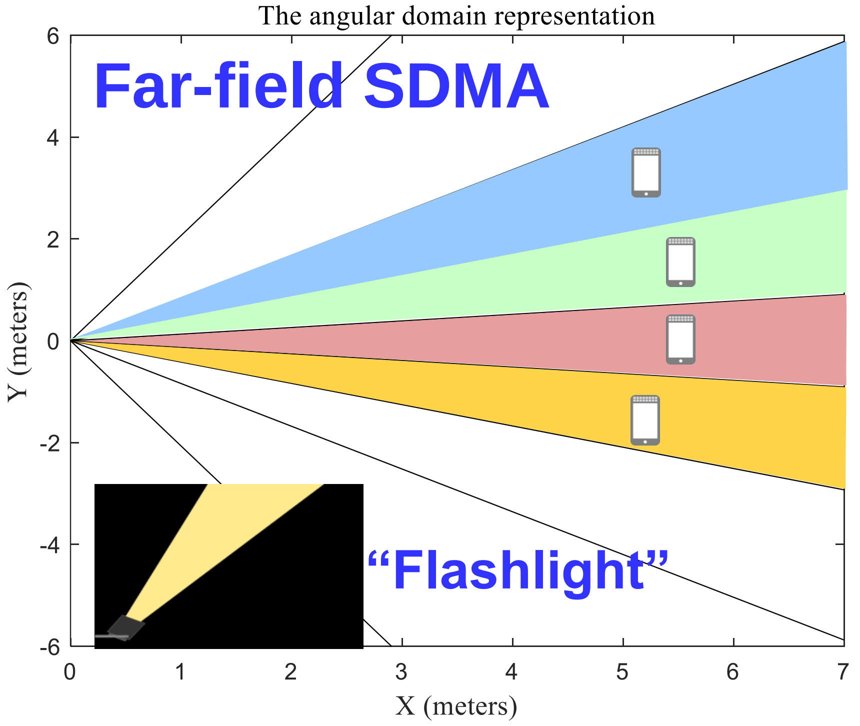


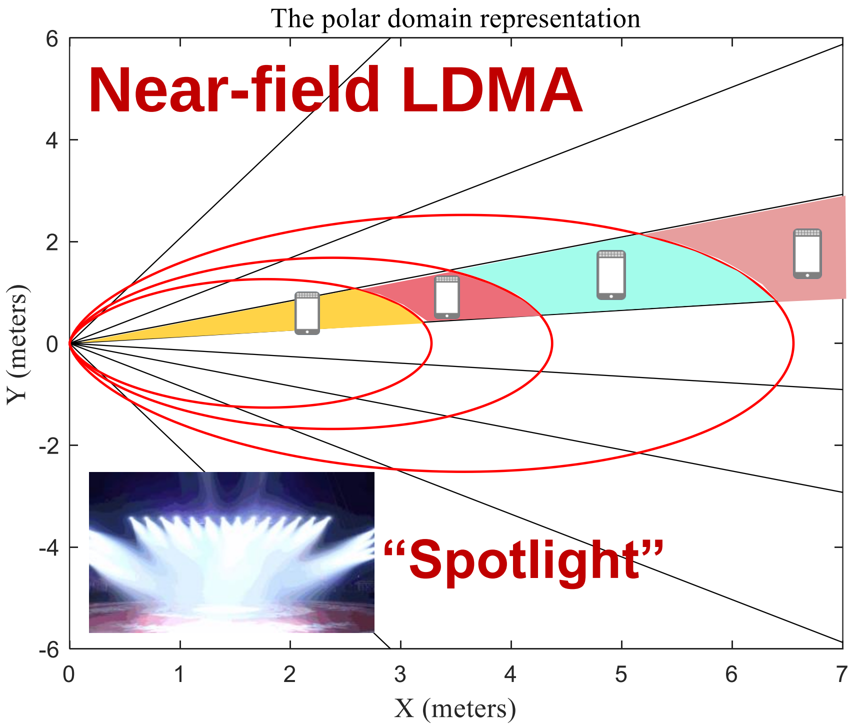


**Compared with far-field SDMA, near-field LDMA provides new possibility for capacity improvement**



Z. Wu and L. Dai, "Multiple access for near-field communications: SDMA or LDMA?" IEEE J. Sel. Areas Commun., Jun. 2023.

# Beamfocusing of Near-Field Beams

Lemma 1: The normalized array gain achieved by $w = a^*(\bar{r}, \theta)$ at any user location $(r, \theta)$ is obtained through Fresnel approximation as

$$f(r, \bar{r}, \theta) = \frac{1}{M}\left|\sum_{n=-N}^{N} e^{jk\left(\bar{r}^{(n)} - r^{(n)}\right)}\right| \approx |G(\beta)| = \left|\frac{C(\beta) + jS(\beta)}{\beta}\right|$$

where $\beta = \sqrt{\frac{M^2 d^2(1-\theta^2)}{2\lambda}\left|\frac{1}{r} - \frac{1}{\bar{r}}\right|}$, $C(\beta) = \int_0^{\beta} \cos\left(\frac{\pi}{2}t^2\right) \mathrm{d}t$ and $S(\beta) = \int_0^{\beta} \sin\left(\frac{\pi}{2}t^2\right) \mathrm{d}t$ are Fresnel functions.

- Beamfocusing property of near-field beams
  - Similar to the beam-width in angular domain of far-field beams, near-field beams possess depth-of-focus in distance domain

$$r \in \left[\frac{\bar{r}D^2(1-\theta^2)}{D^2(1-\theta^2) + 2\lambda\beta_\Gamma^2\bar{r}}, \frac{\bar{r}D^2(1-\theta^2)}{D^2(1-\theta^2) - 2\lambda\beta_\Gamma^2\bar{r}}\right]$$

$G(\beta_\Gamma) = 0.5$

3dB depth-of-focus: $$r_d = \frac{4\lambda\beta_\Gamma^2\bar{r}^2 D^2(1-\theta^2)}{D^4(1-\theta^2)^2 - 4\lambda^2\beta_\Gamma^4\bar{r}^2}$$

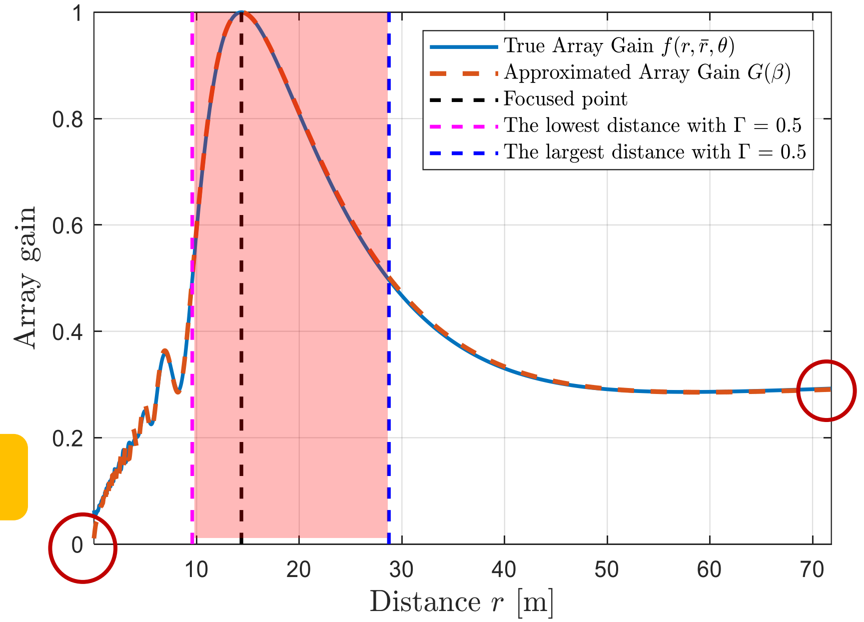


Z. Wu and L. Dai, **"Multiple access for near-field communications: SDMA or LDMA?"** **IEEE J. Sel. Areas Commun., Jun. 2023.**

# Distance Domain Asymptotic Orthogonality

- Far-field orthogonality in angular domain

Phase: $\phi_n^{\text{far}}(\theta) = -\frac{2\pi}{\lambda} n d\theta$

Correlation: $f^{\text{far}} = |\mathrm{a}^H(\theta_1)\mathrm{a}(\theta_2)| = \frac{1}{N}\left|\frac{\sin(\frac{1}{2}Nkd(\sin\theta_1 - \sin\theta_2))}{\sin(\frac{1}{2}kd(\sin\theta_1 - \sin\theta_2))}\right|$

As $N \to \infty$, interference from different angles $I^{\text{far}} \to 0$ $(\theta_1 \neq \theta_2)$

- Lemma 2: Near-field orthogonality in distance domain

Phase: $\phi_n^{near}(\theta) = -\frac{2\pi}{\lambda} n d\theta + \frac{1-\theta^2}{\lambda r}\pi n^2 d^2$

Correlation: $f^{near} = |\mathrm{a}^H(\theta, r_1)\mathrm{a}(\theta, r_2)| \approx |G(\beta)| = \left|\frac{C(\beta)+jS(\beta)}{\beta}\right|$

where $\beta = \sqrt{\frac{N^2 d^2(1-\theta^2)}{2\lambda}\left|\frac{1}{r} - \frac{1}{\bar{r}}\right|}$

As $N \to \infty$, interference from different distances $I^{\text{near}} \to 0$ $(\forall\theta, r_1 \neq r_2)$

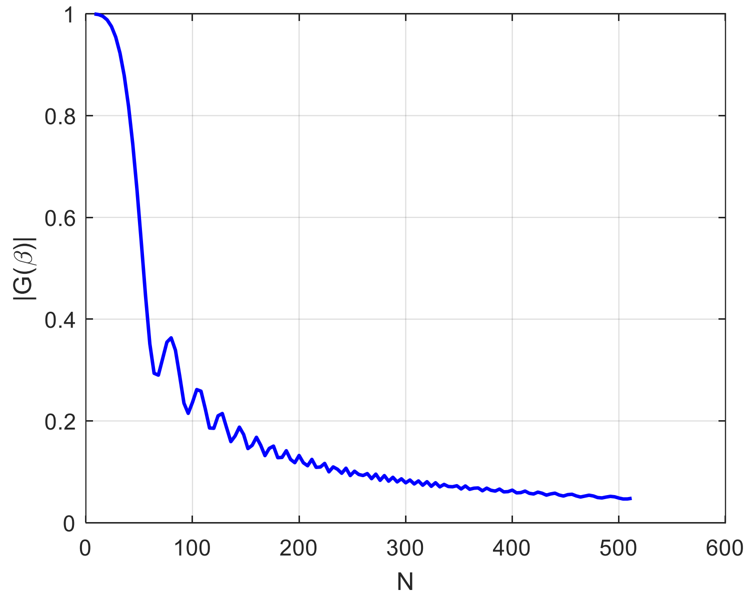


Z. Wu and L. Dai, **"Multiple access for near-field communications: SDMA or LDMA?"** IEEE J. Sel. Areas Commun., **Jun. 2023.**

# Simulation Results for LDMA

- Scenario 1: Users are linearly distributed along the same direction
- Scenario 2: Users are uniformly distributed within a cell

| BS Antennas | UE Antennas | Frequency | UE Numbers | Elevation/ Azimuth Angle Range | Distance Range |
|---|---|---|---|---|---|
| 256 | 1 | 30 GHz | 20 | $[-\pi/2, \pi/2]$ | [4m, 100m] |

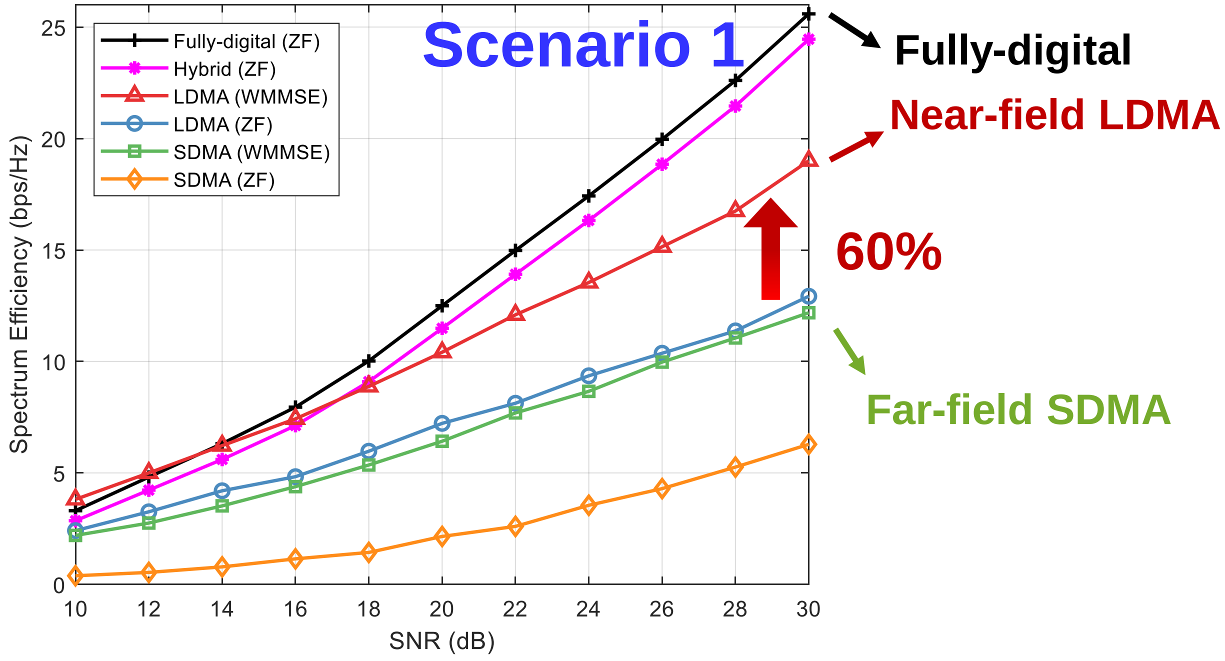


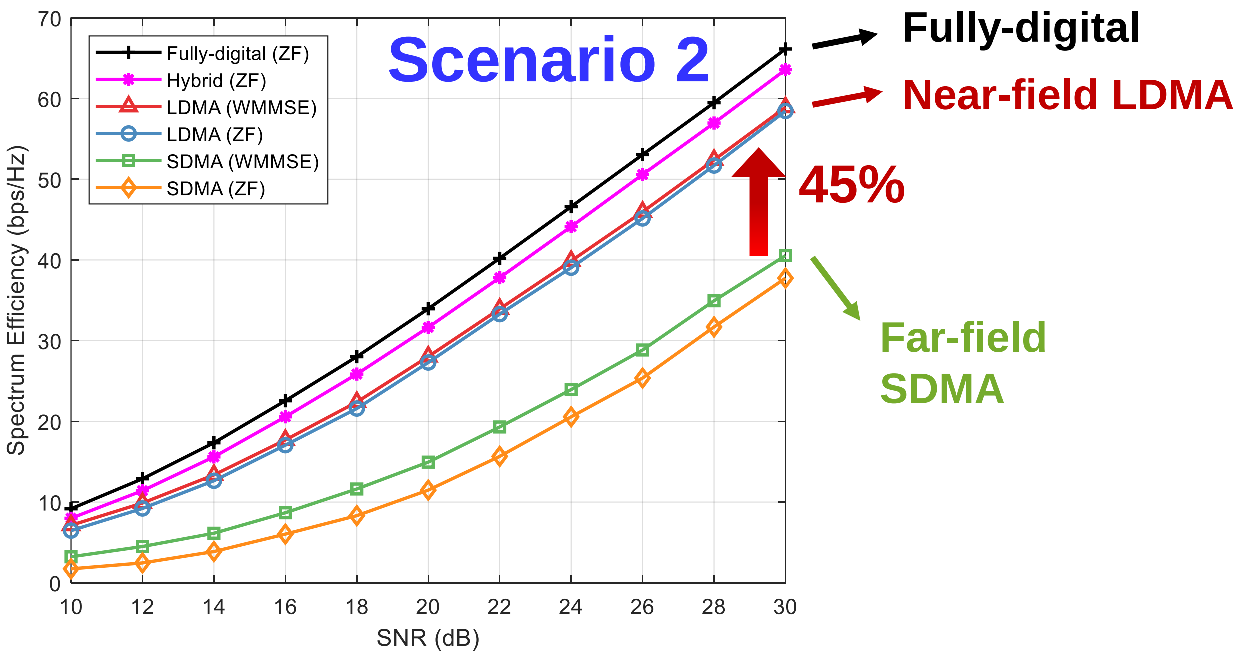


Z. Wu and L. Dai, "Multiple access for near-field communications: SDMA or LDMA?" IEEE J. Sel. Areas Commun., Jun. 2023.

# Outline

- **Chapter 1: Introduction**
    i. Evolution to 6G
    ii. Applications
    iii. Motivations for THz UM-MIMO
- **Chapter 2: THz UM-MIMO Systems**
    i. Electronic and photonic approaches
    ii. New material approaches
    iii. THz UM-MIMO channel
- **Chapter 3: THz Beamforming Technologies**
    i. Fundamentals of beamforming
    ii. State-of-the-art and challenges on beamforming
    iii. Far-field beamforming
    iv. Near-field beamforming/beamfocusing
- **Chapter 4: THz Beam Management**
    i. Fundamentals of beam management
    ii. State-of-the-art and challenges on beam management
    iii. Beam estimation/alignment
    iv. Beam tracking
    v. Beam-guided medium access
- **Chapter 5: Future Directions**
    i. Cross far- and near-field beamforming
    ii. IRS-assisted hybrid beamforming
    iii. Beam management in IRS assisted systems
- **Conclusion**

# Cross Far- and Near-field Communication

Recall Rayleigh distance is a classic boundary between far-field and near-field.

- In THz UM-MIMO system, the increment of the number of antennas and decrease of wavelength result in the growth of the Rayleigh distance

| Rayleigh distance/m | 0.1THz | | 0.3THz | |
|---|---|---|---|---|
| Antennas at Tx and Rx | 1024-64 | 1024-1024 | 1024-64 | 1024-1024 |
| ULA | 1775 | 6291 | 591.9 | 2097 |
| UPA | 4.8 | 12.3 | 1.6 | 4.1 |
| WSMS | 262.8 | 307.2 | 87.6 | 102.4 |

*WSMS is with 64 $\lambda$ subarray spacing and 4 subarrays*

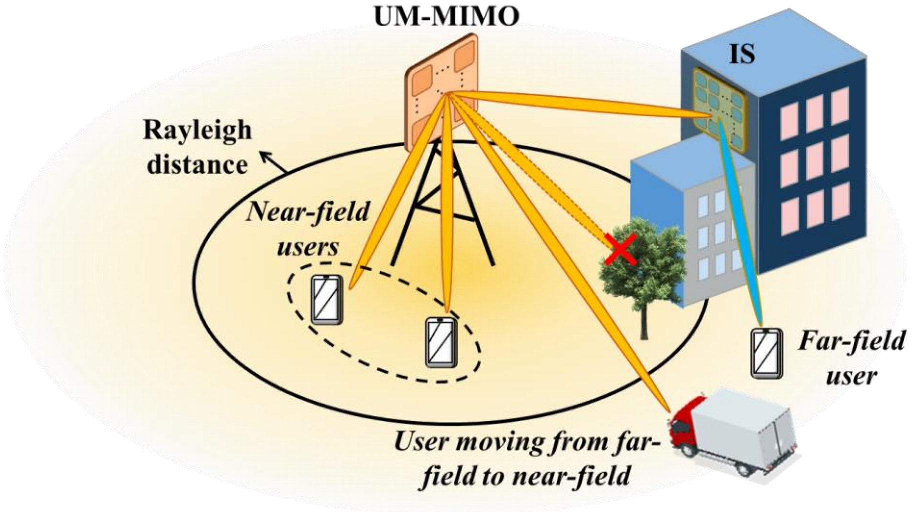


Illustration of THz Hybrid-field communications

- Typical communication distance at THz band **covers both far-field and near-field**



C. Han, Y.-H. Chen, L. Yan, Z. Chen, and L. Dai, **"Cross far- and near-field wireless communications in terahertz ultra-large antenna array systems,"** IEEE Wireless Communications, 2023.

# Practical Hardware Efficient Design

Decrement of distance → Increment of channel capacity

- Far-field
  - ➢ Limited spatial multiplexing
    - → **Less RF chains and phase shifters required**
    - → **Lower hardware cost**

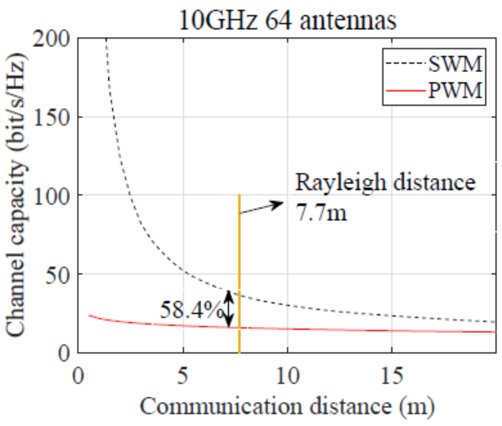

Channel capacity vs. distance

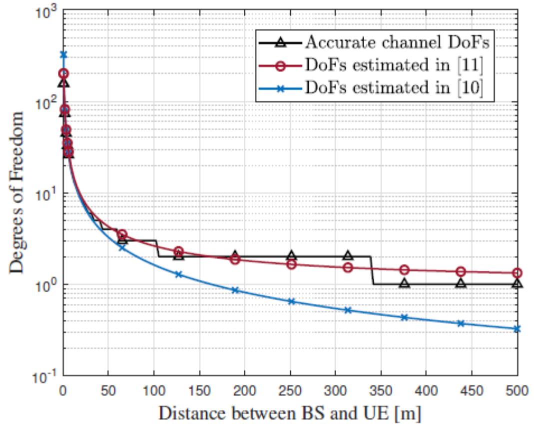

SDoF vs. distance

- Near-field
  - ➢ Non-linear channel phases gives additional spatial degree-of-freedom (SDoF)
  - ➢ To unleash spatial multiplexing
    - → **More RF chains and phase shifters required**
    - → **Higher hardware cost**

**Difficult to simultaneously meet the cross-field spatial multiplexing and hardware cost requirements.**

C. Han, Y.-H. Chen, L. Yan, Z. Chen, and L. Dai, **"Cross far- and near-field wireless communications in terahertz ultra-large antenna array systems,"** IEEE Wireless Communications, 2023.

M. Cui, Z. Wu, Y. Lu, X. Wei, and L. Dai, **"Near-field communications for 6G: Fundamentals, challenges, potentials, and future directions,"** IEEE Commun. Mag., 2022.

# Practical Hardware Efficient Design

Two potential solutions:

- **Widely-Spaced Multi-Subarray (WSMS)**
  - ➢ Enlarge the near-field region to a typical communication distance
- **Distance-aware precoding structure (DAP)**
  - ➢ Insert a selection circuit between phase shifters and RF-chains
  - ➢ Flexibly activate/inactivate each RF-chain according to the SDoFs

The number of RF-chains and phase shifters of both structures are **larger than** structures for far-field transmission.

**More efficient structure is needed to balance spatial multiplexing and hardware cost in cross-field transmission.**

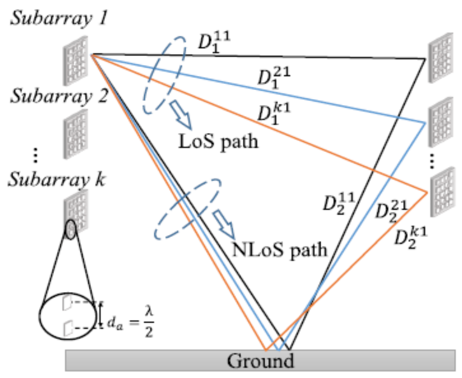


WSMS structure

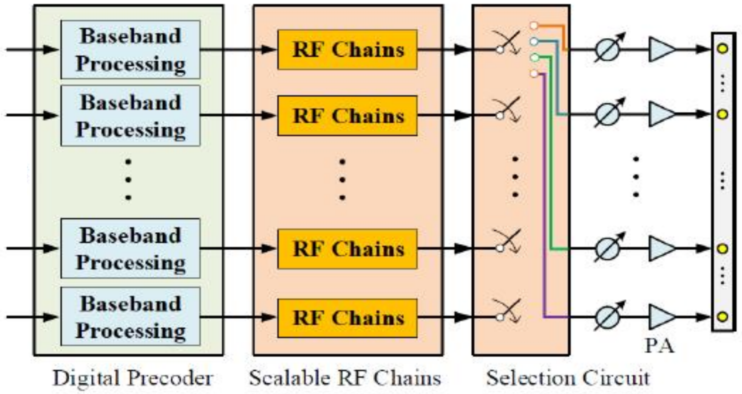


DAP architecture



Z. Wu, M. Cui, Z. Zhang, and L. Dai, **"Distance-aware precoding for near-field capacity improvement in XL-MIMO,"** IEEE VTC, 2022.

# Cross-field Beam Training

Beam training is required to realize **narrow beam pair alignment** between Tx and Rx

- Far-field:
  - Angle domain beam $[\boldsymbol{w}(\theta)]_n = \frac{1}{\sqrt{N}} exp\left(-jk_c\delta_N^{(n)} dsin\theta\right)$

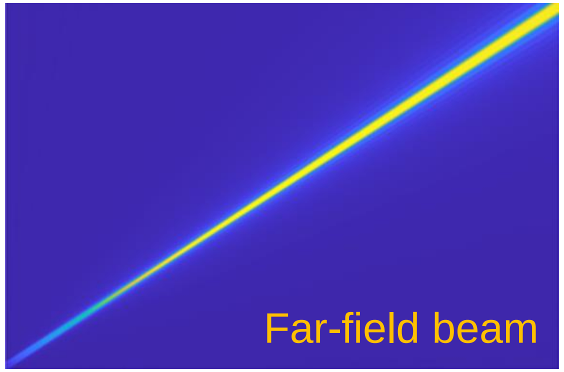


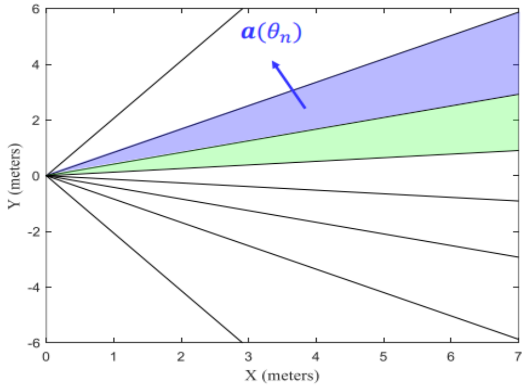


  - Beams only process angular resolution
  - Beam training only needs to search in the angular dimension
  - Inaccurate in the near-field

Chong Han, Linglong Dai, and Zhi Chen ©

M. Cui, L. Dai, R. Schober, and L. Hanzo, **"Near-field wideband beamforming for extremely large antenna array,"** arXiv:2109.10054, Sep. 2021.

# Cross-field Beam Training

- Near-field:
  - ➢ Joint angle and distance domains beam $[\mathbf{w}(r,\theta)]_n = \frac{1}{\sqrt{N}} exp\left(-jk_c r\left(1-\delta_N^{(n)} d sin\theta\right)\right)$

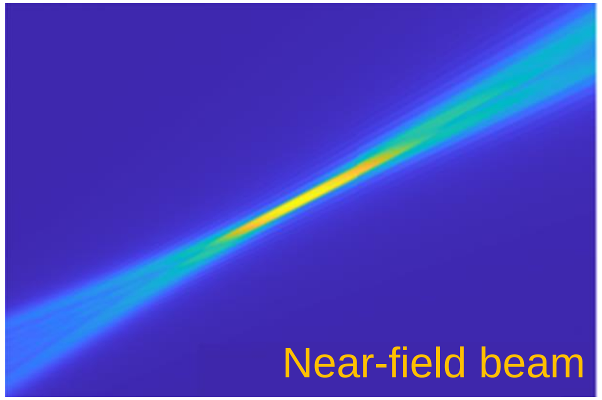


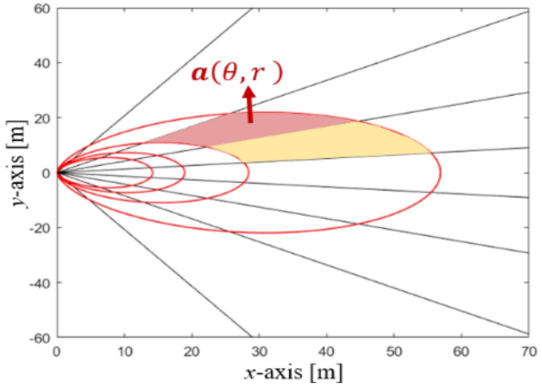


  - ➢ Additional distance domain beam resolution
  - ➢ Beam training jointly searches in the angular and distance domains
  - ➢ Significantly increases the training overhead

**Codebook designs are different for cross-field beam training, and are not universally applicable.**



M. Cui and L. Dai, **"Channel estimation for extremely large-scale MIMO: Far-field or near-field?,"** IEEE Trans. Commun., 2022.

# Multi-user Communications and Networking

Lack of analysis on **medium access control (MAC) and networking** in THz cross-field communication.

- Far-field: spatial division multiple access (SDMA)
- Near-field: location division multiple access (LDMA)
  - Orthogonality in **both angular and distance domains** → increased precision of beamforming
  - **Employ** **near-field location-dependent beam focusing vectors** as analog precoders to serve different UEs located in different locations
  - Enhance the multiple accessibilities **by the distance dimension**
- How to unify the cross-field multiple access?
  - Account for distance and angular beam resolutions in different communication distances

# Beam Split Aggregation and Multiplexing

**BSAM** is a general concept including beam split aggregation and multiplexing

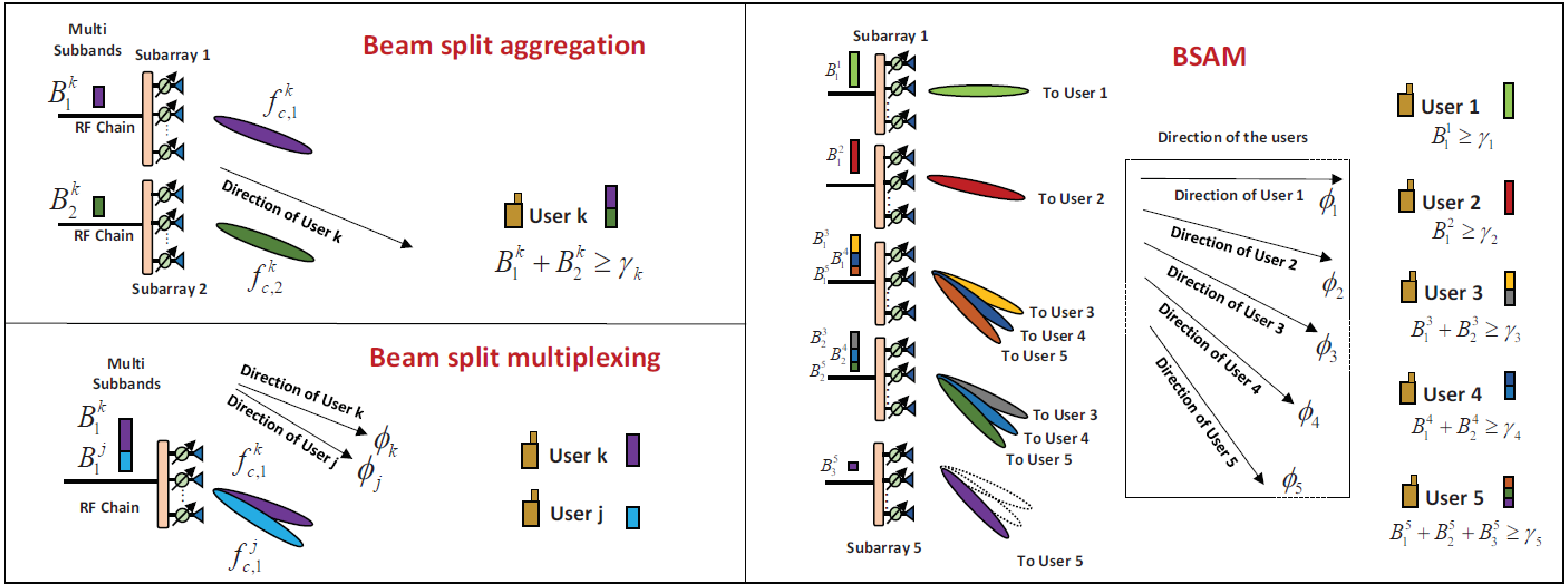


***beam split aggregation***: each user might be served by multiple subarray on different sub-bands
***beam split multiplexing***: each subarray may serve multiple users on different sub-bands



B. Ning, L. Li, W. Chen, and Z. Chen, "Wideband terahertz communications with AoSA: Beam split aggregation and multiplexing," IEEE GLOBECOM, 2022.

# Outline

# Conclusion

- **UM-MIMO** is essential for the viability of terahertz communication.
  - Large array gain
  - Multiplexing gain

  Compensate Loss

- Lots of ideas and algorithms have been proposed for THz band communication. To ensure the practical values, these designs should sufficiently consider **the characteristics of terahertz devices and channels**.

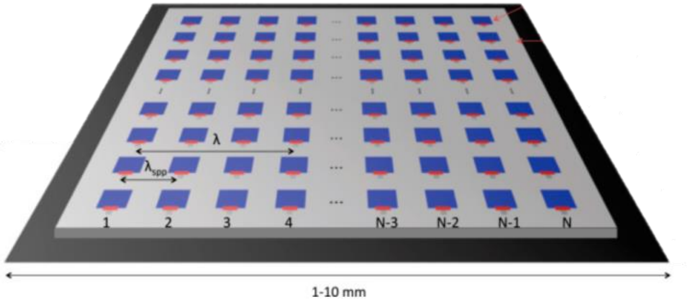



- As an important future direction, the **cross near- and far- field communication** will bring a new paradigm of communication.

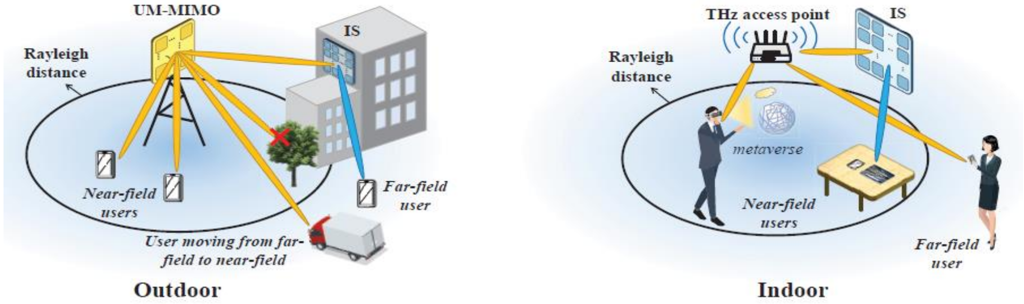

# Thank you very much for your attention!

**Chong Han**
Shanghai Jiao Tong University
chong.han@sjtu.edu.cn

**Linglong Dai**
Tsinghua University
daill@tsinghua.edu.cn

**Zhi Chen**
University of Electronic Science and Technology of China
chenzhi@uestc.edu.cn